2018 Spring

“Advanced Physical Metallurgy”

- Bulk Metallic Glasses -

04.09.2018

Eun Soo Park

Office: 33-313
Telephone: 880-7221
Email: espark@snu.ac.kr
Office hours: by appointment

Contents for previous class

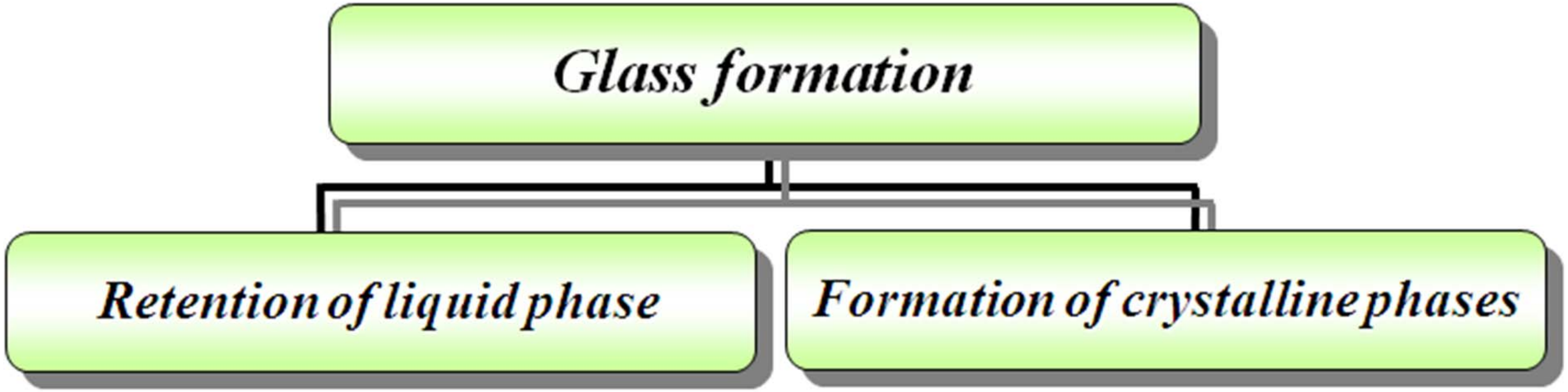

Glass formation

Retention of liquid phase

Formation of crystalline phases

Glass Formation results when

Liquids are cooled to below T_m (T_L) sufficiently fast to avoid crystallization.

Nucleation of crystalline seeds are avoided

Growth of Nuclei into crystallites (crystals) is avoided

Liquid is “frustrated” by internal structure that hinders both events

➡ **“Glass Formation”**

Contents for previous class

2.5.2 Kinetics of Glass Formation

A. Homogeneous Nucleation rate, *I* (by David Turnbull)

$$\boxed{I = \frac{k_n}{\eta(T)} \exp\left[-\frac{b\alpha^3\beta}{T_r(\Delta T_r)^2} \right]} \tag{2.4}$$

where

- b is a shape factor ($= 16\pi/3$ for a spherical nucleus)
- k_n is a kinetic constant
- $\eta(T)$ is the shear viscosity of the liquid at temperature T
- T_r is the reduced temperature ($T_r = T/T_l$)
- ΔT_r is the reduced supercooling ($\Delta T_r = 1 - T_r$)
- α and β are dimensionless parameters related, respectively, to the liquid/solid interfacial energy (σ) and to the molar entropy of fusion, ΔS_f

Thus,

$$\boxed{\alpha = \frac{\left(N_A \overline{V}^2\right)^{1/3} \sigma}{\Delta H_f}} \qquad \boxed{\beta = \frac{\Delta S_f}{R}}$$

where

- N_A is Avogadro's number
- $\overline{V}$ is the molar volume of the crystal
- R is the universal gas constant

A. Homogeneous Nucleation rate, *I* (by David Turnbull)

$$I = \frac{k_n}{\eta(T)} \exp\left[-\frac{b\alpha^3\beta}{T_r(\Delta T_r)^2}\right]$$

$$\alpha = \frac{\left(N_A \overline{V}^2\right)^{1/3} \sigma}{\Delta H_f}$$

$$\beta = \frac{\Delta S_f}{R}$$

1) η ↑ (dense random packed structure) → I ↓

2) For given T and η, $\alpha^3\beta$ ↑ (σ solid interfacial E & ΔS_f ↑/ ΔH_f ↓) → I ↓

3) $\eta \sim T_{rg}$ ($=T_g/T_l$) & $\alpha^3\beta$ ~ thermal stability of supercooled liquid

*** For metallic melt : $\alpha\beta^{1/3} \sim 0.5$**

* if $\alpha\beta^{1/3} > 0.9$, impossible to crystallization by homogeneous nucleation under any cooling condition

* if $\alpha\beta^{1/3} \leq 0.25$, difficult to prevent crystallization

B. Growth rate of a crystal from an undercooled liquid, *U*

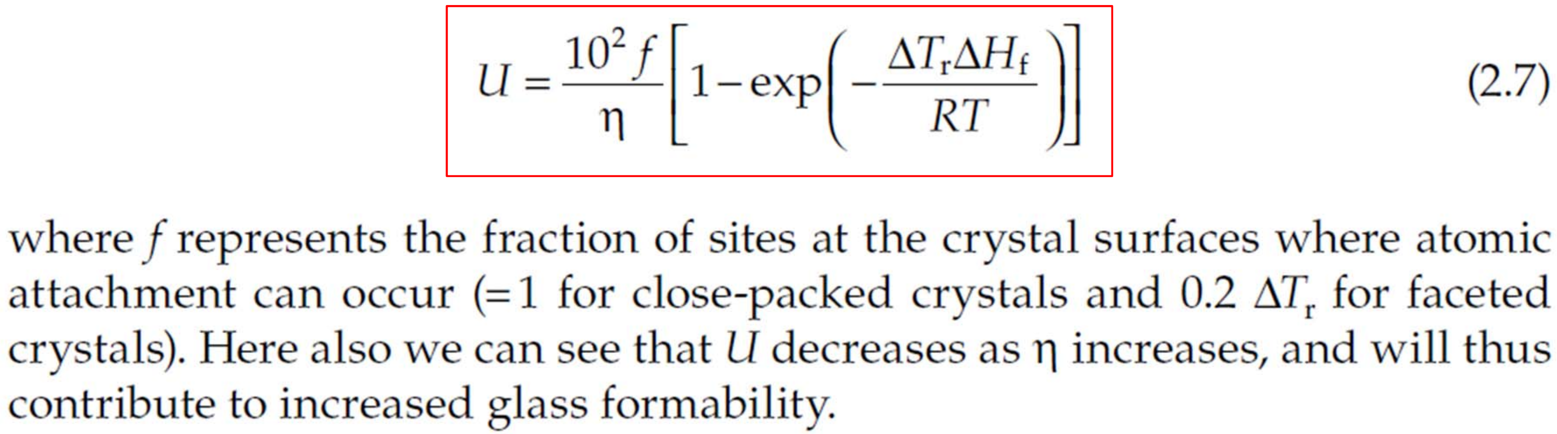

$$\boxed{U = \frac{10^2 f}{\eta}\left[1 - \exp\left(-\frac{\Delta T_r \Delta H_f}{RT}\right)\right]} \qquad (2.7)$$

where f represents the fraction of sites at the crystal surfaces where atomic attachment can occur (=1 for close-packed crystals and 0.2 ΔT_r for faceted crystals). Here also we can see that U decreases as η increases, and will thus contribute to increased glass formability.

1) η ↑ (dense random packed structure) → *U* ↓

2) For given T , *I* & *U* ~ η → T_{rg} or α, β ↑ → GFA ↑

***3)* *f* ↓ through atomic rearrangement like local ordering or segregation → *U* ↓**

*** metallic melt: $\alpha\beta^{1/3} \sim 0.5$ / $T_{rg} > 2/3$ ~ high GFA**

*** Pure metal: $R_c \sim 10^{10\text{-}12}$ K/s, but if $T_{rg} = 0.5$, $R_c \sim 10^6$ K/s**

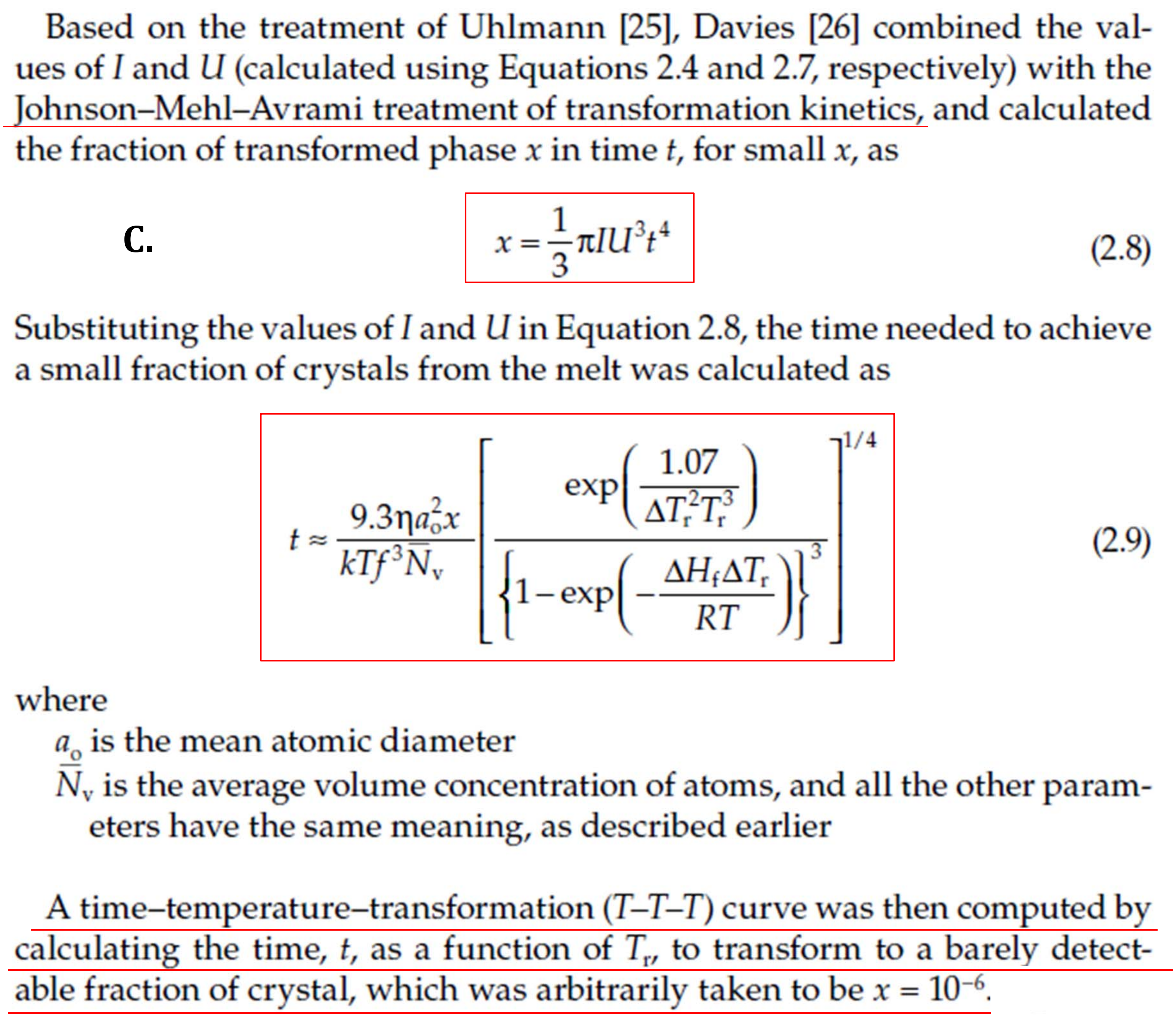

Based on the treatment of Uhlmann [25], Davies [26] combined the values of I and U (calculated using Equations 2.4 and 2.7, respectively) with the Johnson–Mehl–Avrami treatment of transformation kinetics, and calculated the fraction of transformed phase x in time t, for small x, as

C.

$$\boxed{x = \frac{1}{3}\pi I U^3 t^4} \qquad (2.8)$$

Substituting the values of I and U in Equation 2.8, the time needed to achieve a small fraction of crystals from the melt was calculated as

$$\boxed{t \approx \frac{9.3\eta a_o^2 x}{kTf^3\bar{N}_v}\left[\frac{\exp\left(\frac{1.07}{\Delta T_r^2 T_r^3}\right)}{\left\{1-\exp\left(-\frac{\Delta H_f \Delta T_r}{RT}\right)\right\}^3}\right]^{1/4}} \qquad (2.9)$$

where

a_o is the mean atomic diameter

$\bar{N}_v$ is the average volume concentration of atoms, and all the other parameters have the same meaning, as described earlier

A time–temperature–transformation (T–T–T) curve was then computed by calculating the time, t, as a function of T_r, to transform to a barely detectable fraction of crystal, which was arbitrarily taken to be $x = 10^{-6}$.

Constant Nucleation Rate Conditions

- consider impingement + repeated nucleation effects

$$df = (1 - f)df_e \longrightarrow df_e = \frac{df}{1-f}$$

$$f_e = -\ln(1 - f)$$

$$f(t) = 1 - \exp(-f_e(t)) = 1 - \exp\left(-\frac{\pi}{3} I v^3 t^{4}\right)$$

* Short time:
1-exp(z)~Z (z ≪1)

* Long time:
t→∞, *f* →1

Johnson-Mehl-Avrami Equation

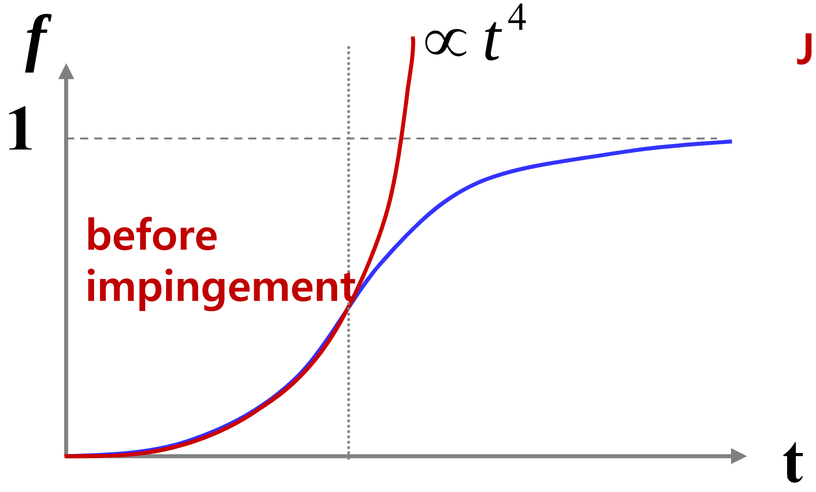

$$f = 1 - \exp(-kt^n)$$

k: T sensitive ***f*(*I*, *v*)** $\quad -\frac{\pi}{3} I v^3$

***n*: 1 ~ 4** (depend on nucleation mechanism)

Growth controlled. Nucleation-controlled.

If no change of nucleation mechanism during phase transformation, n is not related to T.

i.e. 50% transform

Exp (-0.7) = 0.5

$$kt_{0.5}^n = 0.7 \quad t_{0.5} = \frac{0.7}{k^{1/n}}$$

$$\frac{\pi}{3} I v^3 \Rightarrow t_{0.5} = \frac{0.9}{N^{1/4} v^{3/4}}$$

Rapid transformations are associated with (large values of k), or (rapid nucleation and growth rates)

Based on the treatment of Uhlmann [25], Davies [26] combined the values of I and U (calculated using Equations 2.4 and 2.7, respectively) with the Johnson–Mehl–Avrami treatment of transformation kinetics, and calculated the fraction of transformed phase x in time t, for small x, as

C.

$$\boxed{x = \frac{1}{3}\pi I U^3 t^4} \tag{2.8}$$

Substituting the values of I and U in Equation 2.8, the time needed to achieve a small fraction of crystals from the melt was calculated as

$$\boxed{t \approx \frac{9.3\eta a_o^2 x}{kTf^3\bar{N}_v}\left[\frac{\exp\left(\dfrac{1.07}{\Delta T_r^2 T_r^3}\right)}{\left\{1-\exp\left(-\dfrac{\Delta H_f \Delta T_r}{RT}\right)\right\}^3}\right]^{1/4}} \tag{2.9}$$

where

a_o is the mean atomic diameter

$\bar{N}_v$ is the average volume concentration of atoms, and all the other parameters have the same meaning, as described earlier

A time–temperature–transformation (T–T–T) curve was then computed by calculating the time, t, as a function of T_r, to transform to a barely detectable fraction of crystal, which was arbitrarily taken to be $x = 10^{-6}$.

Nucleation and Growth Rates – Poor Glass Formers

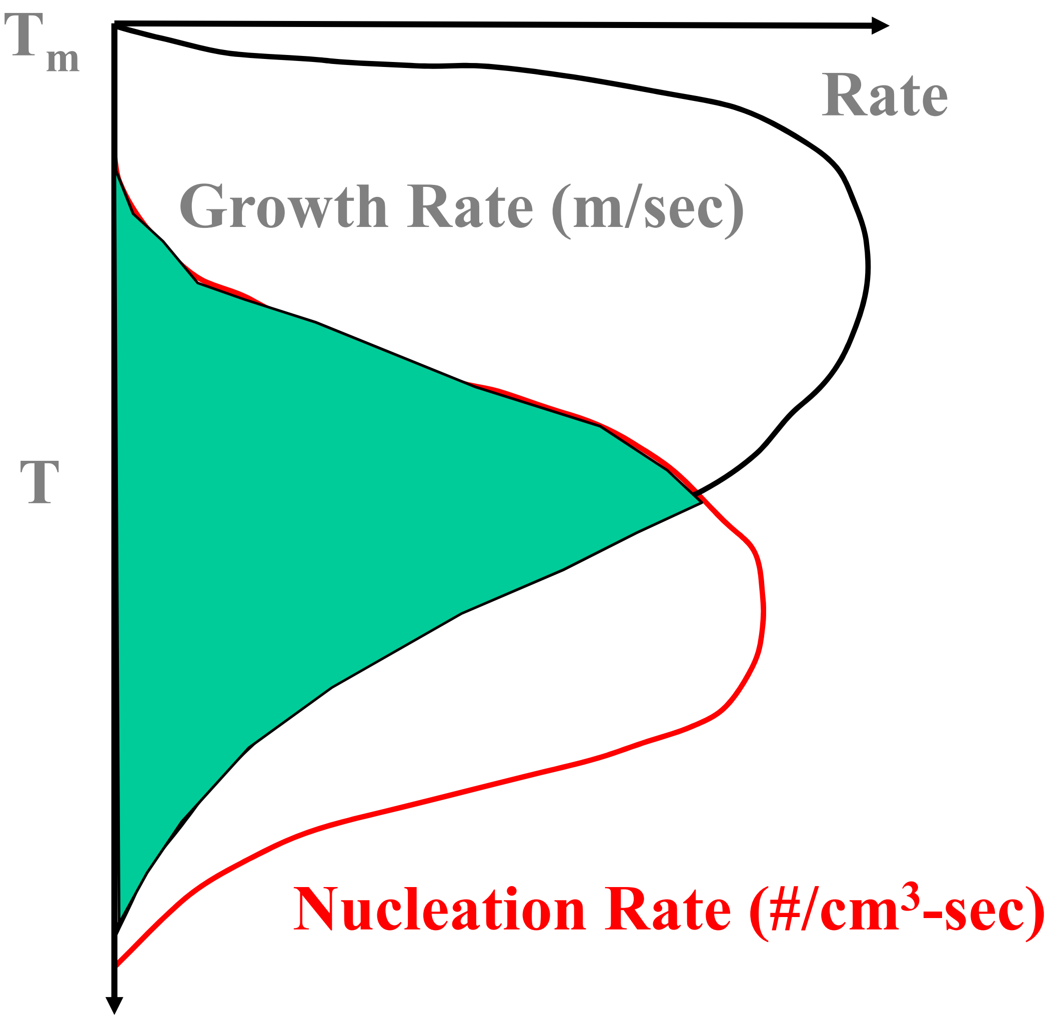

- Strong overlap of growth and nucleation rates
- Nucleation rate is high
- Growth rate is high
- Both are high at the same temperature

Nucleation and Growth Rates – Good Glass Formers

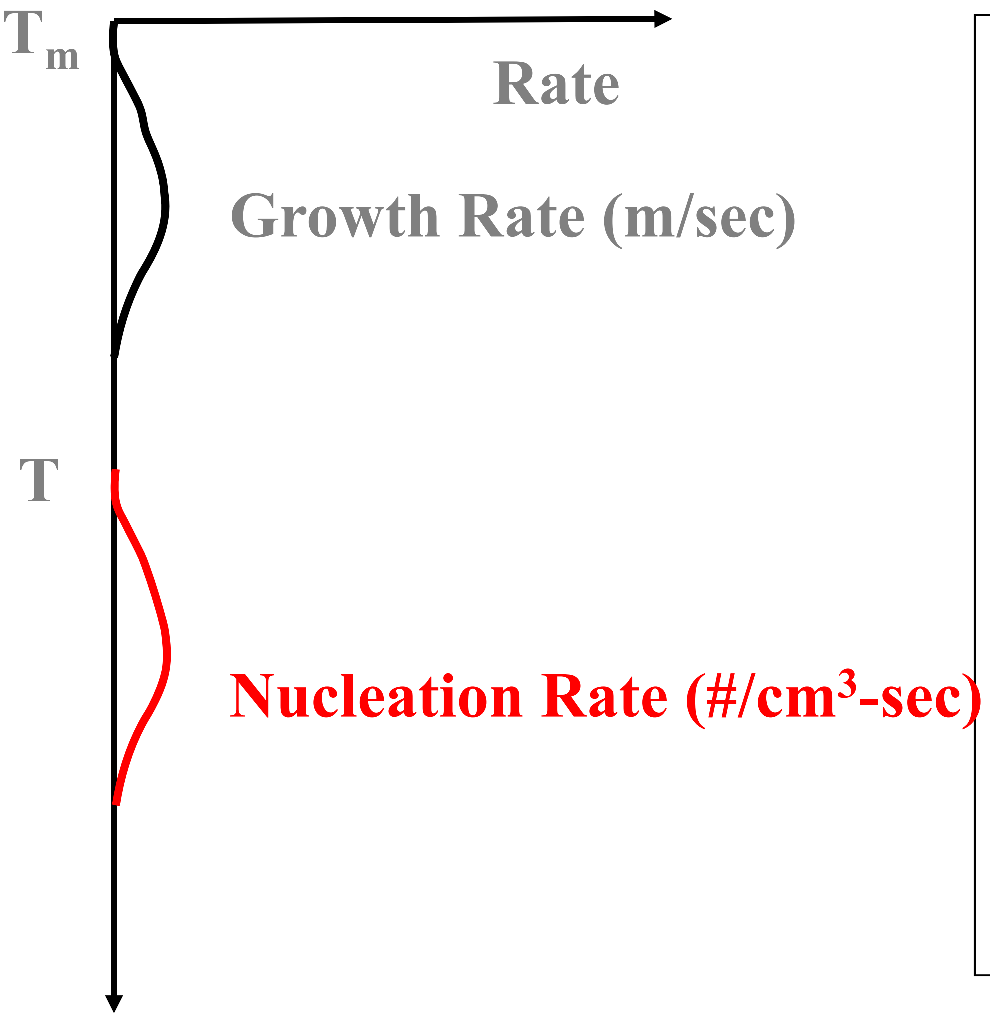

T_m

Rate

Growth Rate (m/sec)

T

Nucleation Rate (#/cm^3-sec)

- No overlap of growth and nucleation rates
- Nucleation rate is small
- Growth rate is small
- At any one temperature one of the two is zero

TTT curves and the critical cooling rate, R_c

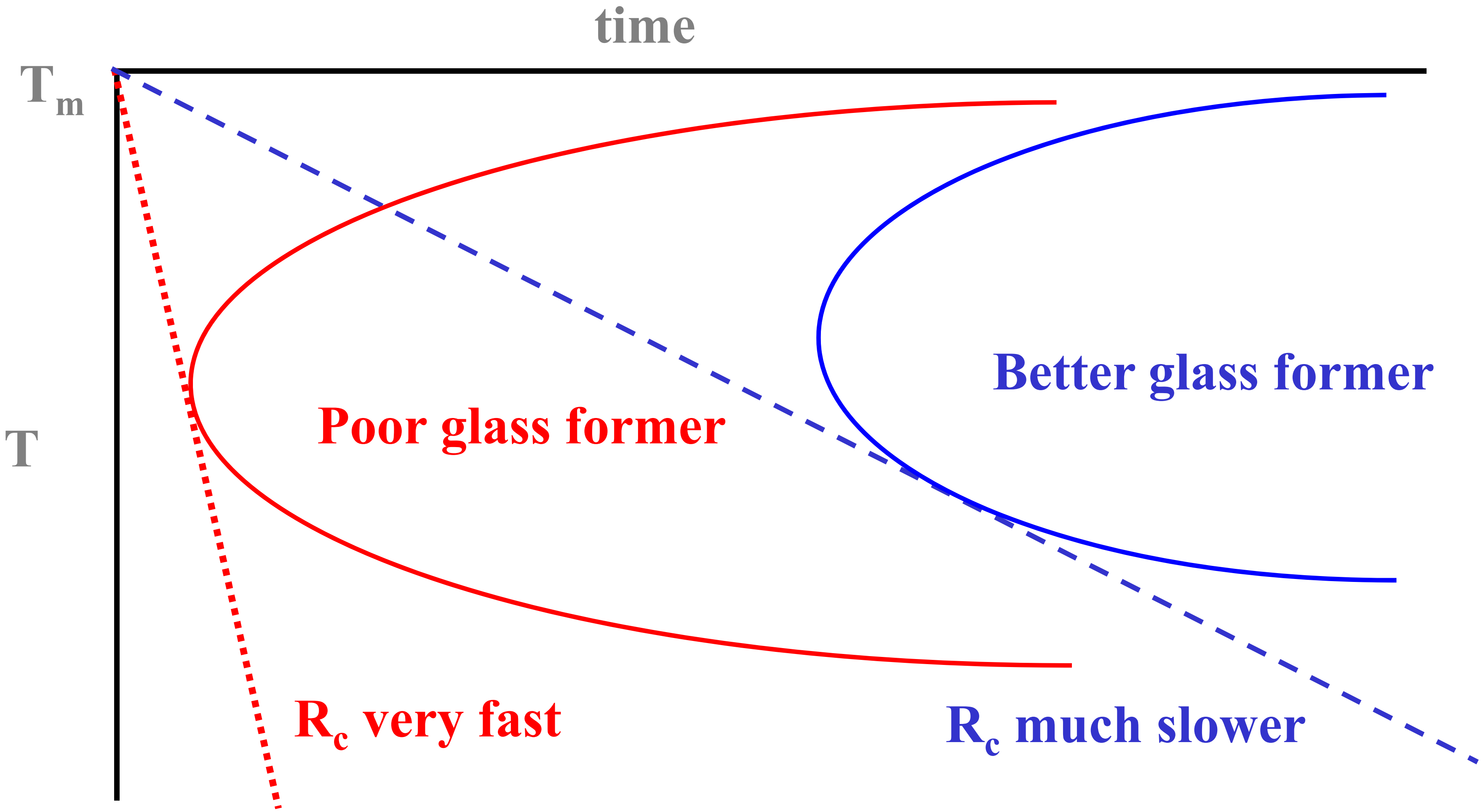

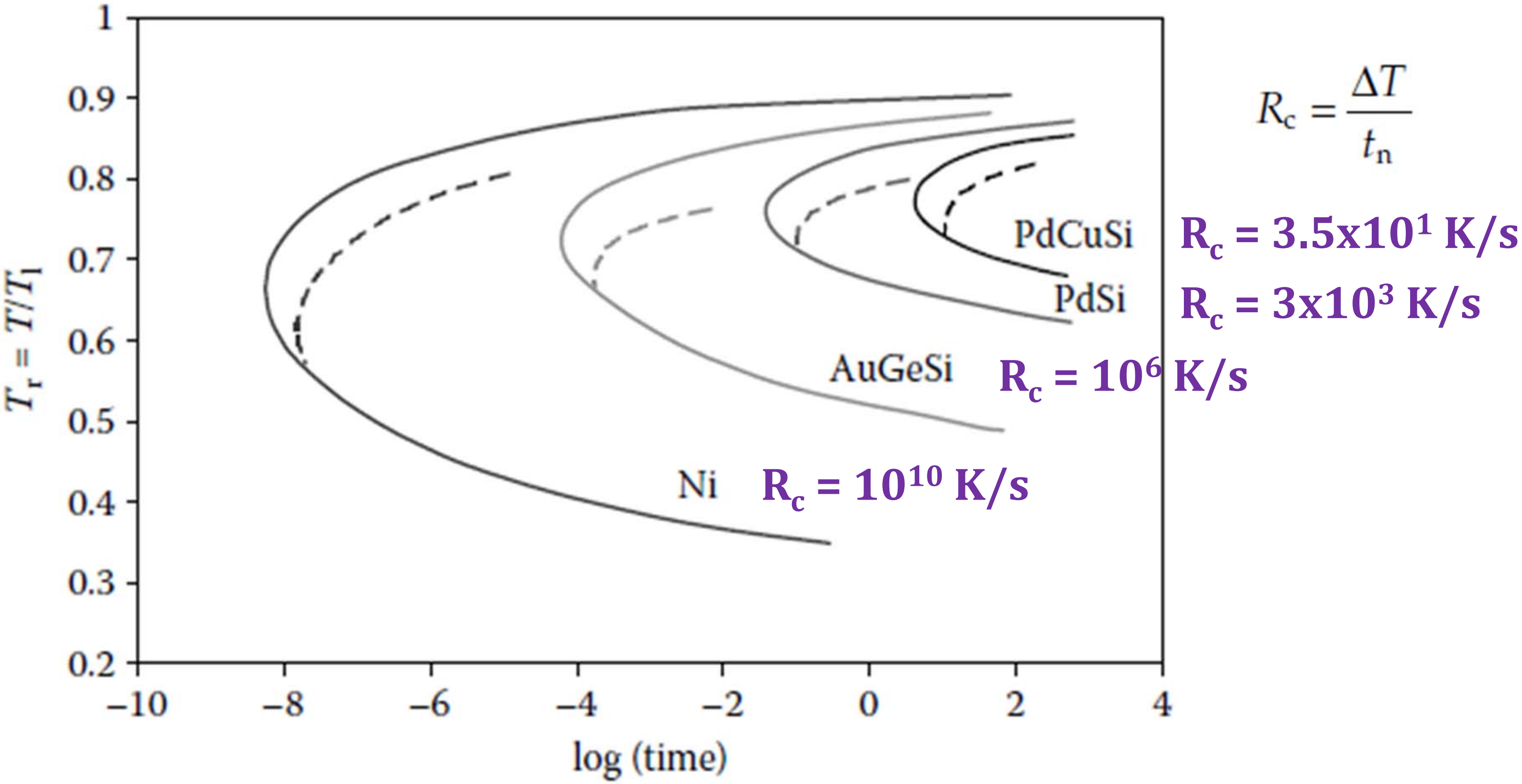

$$R_c = \frac{\Delta T}{t_n}$$

FIGURE 2.3
Time–temperature–transformation (T–T–T) curves (solid lines) and the corresponding continuous cooling transformation curves (dashed lines) for the formation of a small volume fraction for pure metal Ni, and $Au_{78}Ge_{14}Si_8$, $Pd_{82}Si_{18}$, and $Pd_{78}Cu_6Si_{16}$ alloys.

T_{rg}	Ni	$Au_{78}Ge_{14}Si_8$	$Pd_{82}Si_{18}$	$Pd_{78}Cu_6Si_{16}$
		1/4	1/2	2/3

* Time-Temperature-Transformation diagrams

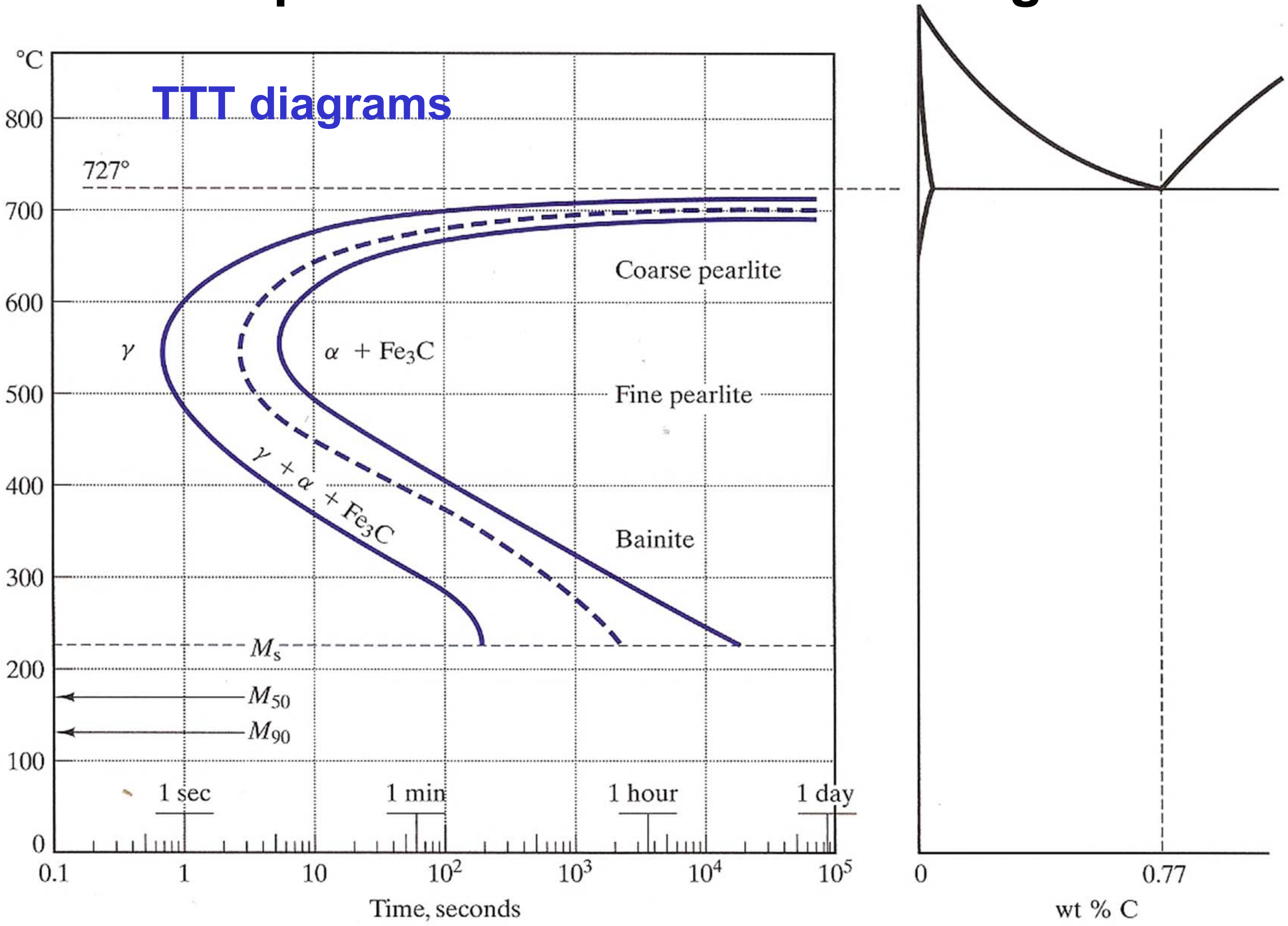

FIGURE 10.11 *A more complete TTT diagram for eutectoid steel than was given in Figure 10.7. The various stages of the time-independent (or diffusionless) martensitic transformation are shown as horizontal lines.* M_s *represents the start,* M_{50} *represents 50% transformation, and* M_{90} *represents 90% transformation. One hundred percent transformation to martensite is not complete until a final temperature (*M_f*) of −46°C.*

* Continuous Cooling Transformation diagrams

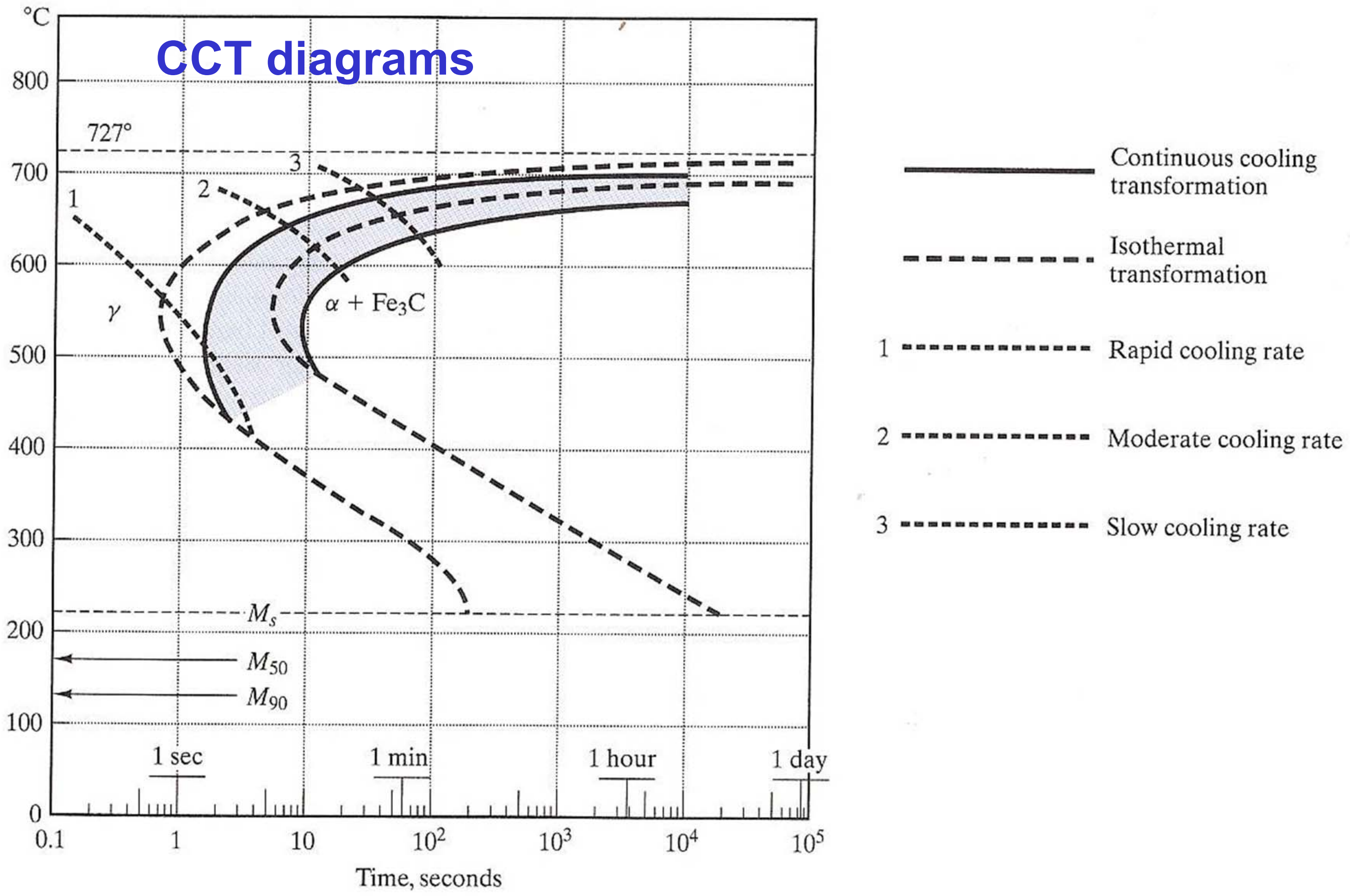

CCT diagrams

FIGURE 10.14 *A continuous cooling transformation (CCT) diagram is shown superimposed on the isothermal transformation diagram of Figure 10.11. The general effect of continuous cooling is to shift the transformation curves downward and toward the right.* (*After* Atlas of Isothermal Transformation and Cooling Transformation Diagrams, *American Society for Metals, Metals Park, OH, 1977.*)

2.6 Methods to Synthesize Metallic Glasses

2.6.1 Vapor-state Processes: expensive & slow, electronic & magnetic applications

Thermal Evaporation/ Sputtering/ Vapor Chemical Deposition

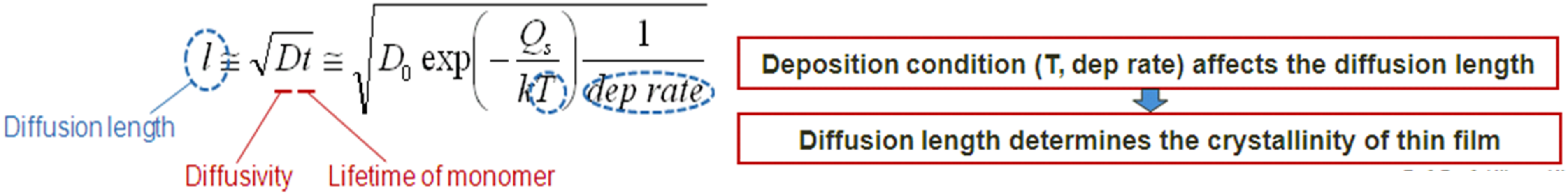

$$l \cong \sqrt{Dt} \cong \sqrt{D_0 \exp\left(-\frac{Q_s}{kT}\right)\frac{1}{dep\ rate}}$$

Deposition condition (T, dep rate) affects the diffusion length

Diffusion length determines the crystallinity of thin film

2.6.2 Liquid-state Processes : Rapid Solidification Process (RSP) $10^{5\text{-}6}$ K/s

most ideal way to obtain metallic glasses, especially the bulk foam

Splat Quenching/ Melt-spinning/ Electro Deposition/ Gas Atomization

2.6.3 Solid-state Processes_Solid state diffusional amorphization

Mechanical Alloying & Milling/Hydrogen-induced Amorphization/ Multilayer Amorphization/ Pressure-induced Amorphization/ Amorphization by Irradiation/ Severe Plastic Deformation_Intense deformation at low temperatures **/Accumulative Roll Bonding (ARB process)**

2.6 Methods to Synthesize Metallic Glasses

2.6.1 Vapor-state Processes: expensive & slow, electronic & magnetic applications

A. Thermal Evaporation

Surface coating

- Thermal evaporation is a common method for thin film deposition.
- The source material is **evaporated** from a source by heating in a **vacuum**.
- The evaporated material is then **condensed** on the substrate.

Vacuum : evaporated particles can travel directly to the substrate

Mean free path :
~ chamber dimensions

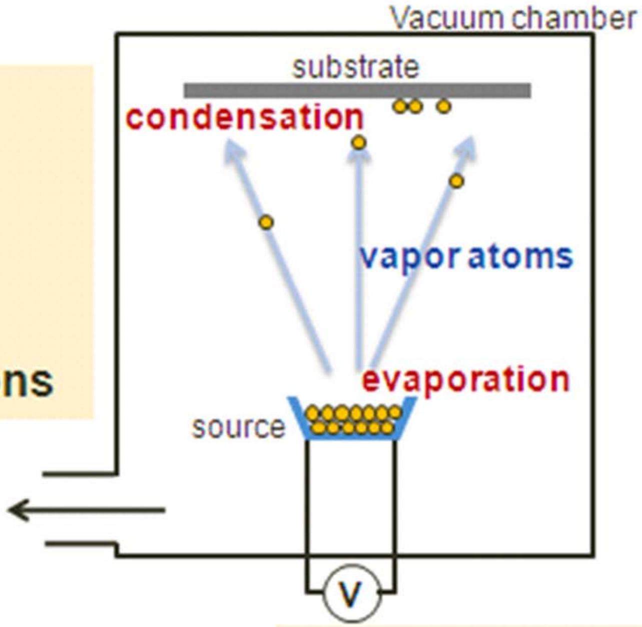

Heating : resistance heating (Joule effect)

First Amorphous Metals: evaporation method

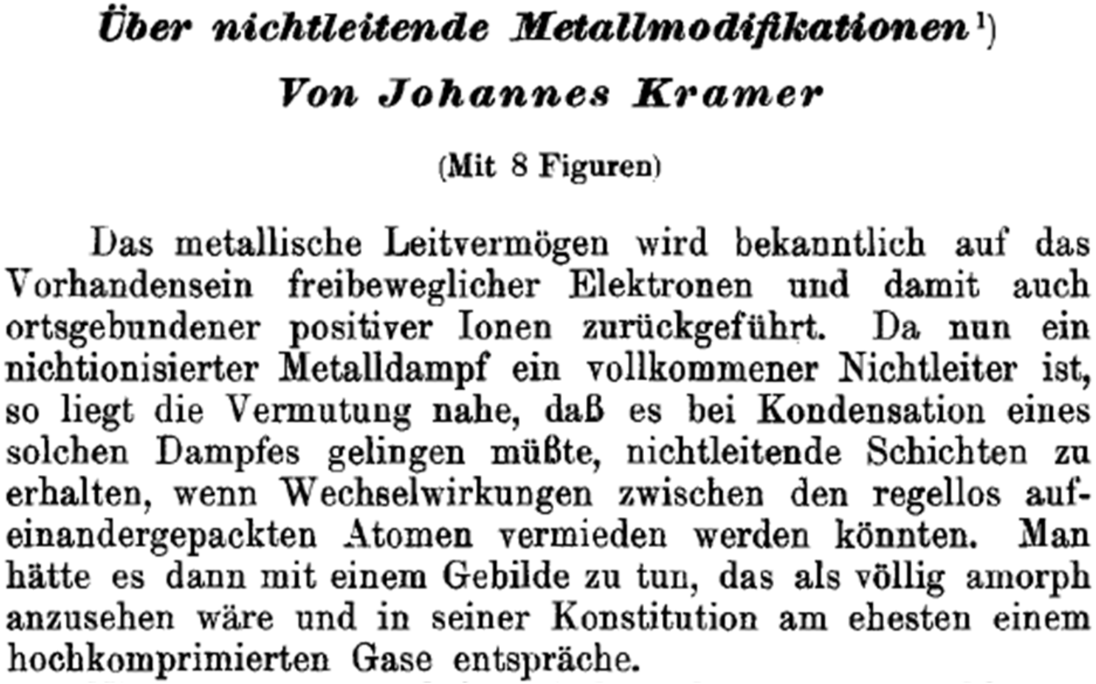

Über nichtleitende Metallmodifikationen 1)

Von Johannes Kramer

(Mit 8 Figuren)

Das metallische Leitvermögen wird bekanntlich auf das Vorhandensein freibeweglicher Elektronen und damit auch ortsgebundener positiver Ionen zurückgeführt. Da nun ein nichtionisierter Metalldampf ein vollkommener Nichtleiter ist, so liegt die Vermutung nahe, daß es bei Kondensation eines solchen Dampfes gelingen müßte, nichtleitende Schichten zu erhalten, wenn Wechselwirkungen zwischen den regellos aufeinandergepackten Atomen vermieden werden könnten. Man hätte es dann mit einem Gebilde zu tun, das als völlig amorph anzusehen wäre und in seiner Konstitution am ehesten einem hochkomprimierten Gase entspräche.

J. Kramer
Nonconducting modifications of metals.
Ann. Physik (Berlin, Germany) 19, 37 (1934)

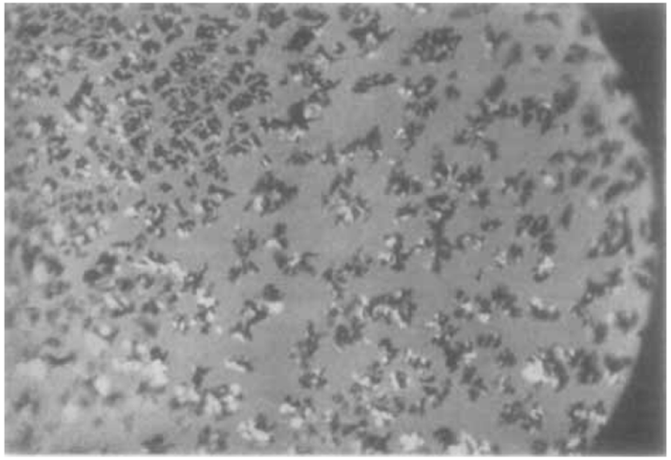

Sb metal → Bi, Ga, and Sn-Bi alloys

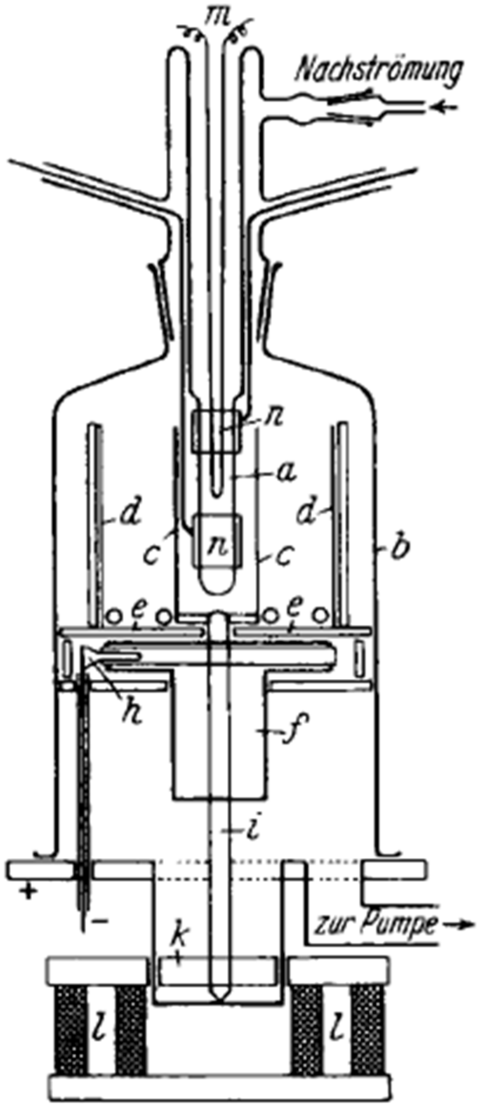

Fig. 1.
Zerstäubungsapparatur

What is Sputtering?

Surface coating

B. **Sputtering** is a common method for **thin film deposition.**

- Process whereby atoms are ejected from a solid target material due to bombardment of the target by energetic particles.
- Ejected atoms are deposited on the substrate, form thin film.

Ref. http://en.wikipedia.org/wiki/Sputtering

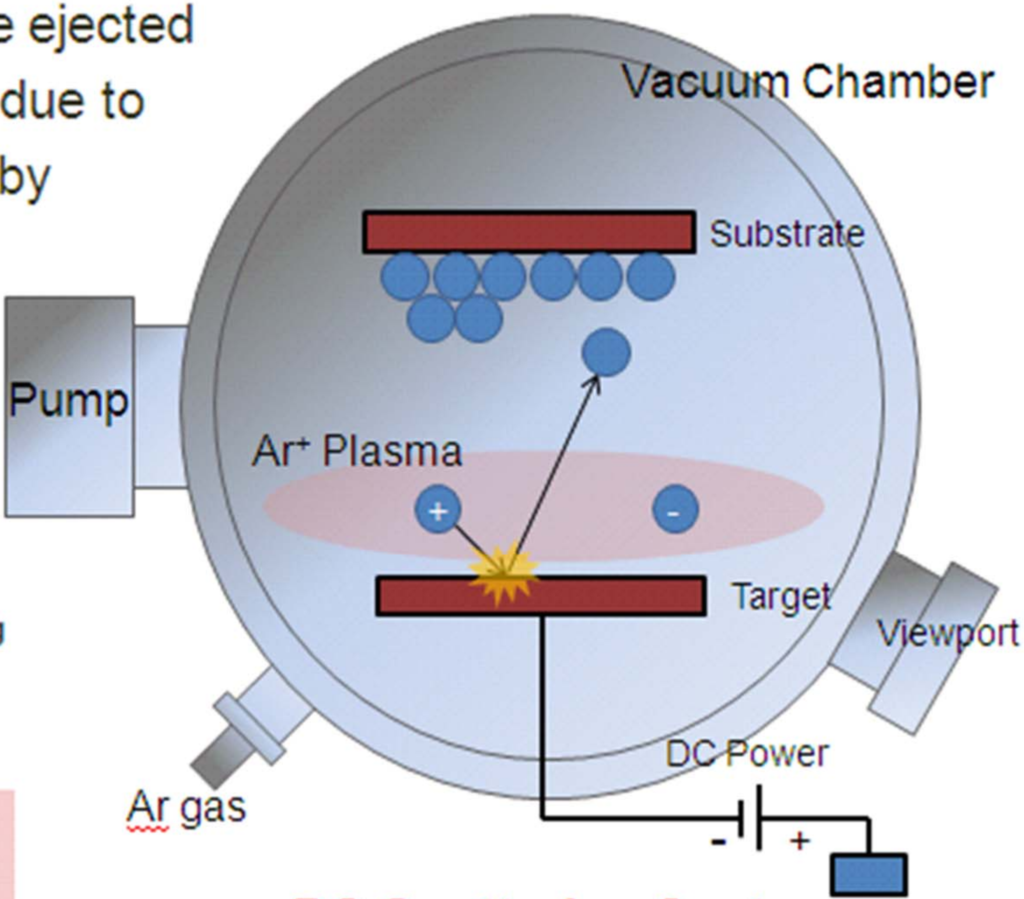

DC Sputtering System

Vacuum : evaporated particles can travel directly to the substrate

2.6.1 Vapor-state Processes

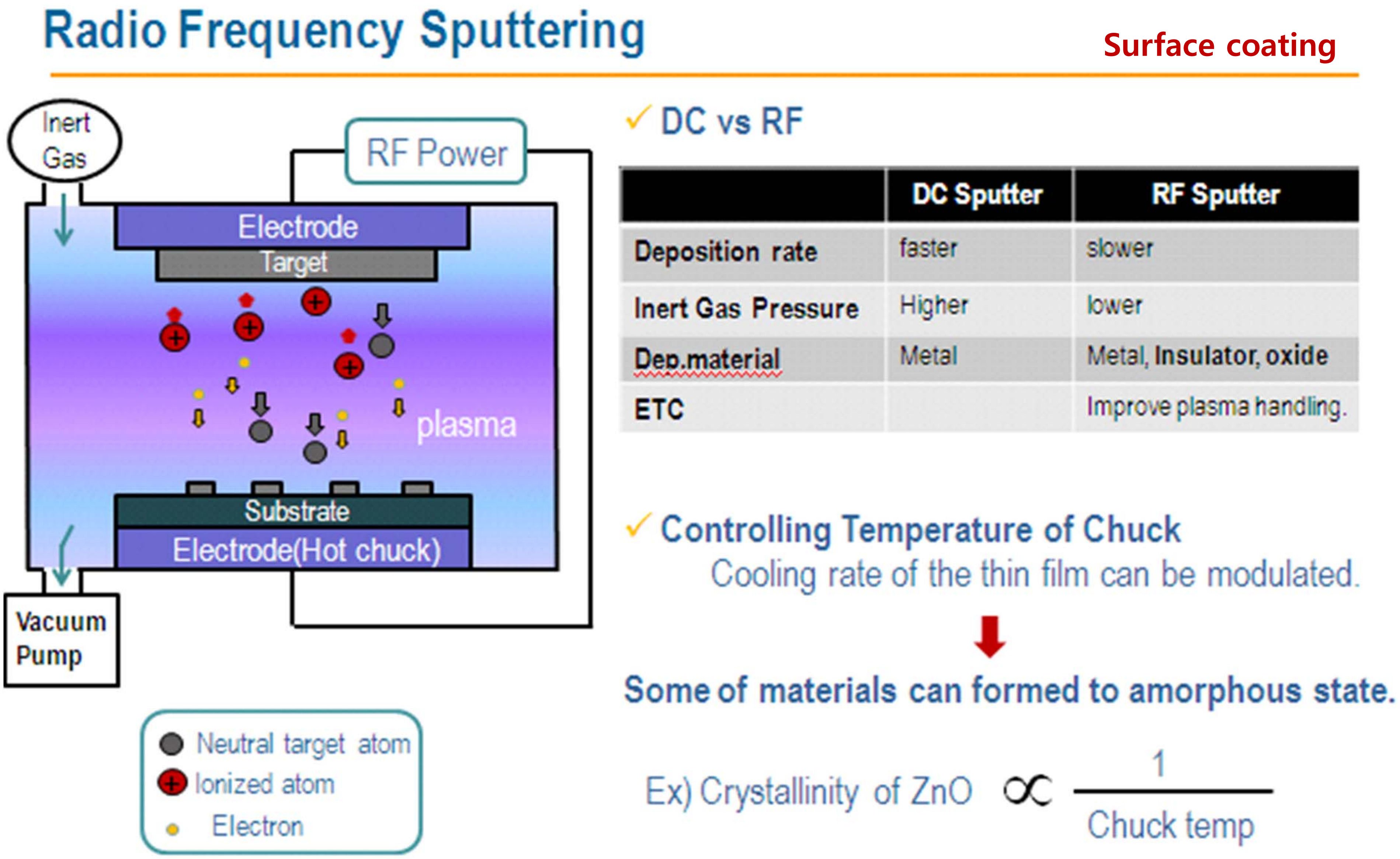

Radio Frequency Sputtering

Surface coating

✓ DC vs RF

	DC Sputter	RF Sputter
Deposition rate	faster	slower
Inert Gas Pressure	Higher	lower
Dep.material	Metal	Metal, **Insulator, oxide**
ETC		Improve plasma handling.

✓ Controlling Temperature of Chuck

Cooling rate of the thin film can be modulated.

⬇

Some of materials can formed to amorphous state.

Ex) Crystallinity of ZnO $\propto \frac{1}{\text{Chuck temp}}$

2.6.1 Vapor-state Processes

C. Principles of CVD

Surface coating

- Substrate is exposed to one or more volatile precursors.
- Precursors will react and/or decompose on substrate to produce the desire deposit.

$3\ SiH_4 + 4\ NH_3 \rightarrow Si_3N_4 + 12\ H_2$

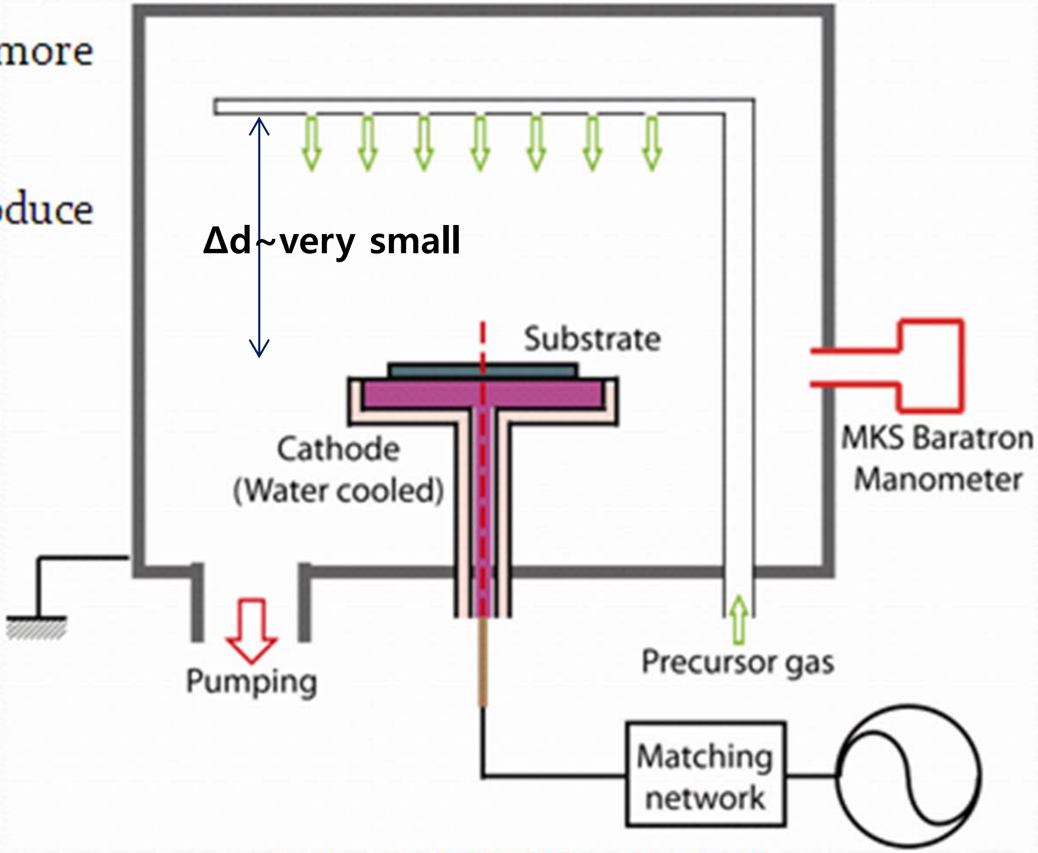

A schematic of r.f.PACVD coating chamber.

- Base and deposition pressure: 10^{-6} and 10^{-2} Torr
- Bias voltage: -400 to -800V
- Deposition temp. : RT

Surface coating

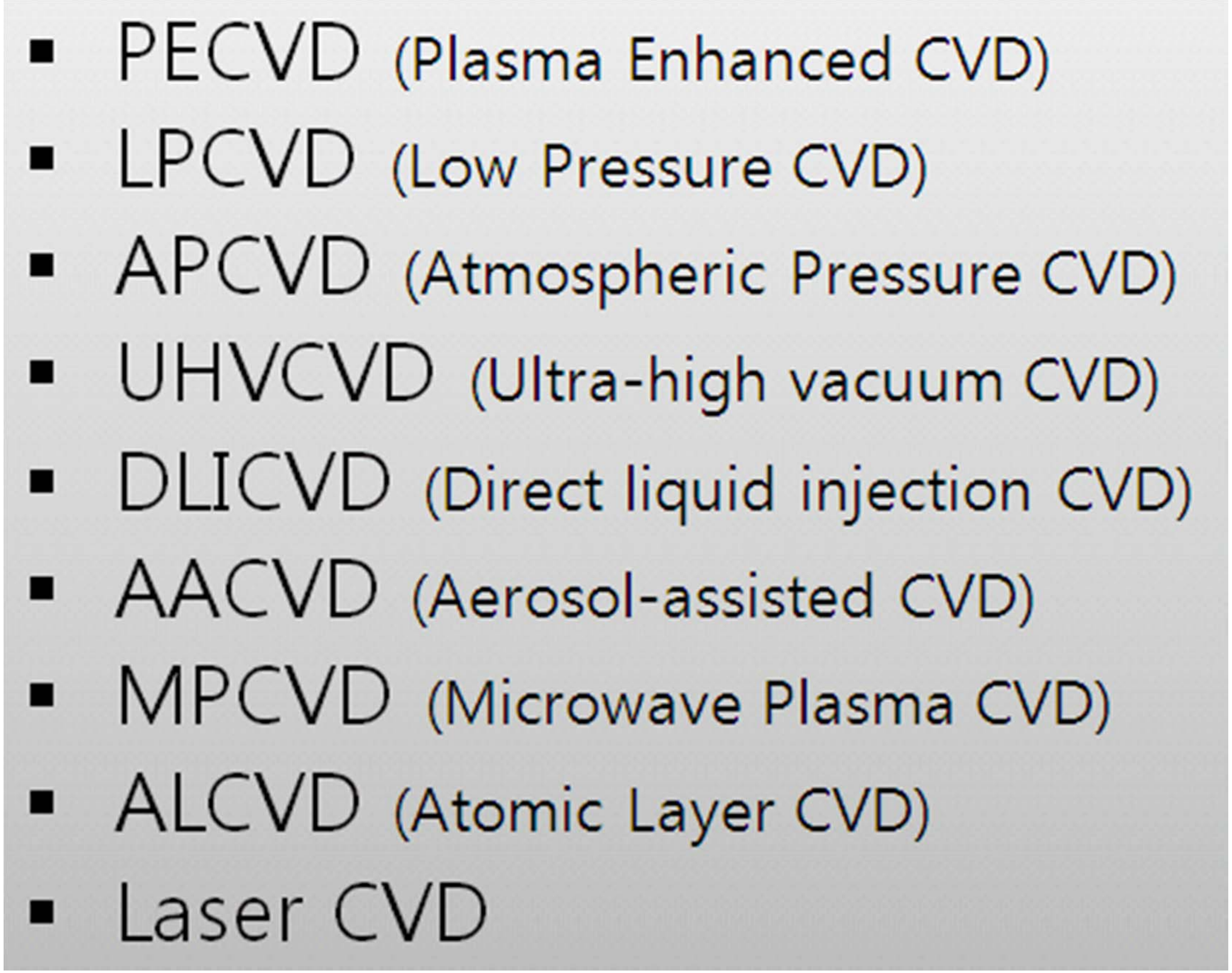

- PECVD (Plasma Enhanced CVD)
- LPCVD (Low Pressure CVD)
- APCVD (Atmospheric Pressure CVD)
- UHVCVD (Ultra-high vacuum CVD)
- DLICVD (Direct liquid injection CVD)
- AACVD (Aerosol-assisted CVD)
- MPCVD (Microwave Plasma CVD)
- ALCVD (Atomic Layer CVD)
- Laser CVD

2.6.1 Vapor-state Processes

Formation of Amorphous Thin Film

Surface coating

Calculation of Diffusion Length

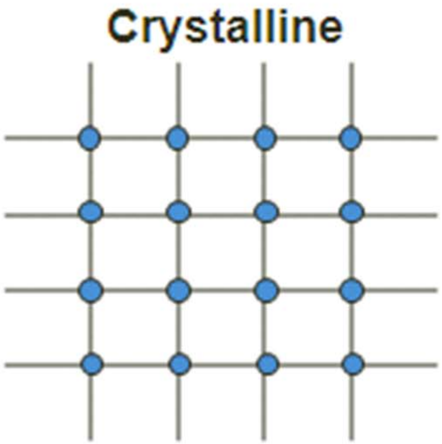
Crystalline

Enough time for locating at right position

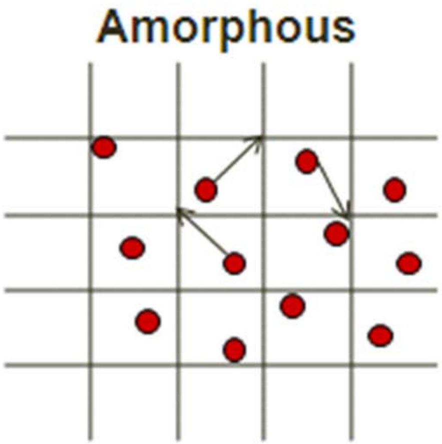
Amorphous

Not enough time for locating at right position

$$l \cong \sqrt{Dt} \cong \sqrt{D_0 \exp\left(-\frac{Q_s}{kT}\right)\frac{1}{dep\ rate}}$$

Diffusion length

Diffusivity

Lifetime of monomer

Deposition condition (T, dep rate) affects the diffusion length

↓

Diffusion length determines the crystallinity of thin film

Ref. Prof. Kibum Kim's lecture

2.6.1 Vapor-state Processes

Formation of amorphous

Surface coating

- Amorphous forming ability is depends on diffusion length
- Diffusion length $\propto \sqrt{Dt}$
- Deposit process is commonly forming amorphous because of low temperature and rapid growth rate
- CVD process is progressed at little high temperature, so metal do not forming amorphous generally

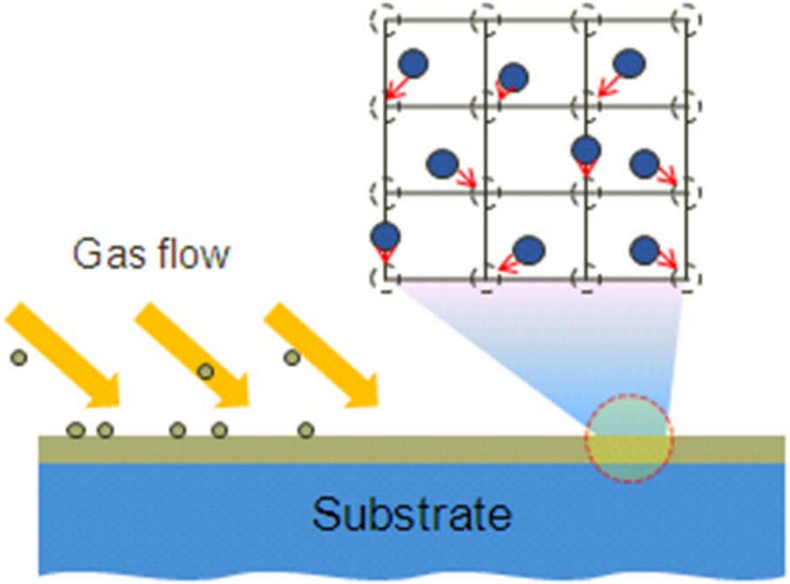

Low temperature, short time

↓

Amorphous

Chemical vapor deposition

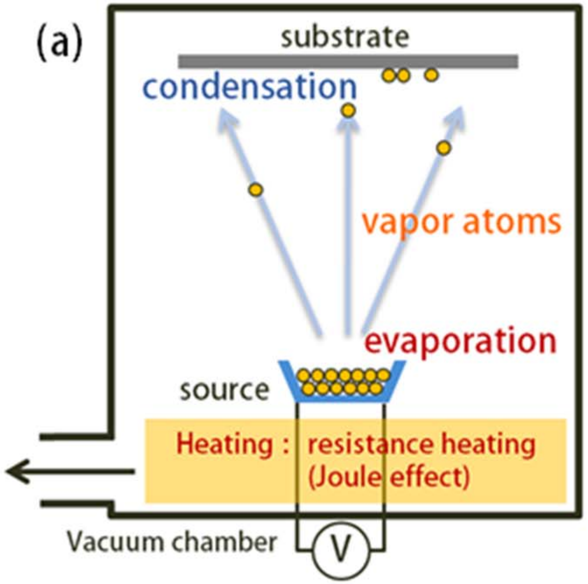

Sputtering

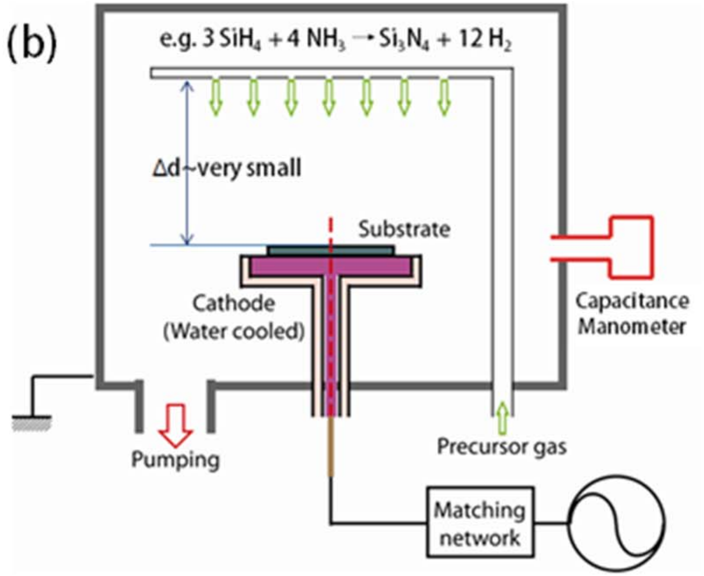

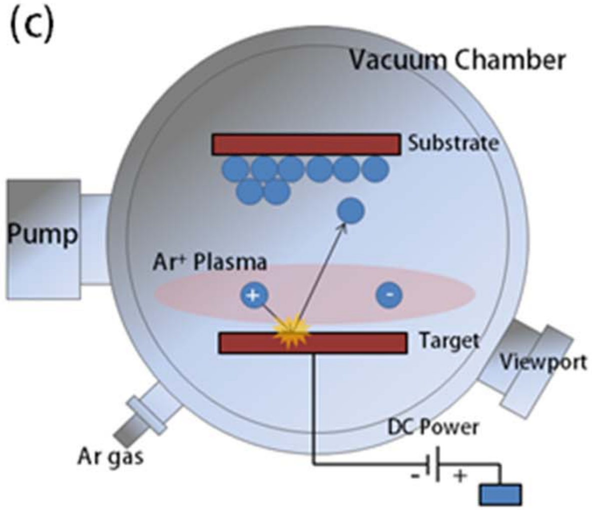

Electron beam evaporation

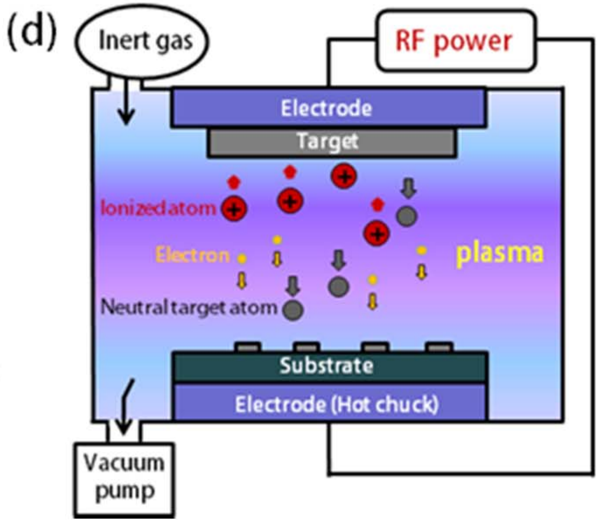

Ion implantation

2.6.2 Liquid-state Processes : Rapid Solidification Process (RSP) 10^{5-6} K/s

most ideal way to obtain metallic glasses, especially the bulk variety

A.

Procedure of Splat Quenching

Thin plate

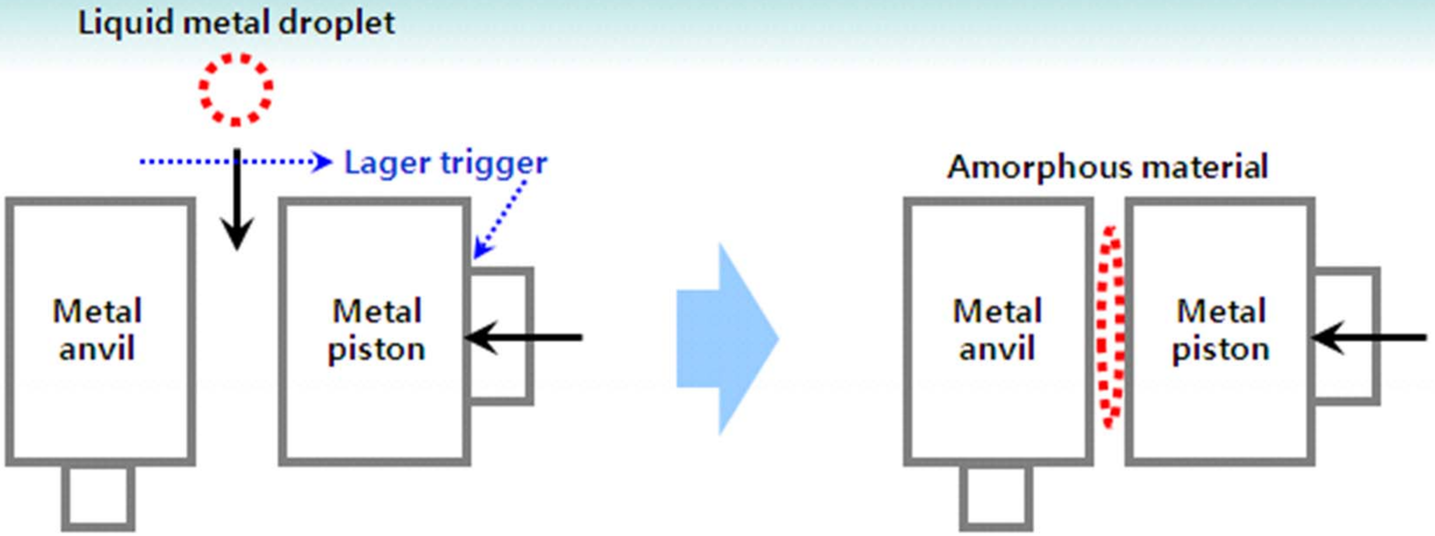

Liquid metal droplet drops

↓

Laser reheats this liquid metal
& signals to sensor for moving piston

→

liquid metal is quenched
& transformed to
amorphous material

Glass formation : stabilizing the liquid phase

- First metallic glass ($Au_{80}Si_{20}$) produced by splat quenching at Caltech by Pol Duwez in 1960.

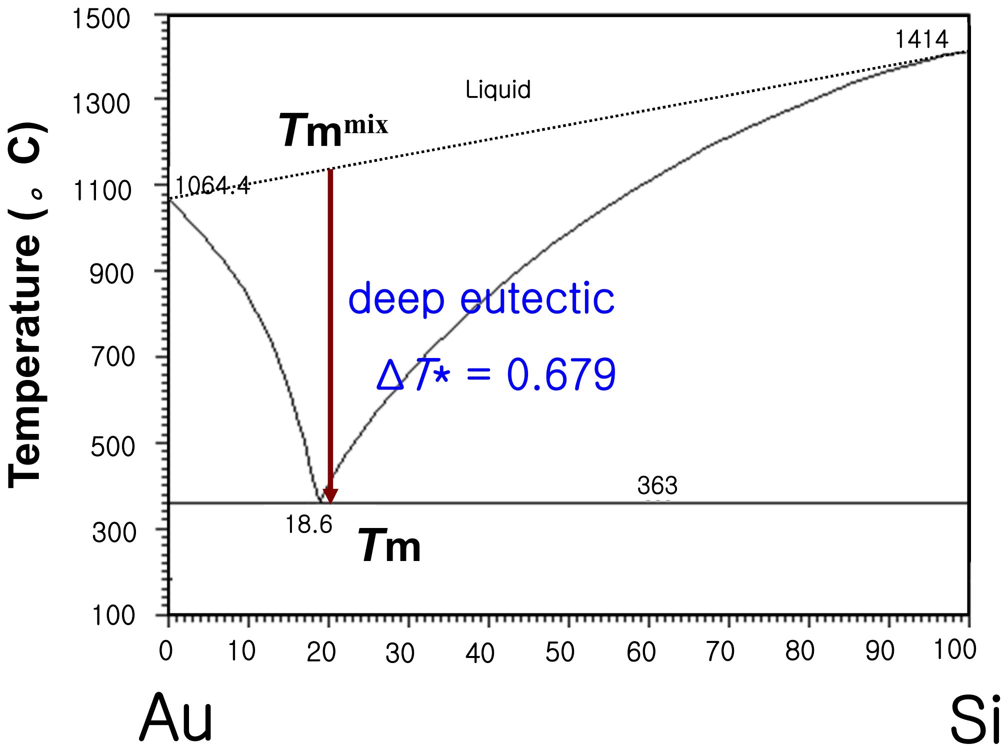

W. Klement, R.H. Willens, P. Duwez, Nature 1960; 187: 869.

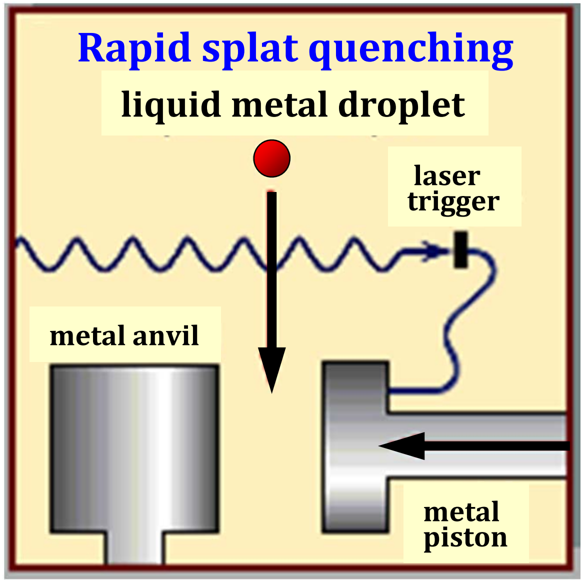

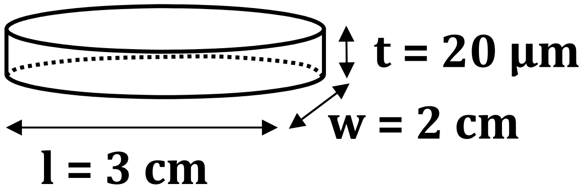

2.6.2 Liquid-state Processes

B. ▣ Brief Definition of Melt Spinning

Thin film

A jet of liquid metal is ejected from a nozzle and impinges on the surface of a rotating substrate, where a thin layer is formed from a melt puddle and rapidly solidifies as a continuous ribbon.

▣ Several Types of Melt Spinning Method

<table>
<tr><th colspan="2">Free Jet Melt spinning (FJMS)</th><th rowspan="2">Planar Flow Melt spinning (PFMS)</th><th rowspan="2">Example (PFMS, Siemens)</th></tr>
<tr><th>Outside of Wheel</th><th>Inside of Wheel</th></tr>
<tr>
<td>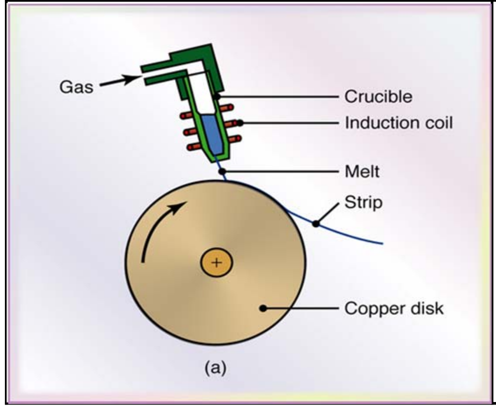
</td>
<td>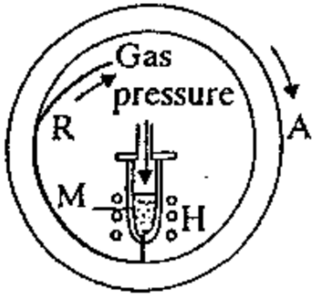
</td>
<td>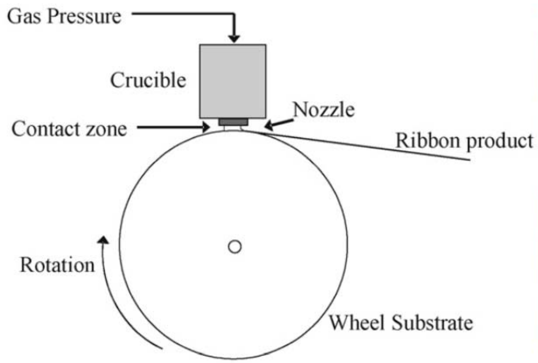
</td>
<td>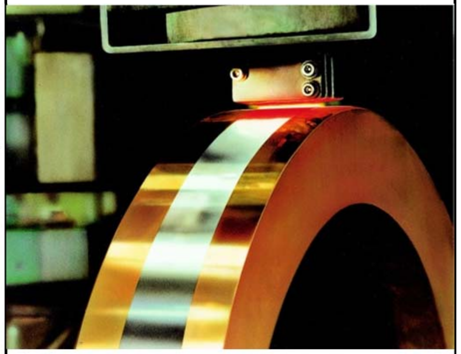</td>
</tr>
</table>

- **Melt-spinning method**

Thin film

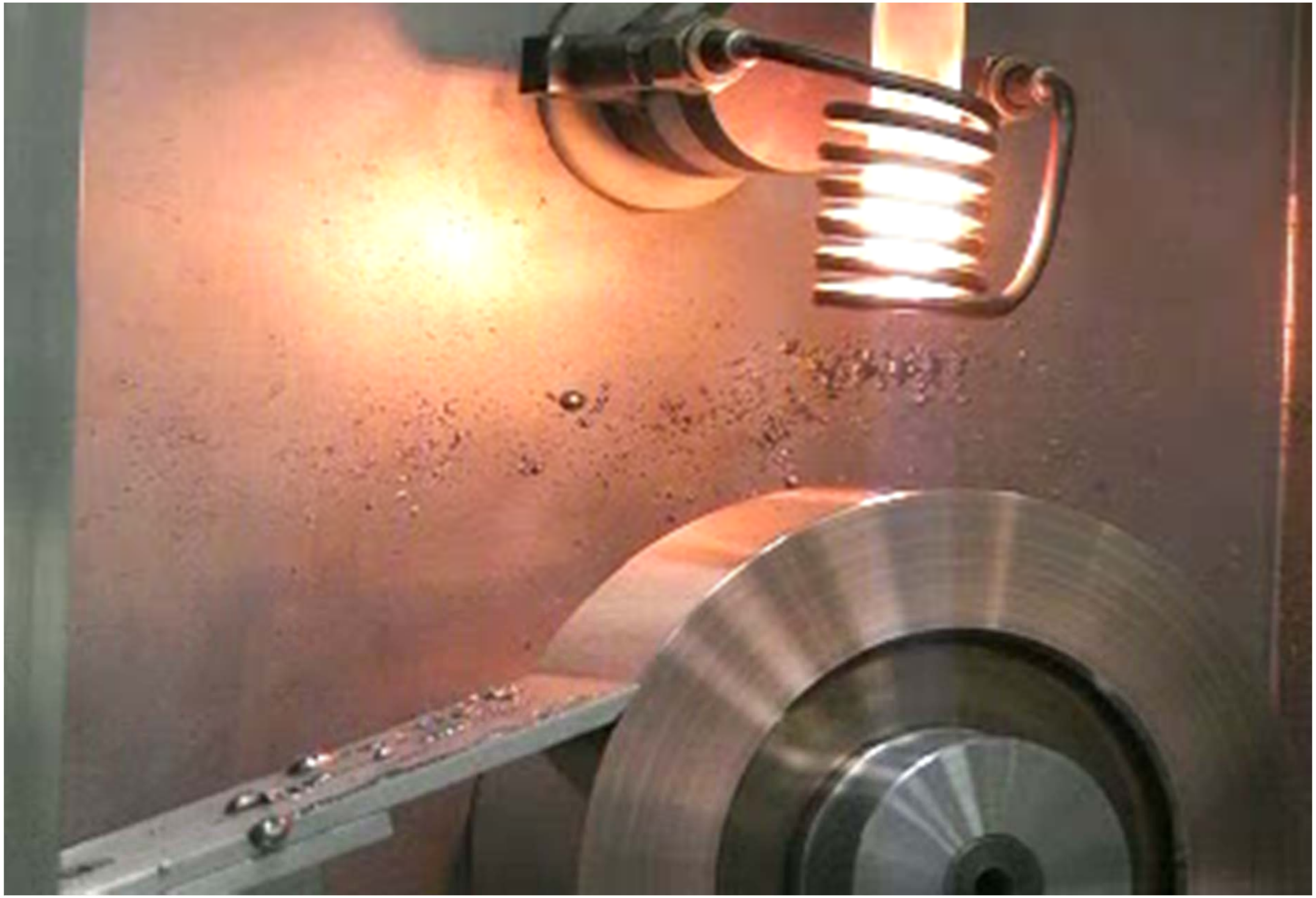

C. Basic Concept of Electrolytic Deposition

Electroplating is a plating process in which metal ions in a solution are moved by an electric field to coat an electrode. The process uses electrical current to reduce cations of a desired material from a solution and coat a conductive object with a thin layer of the material, such as a metal. Electroplating is primarily used for depositing a layer of material to bestow a desired property (e.g., abrasion and wear resistance, corrosion protection, lubricity, aesthetic qualities, etc.) to a surface that otherwise lacks that property. Another application uses electroplating to build up thickness on undersized parts. However, the limited size of the product formed in one experiment puts a limitation on the usefulness of this technique to produce large quantities of metallic glasses

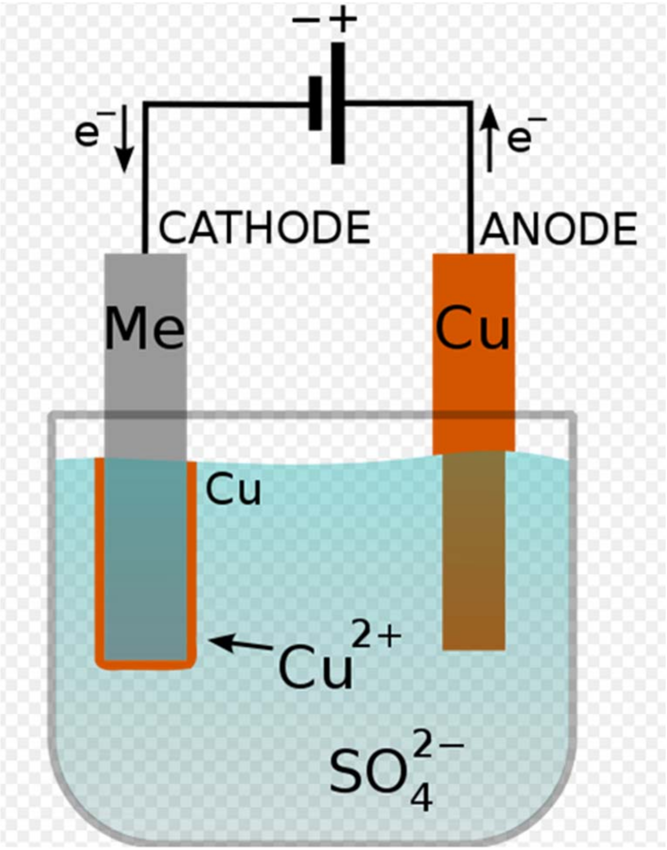

2.6.2 Liquid-state Processes

C. Electro-deposition Methods

It was in 1950, for the first time, that Brenner et al. [38] reported the formation of an amorphous phase in electro-deposited Ni–P alloys containing >10 at.% P. The amorphous nature of the deposit was inferred from the presence of only one broad diffuse peak in the XRD pattern. These alloys have a very high hardness and consequently these are used as wear- and corrosion-resistant coatings [39].

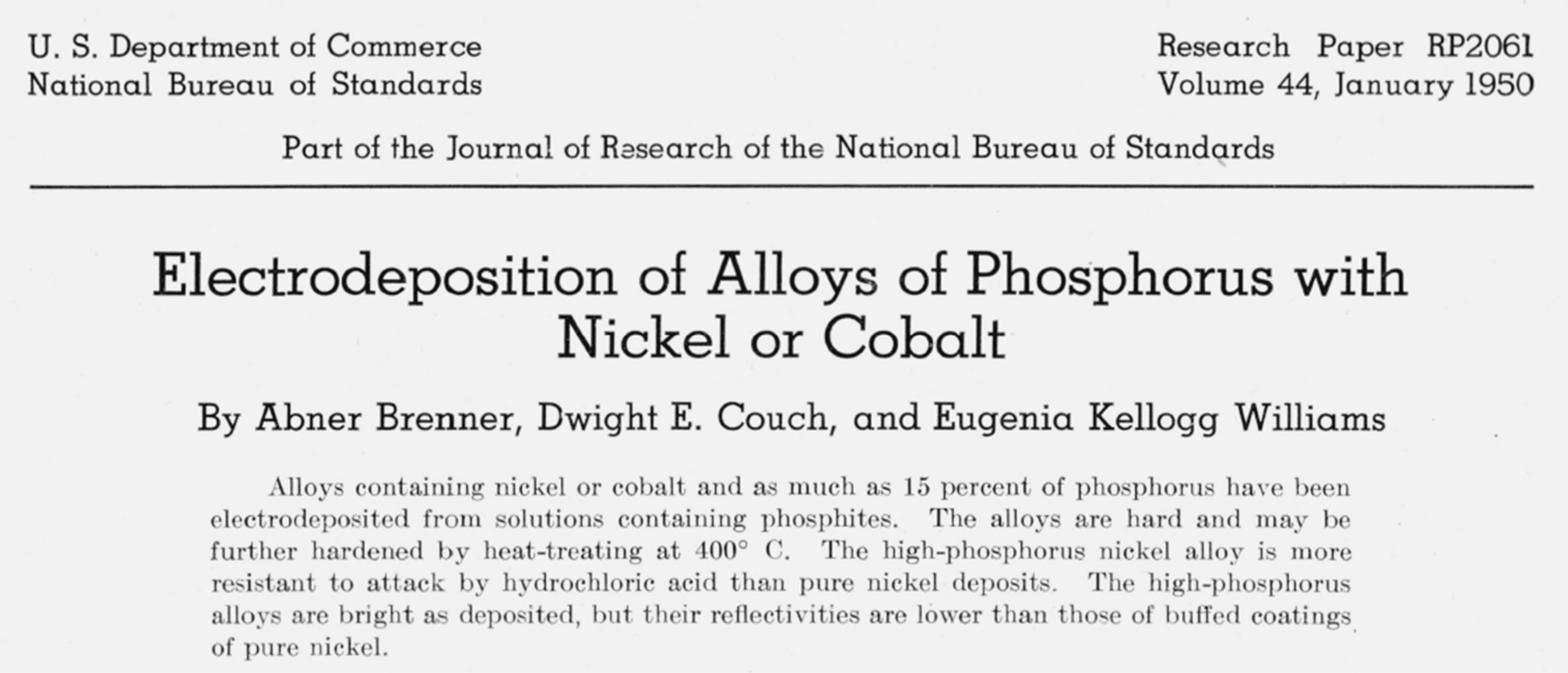

U. S. Department of Commerce
National Bureau of Standards

Research Paper RP2061
Volume 44, January 1950

Part of the Journal of Research of the National Bureau of Standards

---

Electrodeposition of Alloys of Phosphorus with Nickel or Cobalt

By Abner Brenner, Dwight E. Couch, and Eugenia Kellogg Williams

Alloys containing nickel or cobalt and as much as 15 percent of phosphorus have been electrodeposited from solutions containing phosphites. The alloys are hard and may be further hardened by heat-treating at 400° C. The high-phosphorus nickel alloy is more resistant to attack by hydrochloric acid than pure nickel deposits. The high-phosphorus alloys are bright as deposited, but their reflectivities are lower than those of buffed coatings of pure nickel.

Powder

D. Gas Atomization

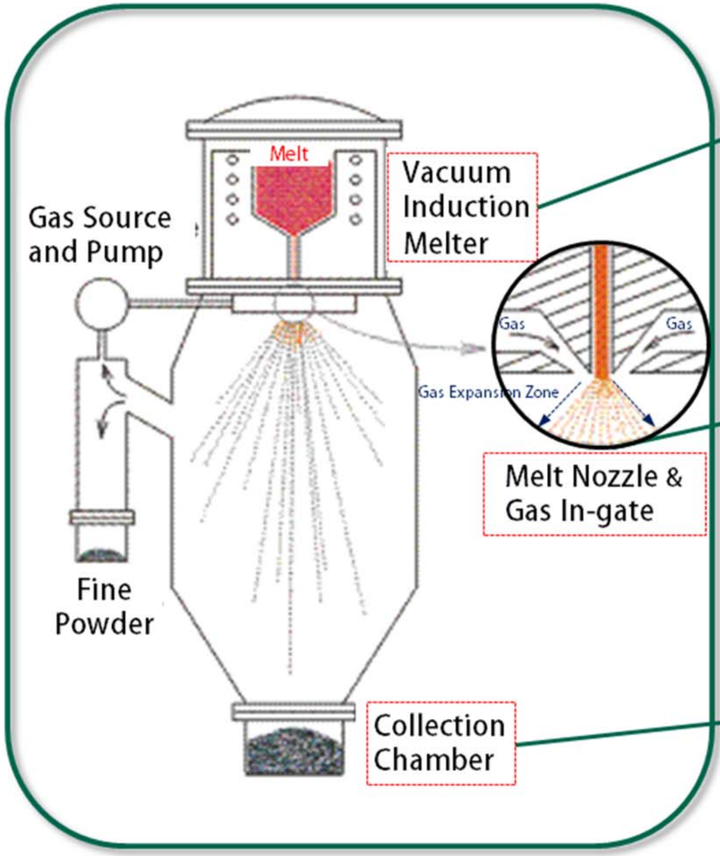

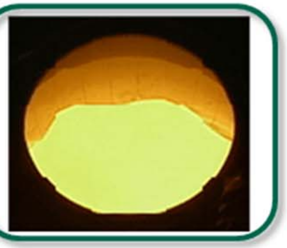

■ Melting Furnace Facility

Melting of Metal or Ceramics

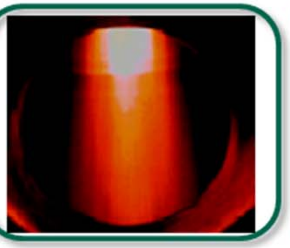

■ Melt Nozzle and Gas In-gate

A rapidly expanding gas breaks up the liquid stream → thin sheet → ligament → ellipsoid → sphere.

■ Collection Chamber

The collection chamber is designed to maximize the yield, minimize contamination, and ease of cleaning.

2.6.3 Solid-state Processes

A. Mechanical alloying/milling

: MA/ MM performed in a high-energy ball mill such as a shaker mill or planetary mill will also induce severe plastic deformation in metals. During milling, particles are fractured and cold welded together, resulting in large deformation.

Schematic Diagram of Mechanical Alloying Process

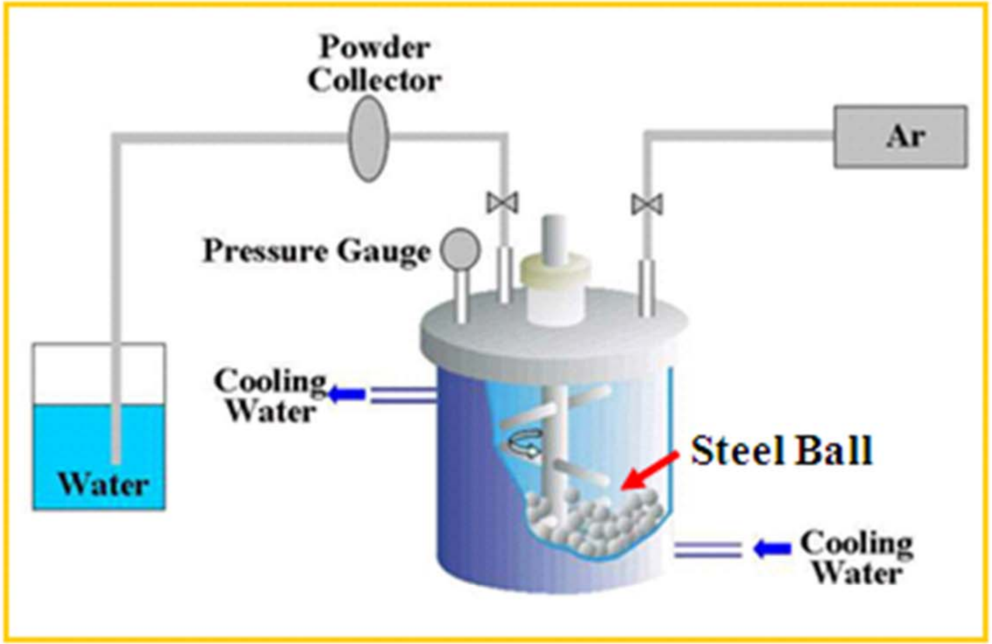

Increased Solid Solubility Limit
Easy to Control the Microstructure
Easy to Fabricate Non-Equilibrium and Nano Phase
Homogeneous Distribution of Fine Strengthener
Excellent Mechanical Properties

Attritor

2.6.3 Solid-state Processes

A. Mechanical alloying/milling

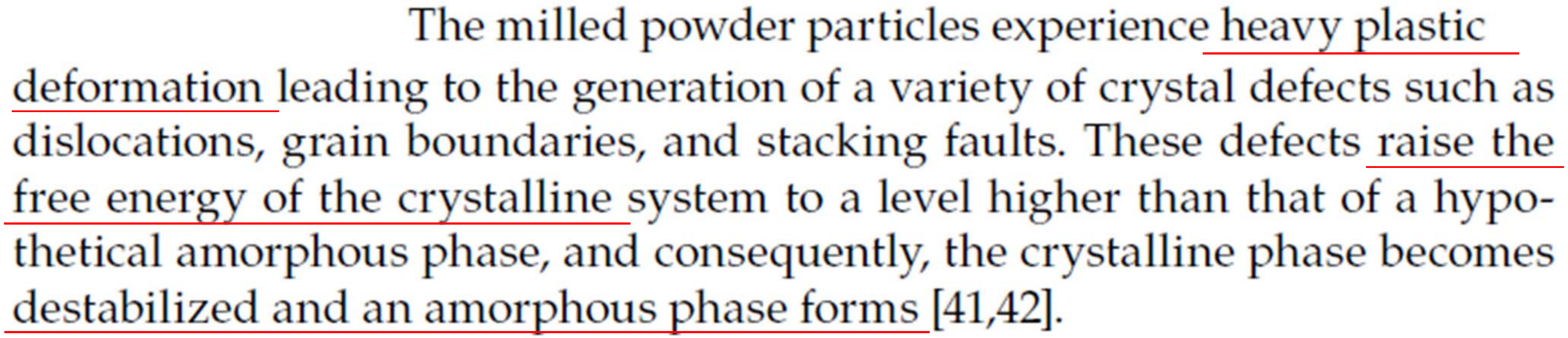

The milled powder particles experience heavy plastic deformation leading to the generation of a variety of crystal defects such as dislocations, grain boundaries, and stacking faults. These defects raise the free energy of the crystalline system to a level higher than that of a hypothetical amorphous phase, and consequently, the crystalline phase becomes destabilized and an amorphous phase forms [41,42].

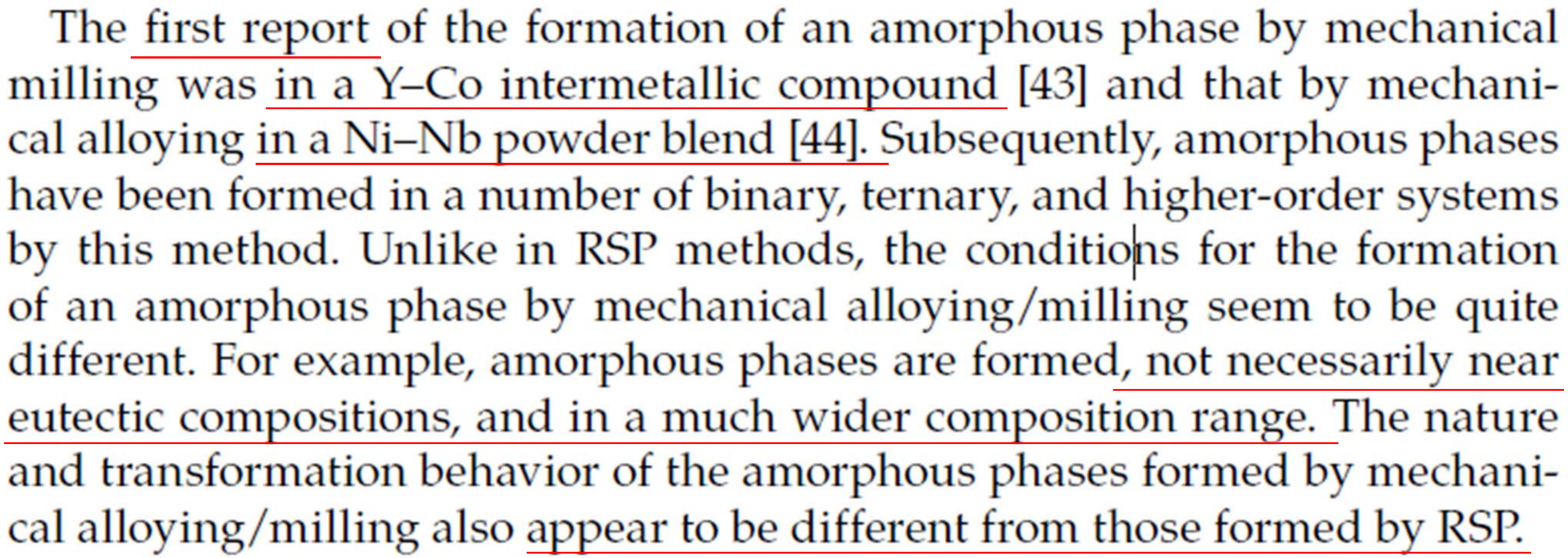

The first report of the formation of an amorphous phase by mechanical milling was in a Y–Co intermetallic compound [43] and that by mechanical alloying in a Ni–Nb powder blend [44]. Subsequently, amorphous phases have been formed in a number of binary, ternary, and higher-order systems by this method. Unlike in RSP methods, the conditions for the formation of an amorphous phase by mechanical alloying/milling seem to be quite different. For example, amorphous phases are formed, not necessarily near eutectic compositions, and in a much wider composition range. The nature and transformation behavior of the amorphous phases formed by mechanical alloying/milling also appear to be different from those formed by RSP.

2.6.3 Solid-state Processes

A. Mechanical alloying/milling

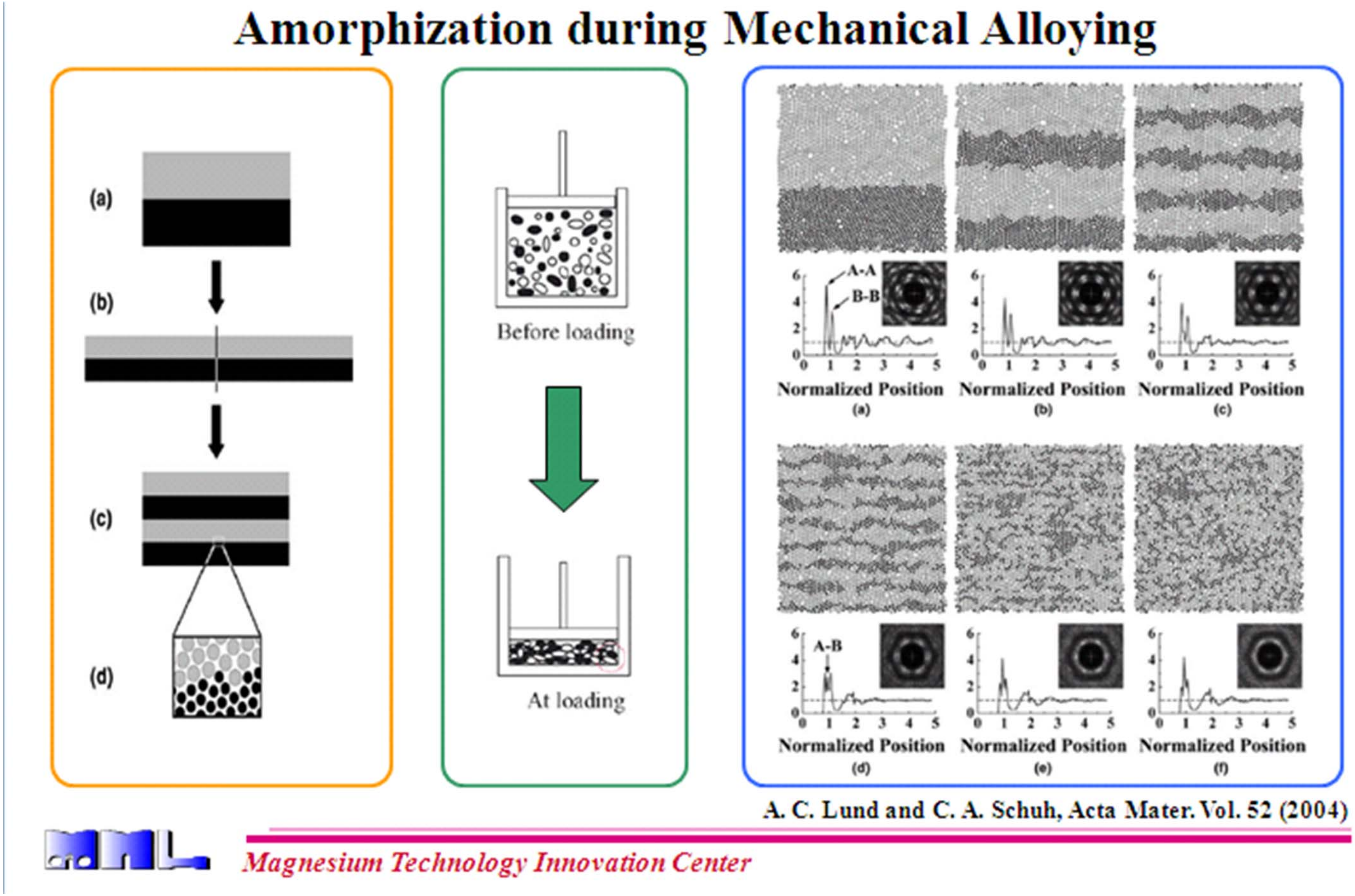

Amorphization during Mechanical Alloying

A. C. Lund and C. A. Schuh, Acta Mater. Vol. 52 (2004)

Magnesium Technology Innovation Center

Mechanical Alloying/ Milling

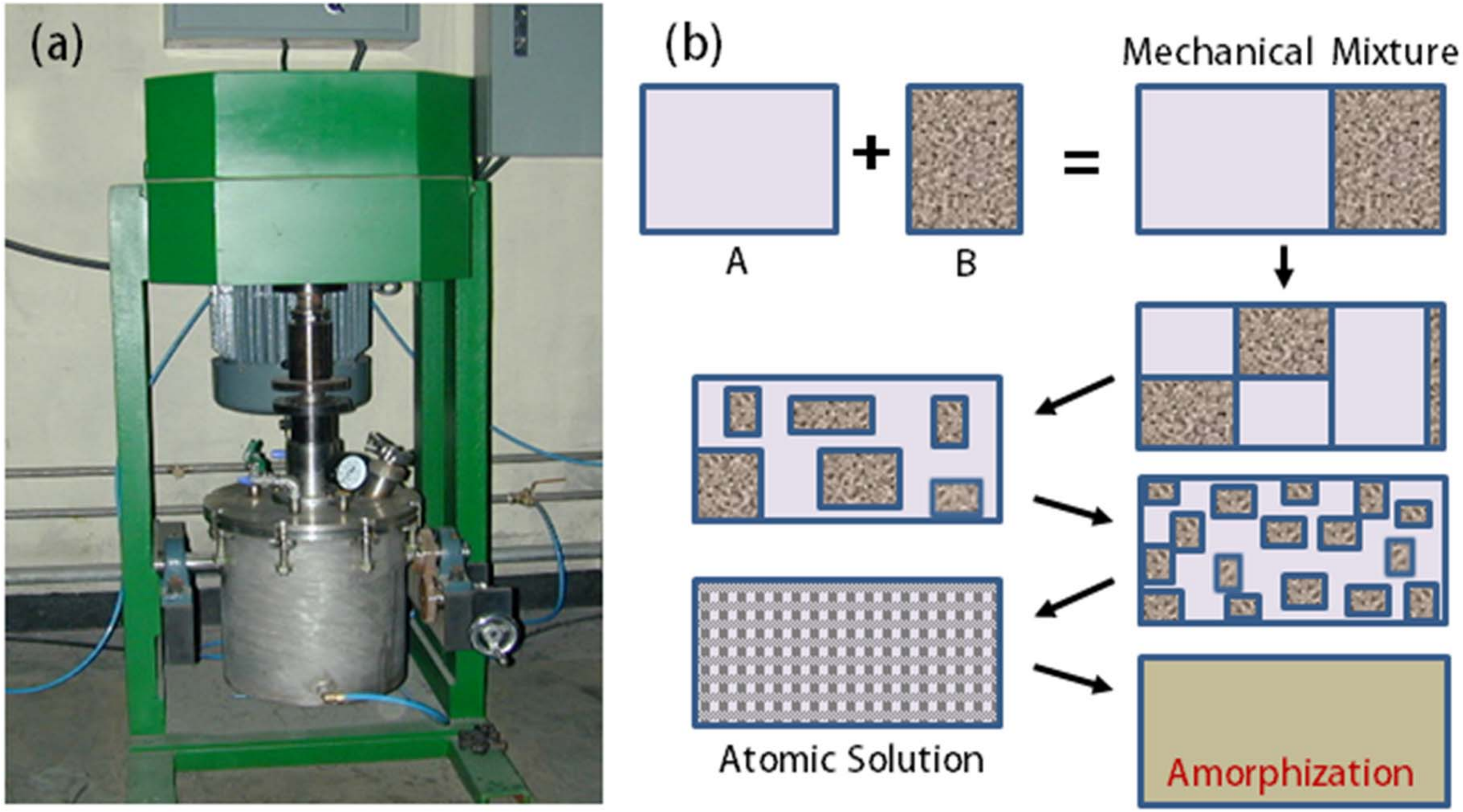

2.6.3 Solid-state Processes

B. Hydrogen-induced Amorphization

- Yeh et al. [45] reported the formation of an amorphous metal hydride $Zr_3RhH_{5.5}$ by a reaction of hydrogen with a metastable crystalline Zr_3Rh compound at sufficiently low temperatures (< about 200°C). A similar amorphous hydride phase was also reported to form when the amorphous Zr_3Rh alloy obtained in a glassy state was also reacted with hydrogen.
- Aoki [46] has reported that hydrogen-induced amorphization is possible in many binary metal compounds.

C. Multilayer Amorphization

- An amorphous phase was found to form when thin metal films (10–50 nm in thickness) of La and Au were allowed to interdiffuse at relatively low temperatures (50°C–100°C). Similar to the case of hydrogen-induced amorphization, here also the large asymmetry in the diffusion coefficients of the two elements was found to be responsible for the formation of the amorphous phase [47]. Since then, a large number of cases where multilayer amorphization occurs have been reported.

Ex) cold rolling of thin foils of Ni and Zr, and then annealing them at a low temperature.

Solid-State Diffusional Amorphization

✓ Alternate layers of crystalline metallic films (‘diffusion couples’) **interdiffuse** under isothermal conditions, with the eventual amorphization of the **entire** multilayer.

✓ **Couple: late transition metal with early transition metal**
ex. Au-La, Au-Zr, Au-Y, Cu-Zr, Cu-Er, Ni-Er, Ni-Ti, Ni-Hf, Fe-Zr,
Co-Zr, Ni-Zr

✓ Low temperature annealing **below the crystallization temperature**
(the nucleation or growth of crystalline phases cannot occur)

* Diffusion in multiple binary system

A diffusion couple made by welding together pure A and pure B

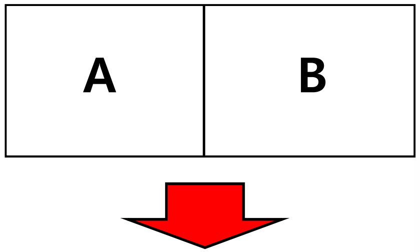

What would be the microstructure evolved after annealing at T_1 ?

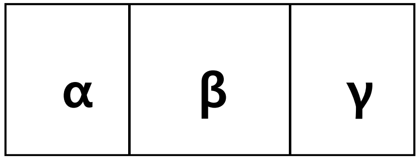

→ a layered structure containing α, β & γ.

Draw a phase distribution and composition profile in the plot of distance vs. X_B after annealing at T_1.

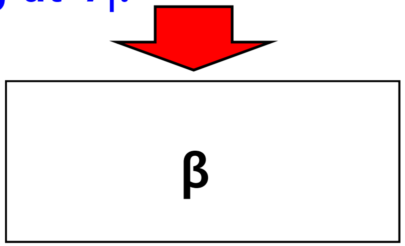

Draw a profile of activity of B atom, in the plot of distance vs. a_B after annealing at T_1.

A or B atom → easy to jump interface (local equil.)

→ $\mu_A^\alpha = \mu_A^\beta$, $\mu_A^\beta = \mu_A^\gamma$ at interface

$(a_A^\alpha = a_A^\beta,\ a_A^\beta = a_A^\gamma)$

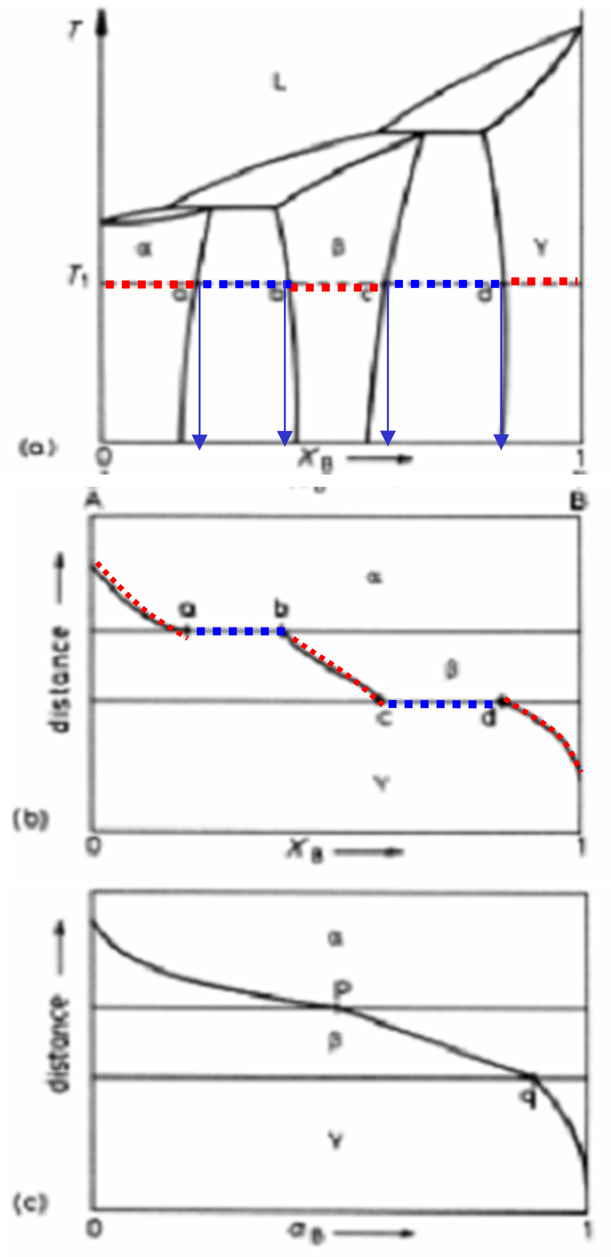

Solid-State Diffusional Amorphization

Schematic Diagram

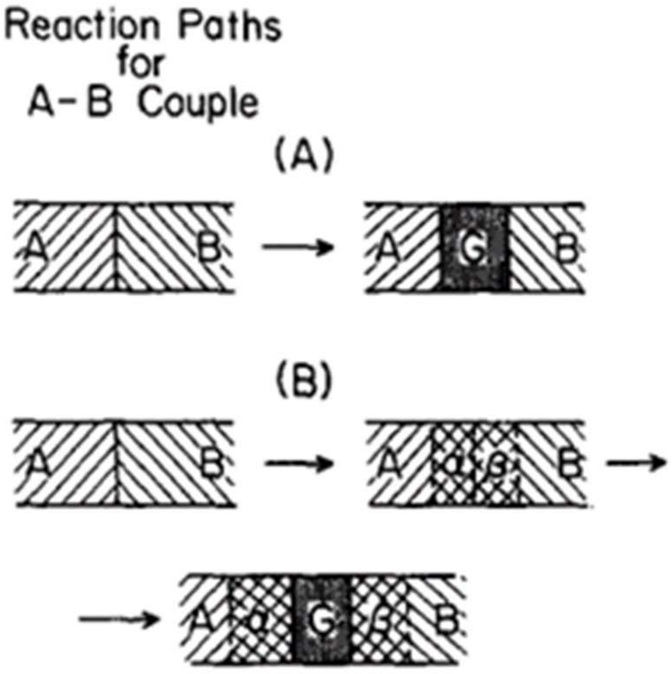

Example (Co-Zr)

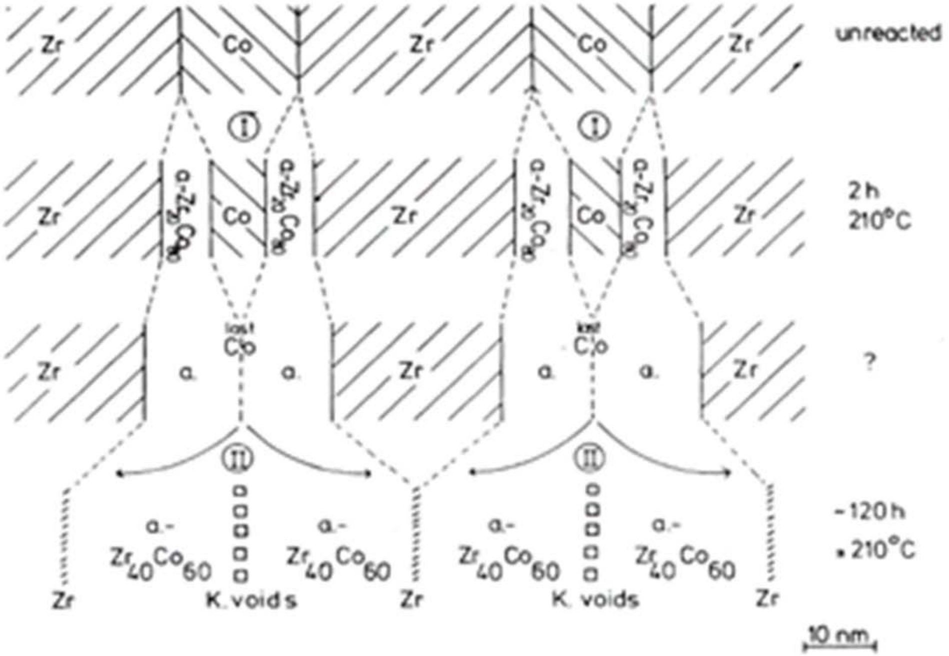

(A) Direct nucleation of the amorphous phase

(B) Substantial mutual dissolution of the parent metals leading to unstable solid solutions

Two Main Attributes

- **A strong thermodynamic driving force**

i.e. a large negative heat of mixing

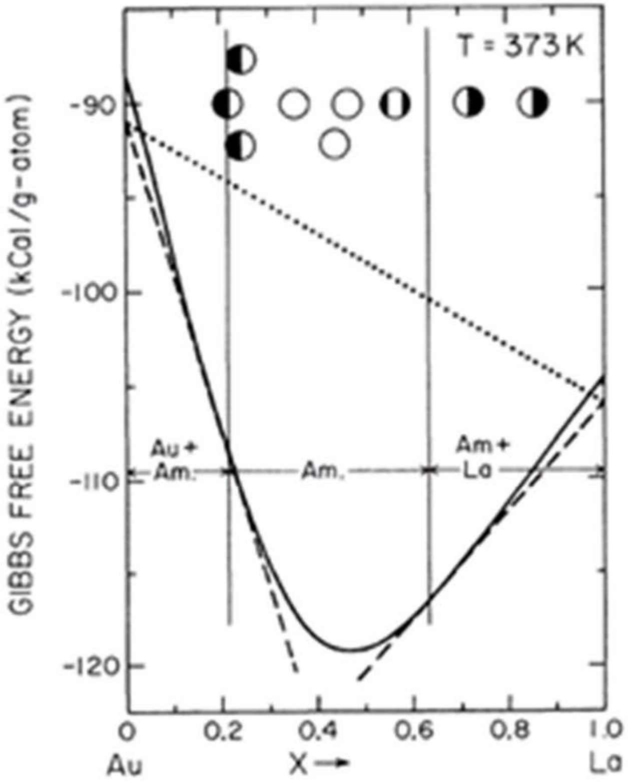

- **Diffusional asymmetry**

i.e. one element diffuses anomalously fast in the other, but not vice versa

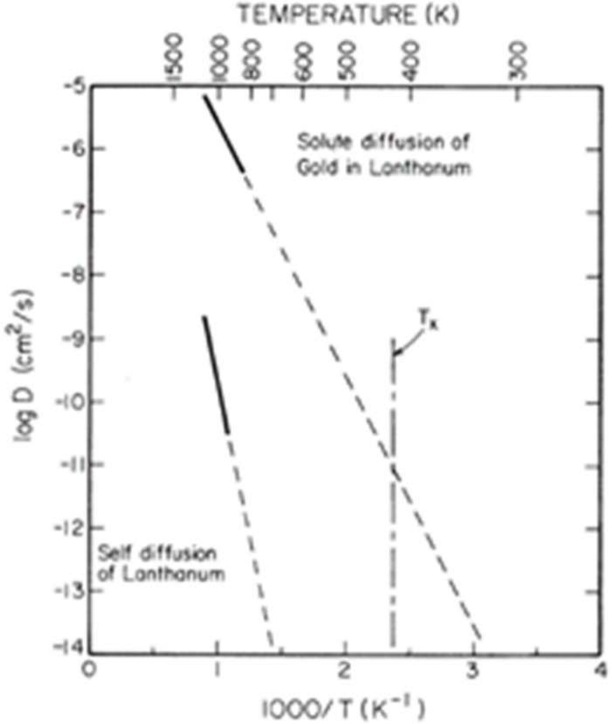

2.6.3 Solid-state Processes

D. Pressure-induced Amorphization

- Alloys in the systems Cd–Sb, Zn–Sb, and Al–Ge were subjected to high pressures when they formed unstable crystalline phases and then decayed in a short time to amorphous phases [50]. An amorphous phase was also found to form in Cu–12–17 at.% Sn alloys when they were heated to high temperatures in a confined pressure, and turning off the power suddenly.

e. Amorphization by Irradiation

- A number of intermetallics, for example, NiTi, Zr_3Al, Cu_4Ti_3, $CuTi_2$, FeTi, etc., have been amorphized by irradiation with high-energy electrons, heavy ions, or fission fragments [18]. It is only intermetallics, and not solid solutions, that have been amorphized this way. Several different criteria have been proposed for this purpose, which include low temperature, high doses, high dose rates, intermetallics with an extremely narrow homogeneity range, permanently ordered compounds (i.e., intermetallics which are ordered up to the melting temperature and do not show an order–disorder transformation), which also have high-ordering energies, destruction of long-range order by irradiation, etc. Fecht and Johnson [52] have analyzed the fundamental issues involved in the amorphization of intermetallics by irradiation methods.

Preparation of amorphous materials by irradiation

Two kinds of irradiation effects

- Laser/electron irradiation:

Small area melting → cooling → amorphous layer/crystalline

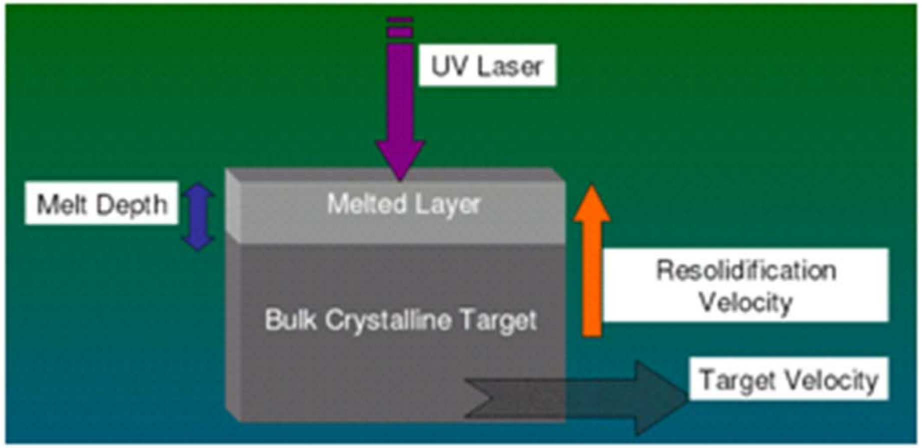

- Neutron and heavy ion irradiation:

Atomic displacement → recovery → amorphous phase

- **Mechanism of irradiation amorphization:**

- The kinetic knock-off of atoms from their lattice positions
- Very high temperature is expected in a very small volume during a short time (ps), which causes melting of material in a local small point.

- **Two opposing radiation-induced processes can be operative:**

- **Radiation-induced chemical disordering** of atoms on lattice sites will tend to promote amorphization;
- **Radiation-induced defect migration** will tend to restore ordering.

➡ **The irradiation be <u>carried out at sufficiently low temperature</u> to suppress the defect migration.**

Radiation damage: damage by collision between high energy particle and materials

- **Basic defect by collision with high E particle: Vacancy & Interstitial**
  (Frenkel pair)

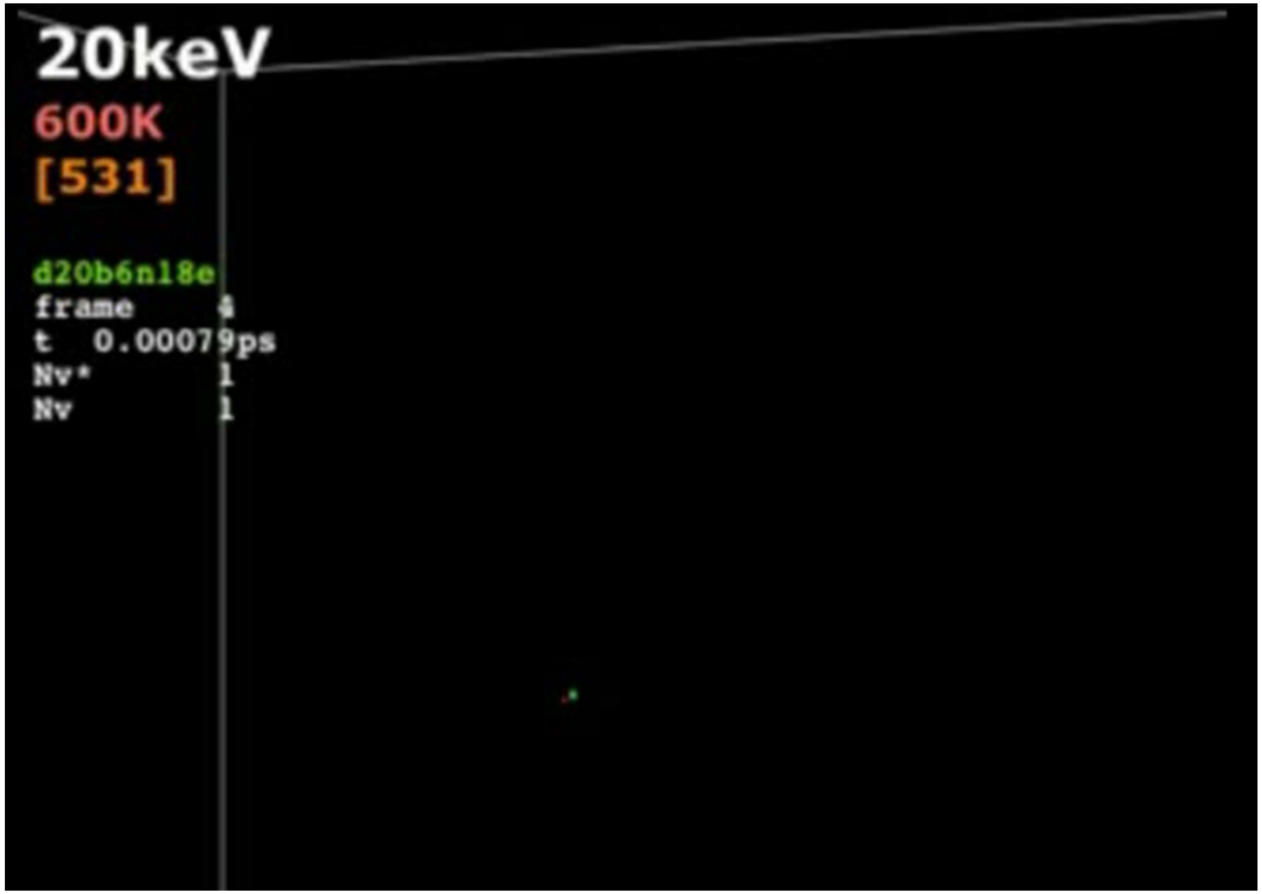

20keV Fe displacement cascade in bcc Fe at 600K

http://www.youtube.com/watch?v=0btHd_8JFV4

*** A primary knock-on atom (PKA) displaces neighbouring atoms, resulting in <u>an atomic displacement cascade</u>, leading to formation of point defects and defect clusters of vacancies and interstitial atoms.**

Seeger et al., Proc. Symp. Radiat. Damage Solids React. 1 (1962) 101-1056.

Radiation damage: damage by collision between high energy particle and materials

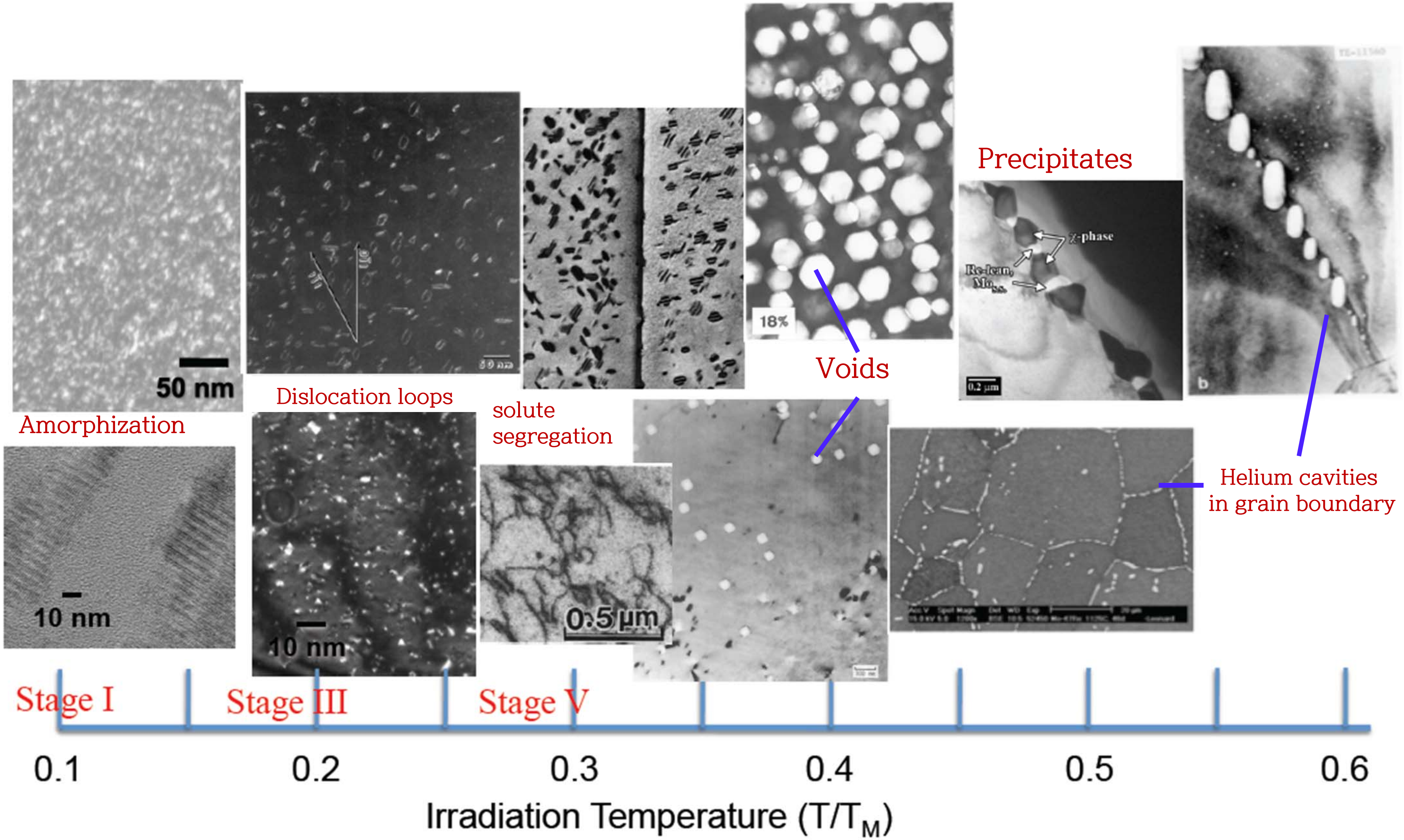

Precipitates

Amorphization

Dislocation loops

solute
segregation

Voids

Helium cavities
in grain boundary

Stage I

Stage III

Stage V

0.1

0.2

0.3

0.4

0.5

0.6

Irradiation Temperature (T/T_M)

S. Zinkle, Defects, deformation and damage in structural materials, 2012

Sample Preparation : Surface Damage

Ion beam induced amorphous formation in Silicon (100)

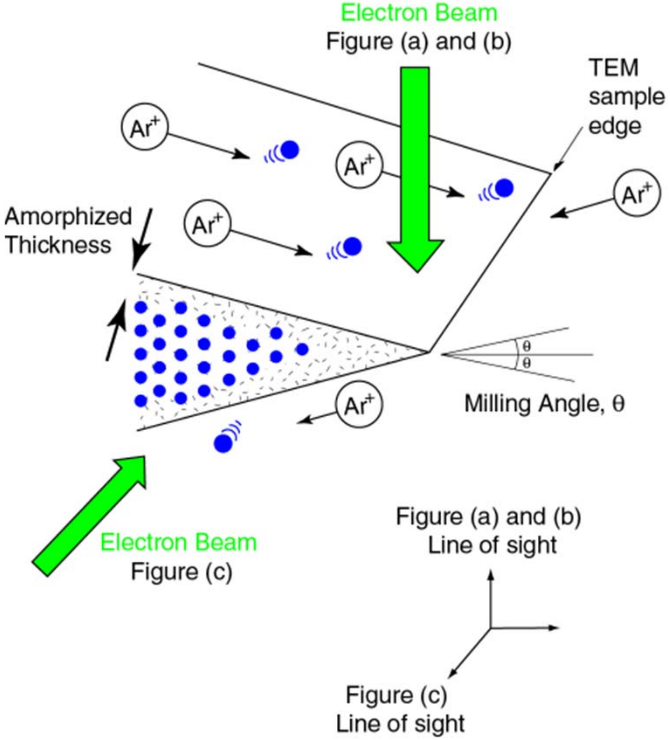

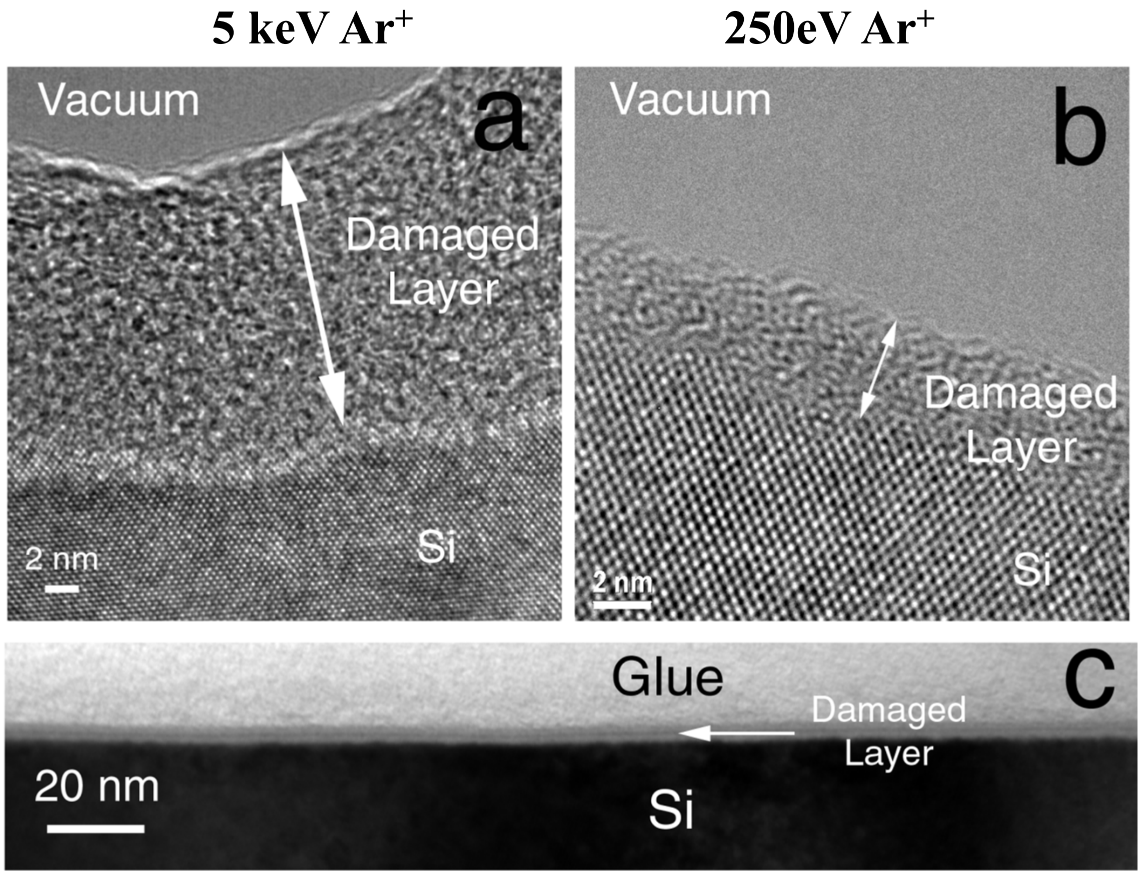
5 keV Ar^+

250eV Ar^+

Y.W. Kim, Metals and Materials International, 7, 499 (2001)

The schematic diagram of High Energy Electron beam accelerator

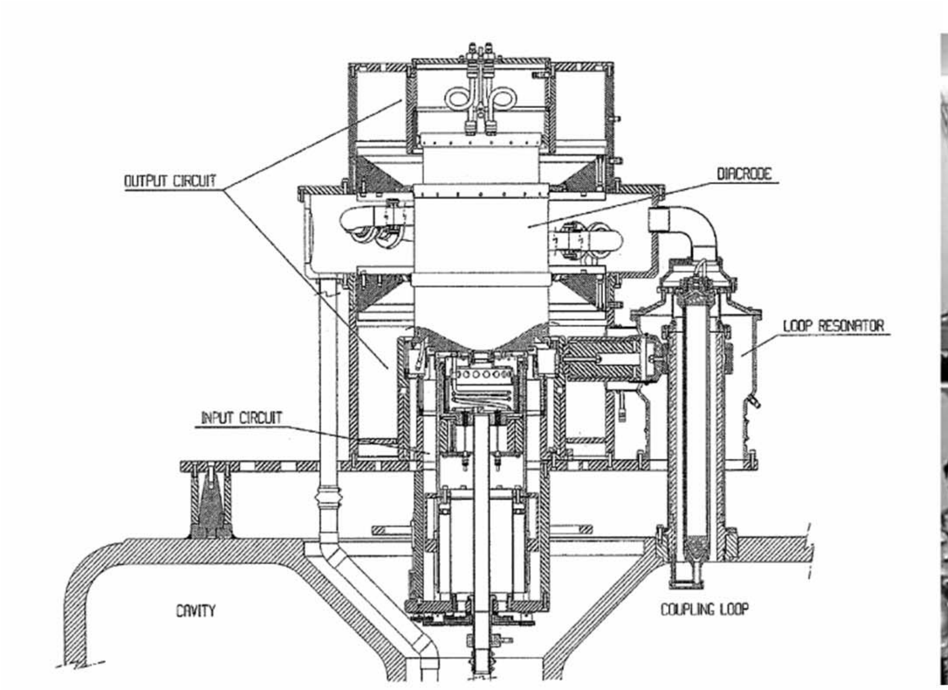

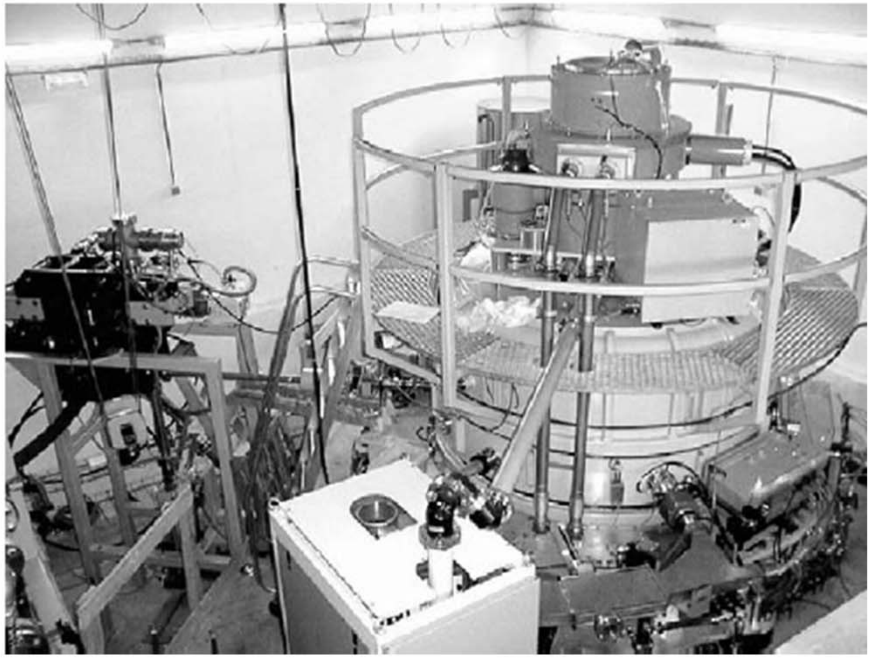

TT1000 prototype picture

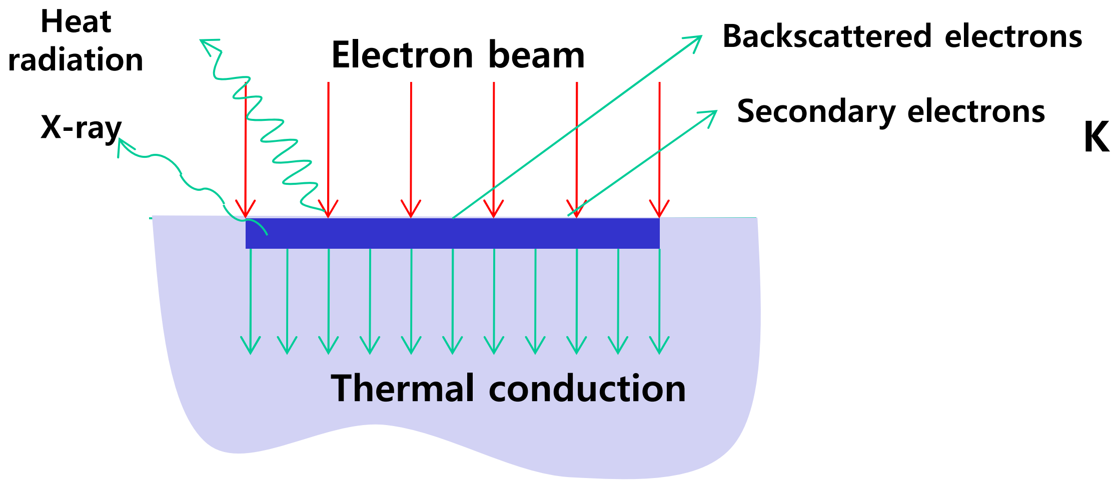

Kinetic energy of accelerated electron

↓ Collided with electrons of materials

To transform thermal energy

The making method of amorphous materials by Irradiation

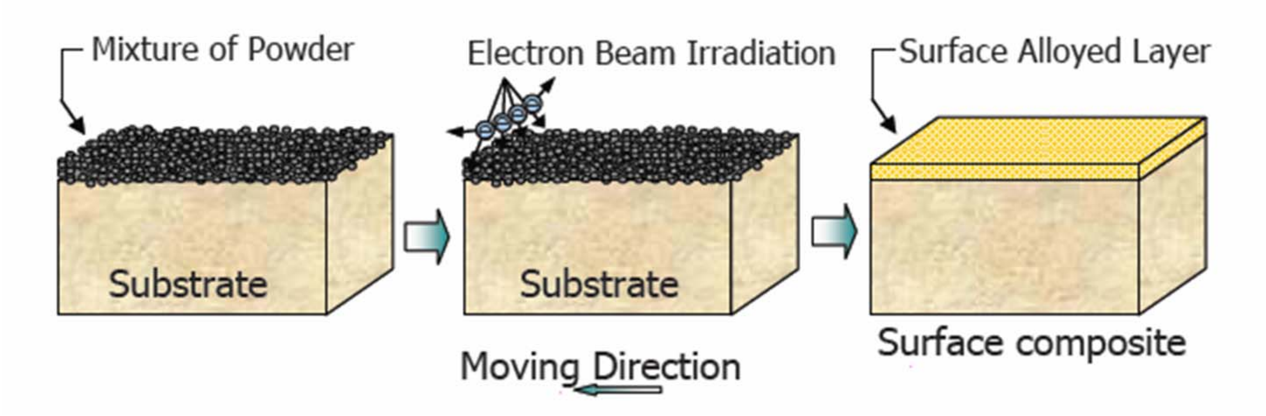

❖ Electron beam irradiation is heating the mixture of powder.

❖ The temperature of substrate is so low that surface is super-cooling.

Surface : Amorphous alloy

Surface gloss, Hardness, corrosion resistance,

Substrate : Cu(or Ti, Fe) alloy

Ductility, limited size of amorphous materials,

It is possible to make mass production and reduce weight

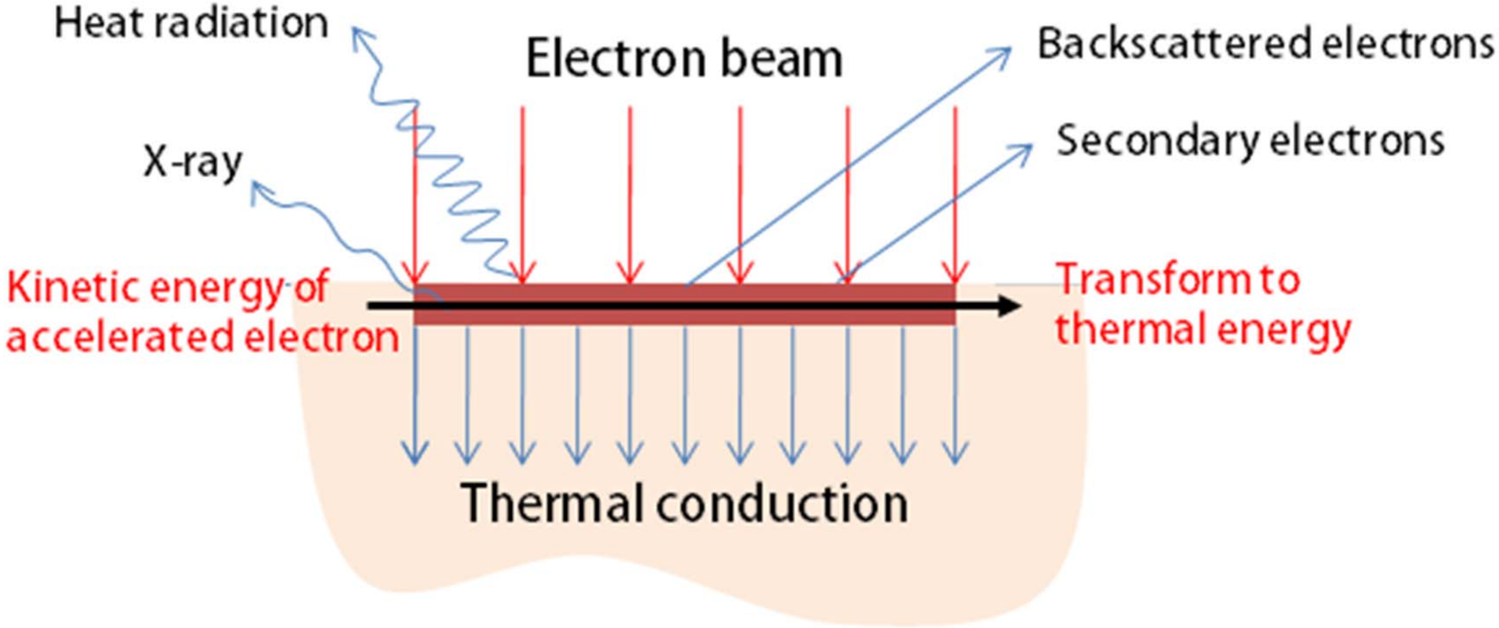
Heat radiation
Electron beam
Backscattered electrons
Secondary electrons
X-ray
Kinetic energy of accelerated electron
Transform to thermal energy
Thermal conduction

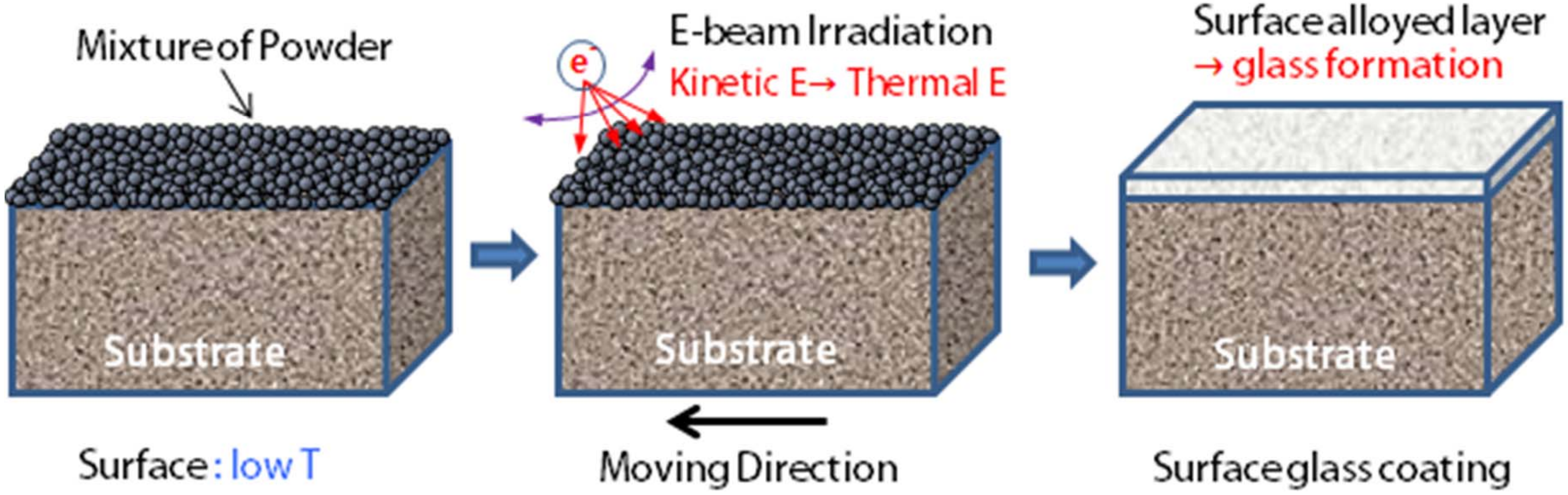
Mixture of Powder
e-
E-beam Irradiation
Kinetic E→ Thermal E
Surface alloyed layer
→ glass formation
Substrate
Substrate
Substrate
Surface : low T
Moving Direction
Surface glass coating

2.6.3 Solid-state Processes

f. Severe Plastic Deformation : Intense deformation at low temperatures (SPD methods)

Developed in the 1970s

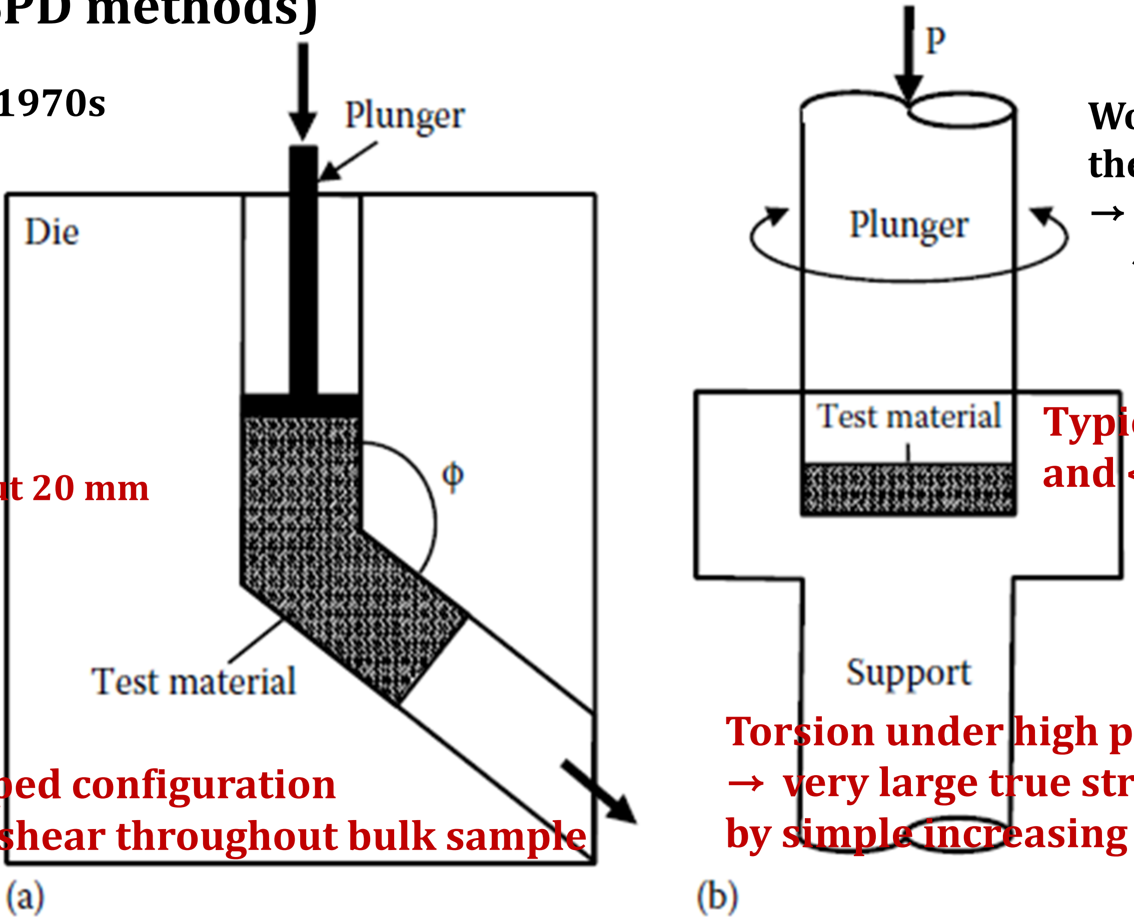

(a) (b)

Billet diameter
~Not exceeding about 20 mm

Bent into an L-shaped configuration
→ Uniform simple shear throughout bulk sample

Won Percy Bridgman the 1946 Nobel prize
→ metal processing
~ more recent in 2003

Typically 10 mm in dia. and < 1mm in height

Torsion under high pressure
→ very large true strain
by simple increasing the # of rotations

FIGURE 2.4 equal channel angular extrusion (ECAE)

Schematic diagrams showing the (a) equal channel angular pressing (ECAP) and (b) high-pressure torsion (HPT) processes.

HPT process: Equivalent strain induced on sample

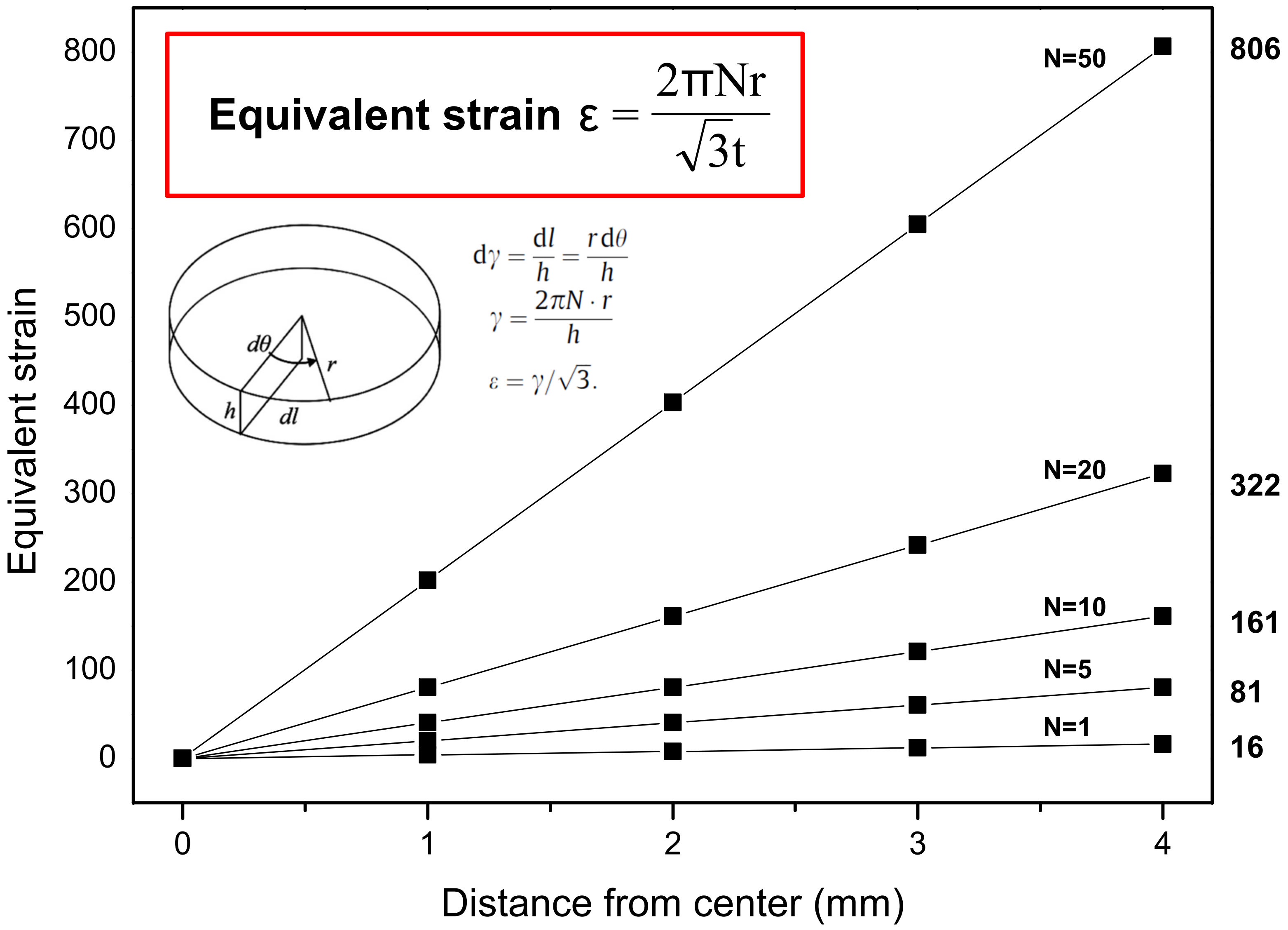

Equivalent strain $\varepsilon = \dfrac{2\pi N r}{\sqrt{3} t}$

$$d\gamma = \frac{dl}{h} = \frac{r\,d\theta}{h}$$

$$\gamma = \frac{2\pi N \cdot r}{h}$$

$$\varepsilon = \gamma/\sqrt{3}.$$

HPT: severe plastic deformation, but Inhomogeneous process

2.6.3 Solid-state Processes

f. Severe Plastic Deformation : Intense deformation at low temperatures (SPD methods)

- The SPD methods have some advantages over other methods in synthesizing ultrafine-grained materials. Firstly, ultrafine-grained materials with high-angle grain boundaries could be synthesized. Secondly, the samples are dense and there is no porosity in them since they have not been produced by the consolidation of powders. Thirdly, the grain size is fairly uniform throughout the structure. Lastly, the technique may be applied directly to commercial cast metals.
- However, the limitations of this technique are that the minimum grain size is not very small (typically it is about 200–300 nm), and that amorphous phases or other metastable phases have not been synthesized frequently. But, these methods are very useful in producing bulk ultrafine-grained materials.
- The methods of SPD described above have two drawbacks. Firstly, forming machines with large load capacities and expensive dies are required. Secondly, the productivity is relatively low.

2.6.3 Solid-state Processes

g. Accumulative Roll Bonding (ARB process)

: 2 sheets of the same material are stacked, heated (to below the recrystallization temperature), and rolled, bonding the 2 sheets together. This sheet is cut in half, the 2 halves are stacked, and the process is repeated several times. Compared to other SPD processes, ARB has the benefit that it does not require specialized equipment. However, the surfaces to be joined must be well cleaned before rolling to ensure good bonding.

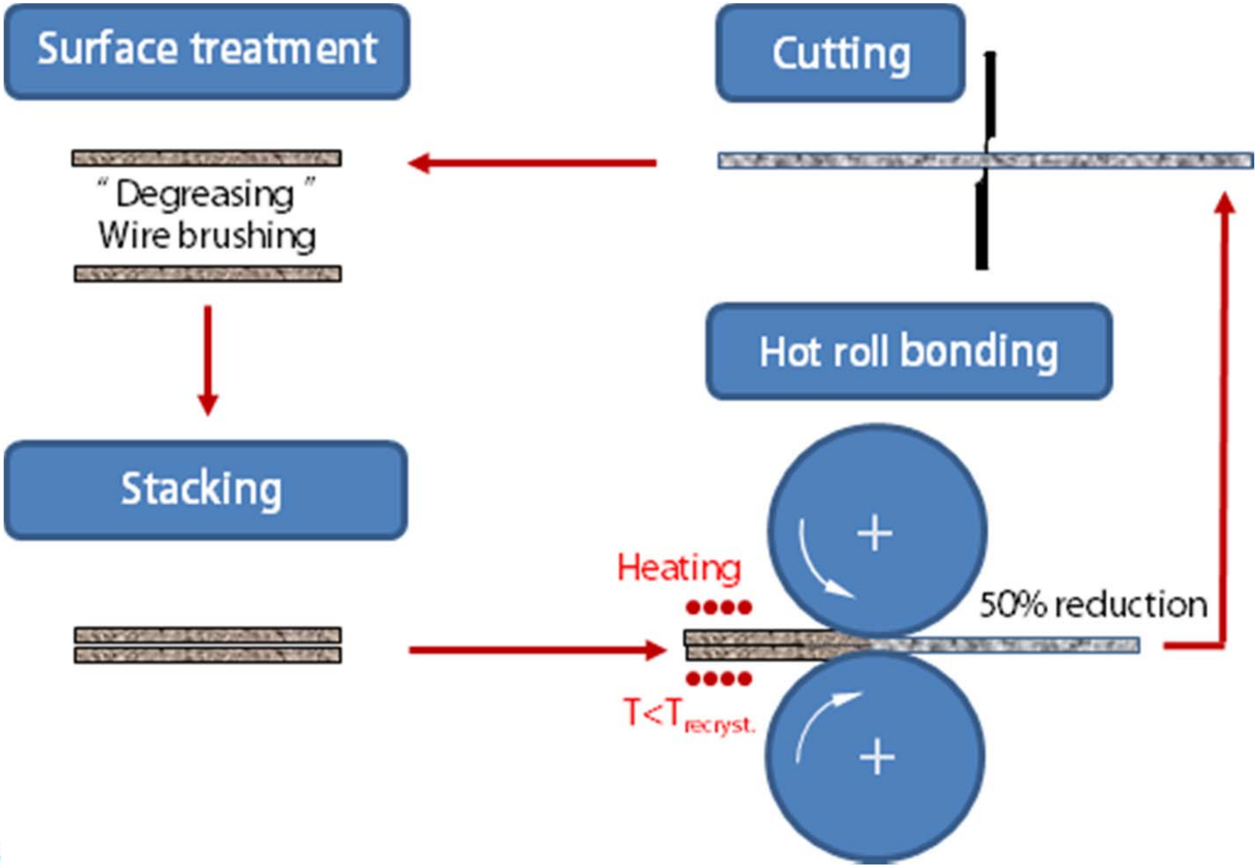

FIGURE 2.5
Schematic of the accumulative roll-bonding (ARB) process.

2.7 Bulk Metallic Glasses (BMGs)

- More commonly, metallic glasses with at least a diameter or section thickness of 1 mm are considered "bulk." (Nowadays researchers tend to consider 10 mm as the minimum diameter or section thickness at which a glass is designated bulk.)

2.7.1 Characteristics of Bulk Metallic Glasses

- The alloy systems have a minimum of three components; more commonly the number is much larger and that is why they are frequently referred to as multicomponent alloy systems.
- They can be produced at slow solidification rates, typically 10^3 K s^{-1} or less. The lowest solidification rate at which BMGs have been obtained was reported as 0.067 K s^{-1}, that is, 4 K min^{-1} [61]; a really slow solidification rate indeed!
- BMGs exhibit large section thicknesses or diameters, a minimum of about 1 mm. The largest diameter of a bulk metallic glass rod produced till date is 72 mm in a $Pd_{40}Cu_{30}Ni_{10}P_{20}$ alloy [62].
- They exhibit a large supercooled liquid region. The difference between the glass transition temperature, T_g, and the crystallization temperature, T_x, that is, $\Delta T_x = T_x - T_g$, is large, usually a few tens of degrees, and the highest reported value so far is 131 K in a $Pd_{43}Ni_{10}Cu_{27}P_{20}$ alloy [17].

When the as-cast alloy is characterized by XRD techniques, the presence of a broad and diffuse peak is often taken to be evidence for the presence of a glassy phase. This is normally true. But, it should be realized that the technique of XRD is not very sensitive to the presence of a small volume fraction of a crystalline phase in a glassy phase, especially when the crystals are in nanocrystalline condition. Therefore, even if the XRD pattern shows a broad halo, the material may contain a small volume fraction of a crystalline phase dispersed in the glassy matrix. Further, a structure consisting of a glassy phase, or extremely fine grains, or a nanocrystalline material with a small grain size of about <10 nm, will all produce a broad and diffuse halo. Therefore, it is always desirable to confirm the lack of crystallinity in the material by conducting (high-resolution) transmission electron microscopy investigations.

2.7.2 The Origins of BMGs

* History of Metallic Glasses

- **First amorphous metal produced by evaporation in 1934.**

  ** j. Kramer, Annalen der Phys. 1934; 19: 37.*

- **First amorphous alloy(CoP or NiP alloy)**

  produced by electro-deposition in 1950.

  ** A. Brenner, D.E. Couch, E.K. Williams, J. Res. Nat. Bur. Stand. 1950: 44; 109.*

- **First metallic glass ($Au_{80}Si_{20}$)**
  produced by splat quenching at Caltech by Pol Duwez in 1957.

  ** W. Klement, R.H. Willens, P. Duwez, Nature 1960; 187: 869.*

- **First bulk metallic glass ($Pd_{77.5}Cu_6Si_{16.5}$)**
  produced by droplet quenching at Harvard Univ.
  by H.S. Chen and D. Turnbull in 1969

  ** H.S. Chen and D. Turnbull, Acta Metall. 1969; 17: 1021.*

  produced by water quenching of PdTMSi, Pt-Ni-P and Pd-Ni-P system
  by H.S. Chen in 1974 (long glassy roads, 1-3 mm in diameter and several centimeters in length)

  ** H.S. Chen, Acta Metall. 1974; 22: 1505*

- # First bulk metallic glass: $Pd_{77.5}Cu_6Si_{16.5}$ (T_{rg}=0.64)

By droplet quenching (CR~800 K/s)

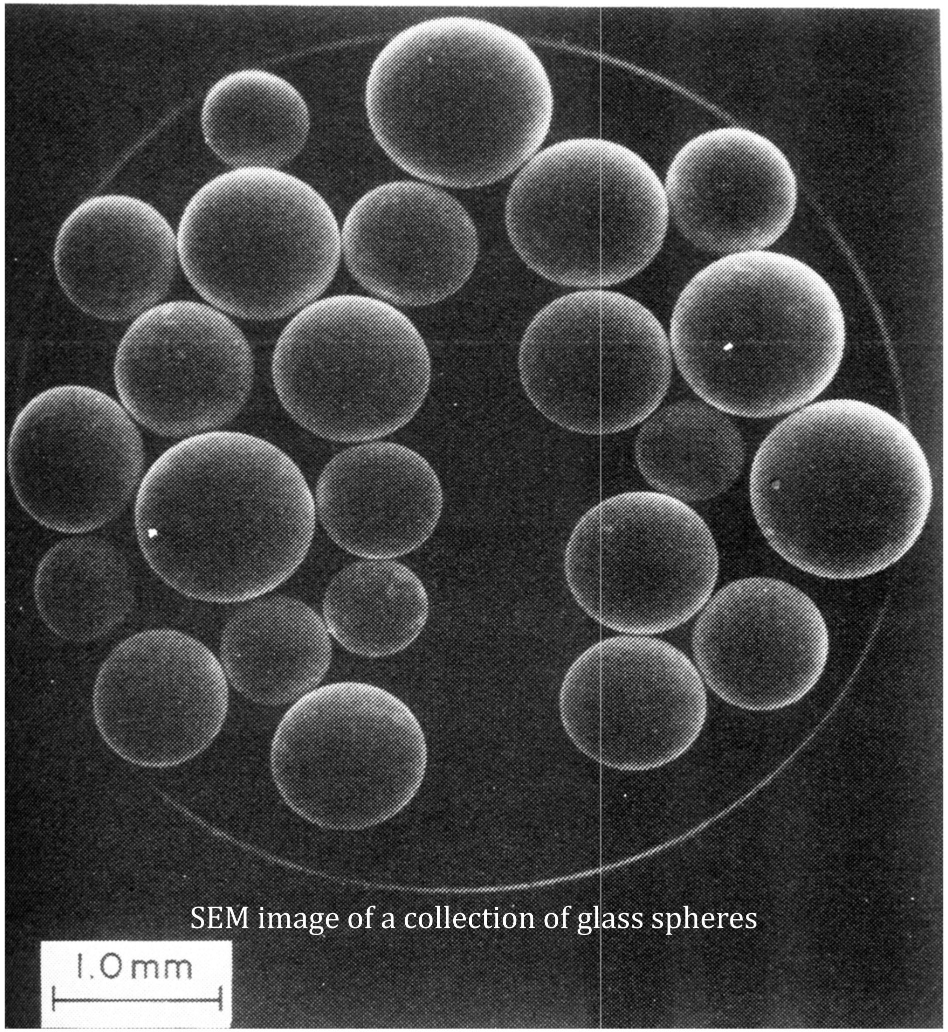

SEM image of a collection of glass spheres

** H.S. Chen and D. Turnbull, Acta Metall. 1969; 17: 1021.*

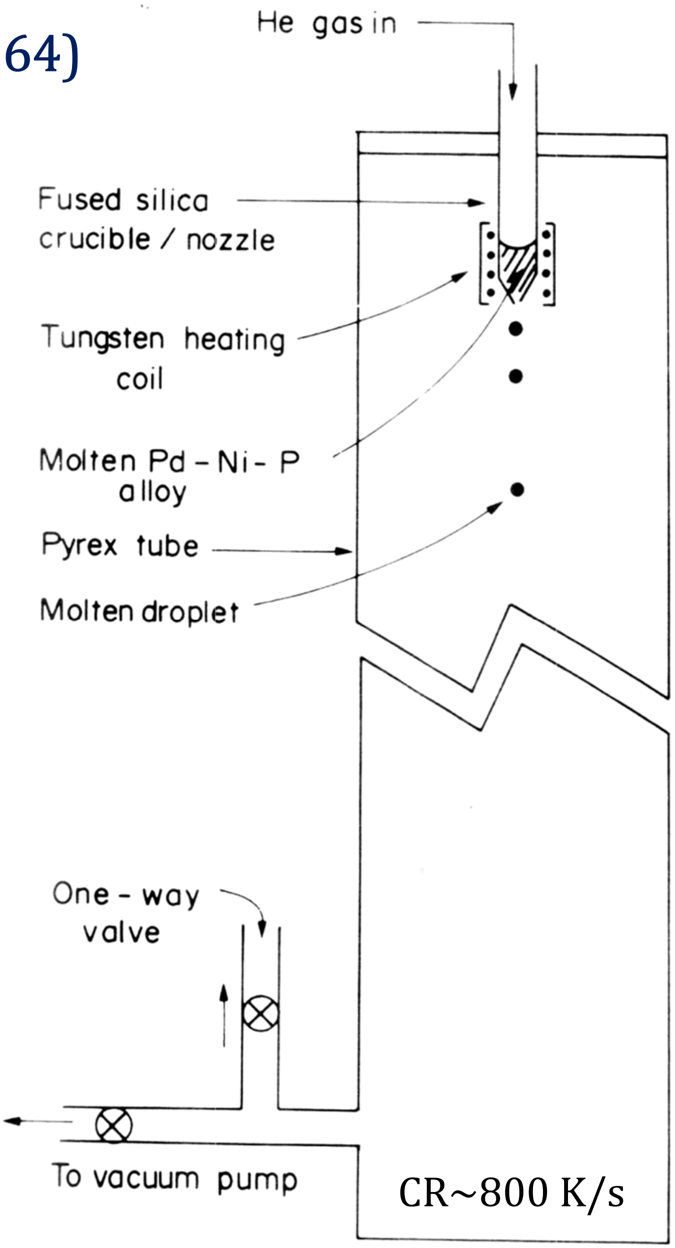

CR~800 K/s

Bulk formation of a metallic glass: $Pd_{40}Ni_{40}P_{20}$

- **Alloy Selection: Consideration of T_{rg}**

*** $Pd_{82}Si_{18}$ ➡ T_{rg}=0.6**

- Homogeneous nucleation rate: >10^5/cm^{3}s

- Critical cooling rate: > 800 K/s

*** $Pd_{77.5}Cu_6Si_{16.5}$ ➡ T_{rg}=0.64**

*** $Pd_{40}Ni_{40}P_{20}$ ➡ T_{rg}=0.67**
T_g=590 K, T_e = 880 K, T_l = 985 K

- **Suppression of Heterogeneous nucleation**

1. Surface Etching of ingot in a mixture of HCL and H_2O_2
: elimination of surface heterogeneities

2. Thermal cycling –5 cycles
: dissolution of nucleating heterogeneities
⟶ reduce the temperature at which nucleation occurred

<Schematic diagram of apparatus>

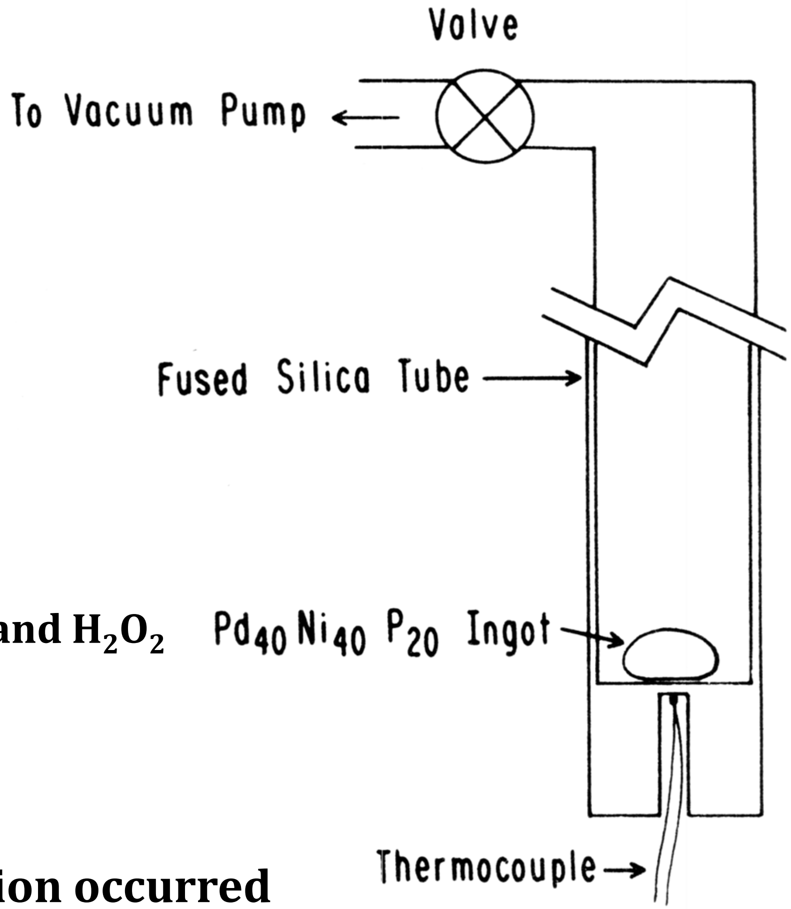

Bulk formation of a metallic glass: $Pd_{40}Ni_{40}P_{20}$

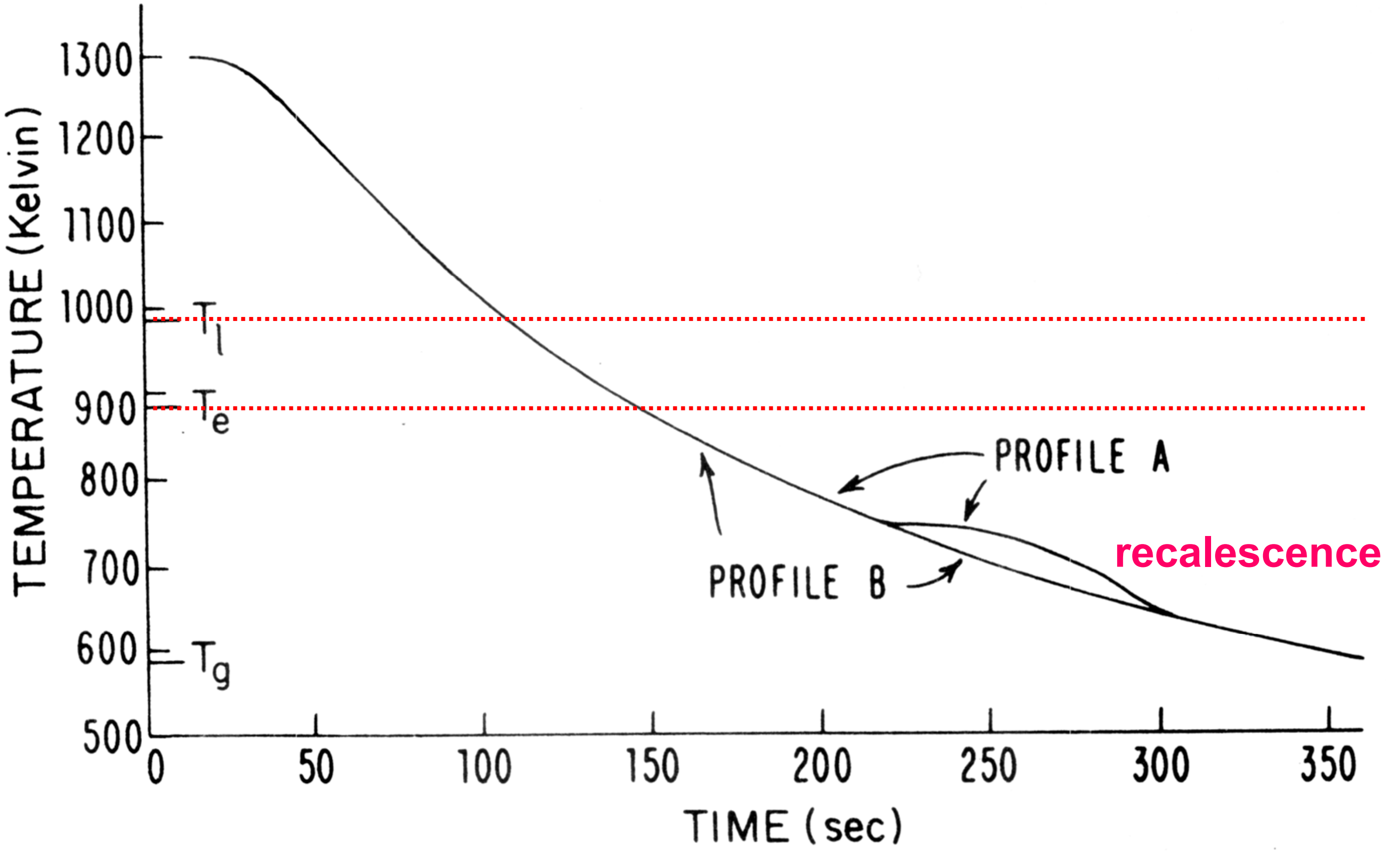

FIG. 2. Superposition of two cooling profiles: A—bulk crystallization which began at 740 K. B—formation of a glassy ingot.

A.J. Drehman, A.L. Greer, D. Turnbull, Appl. Phys. Lett. 1982; 41: 716.

Bulk formation of a metallic glass: $Pd_{40}Ni_{40}P_{20}$

- **Largest ingot**

- minimum dimension 0.6 cm and mass of 2.3 g

- Critical cooling rate: ~ 1.4 K / sec.

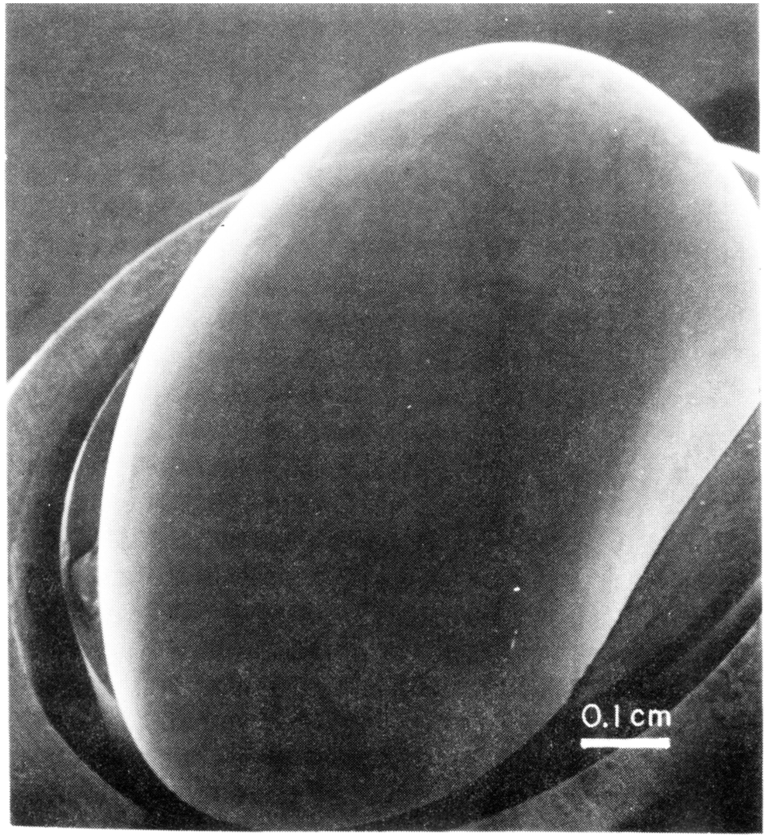

Appl. Phys. Lett. 1982; 41: 716.

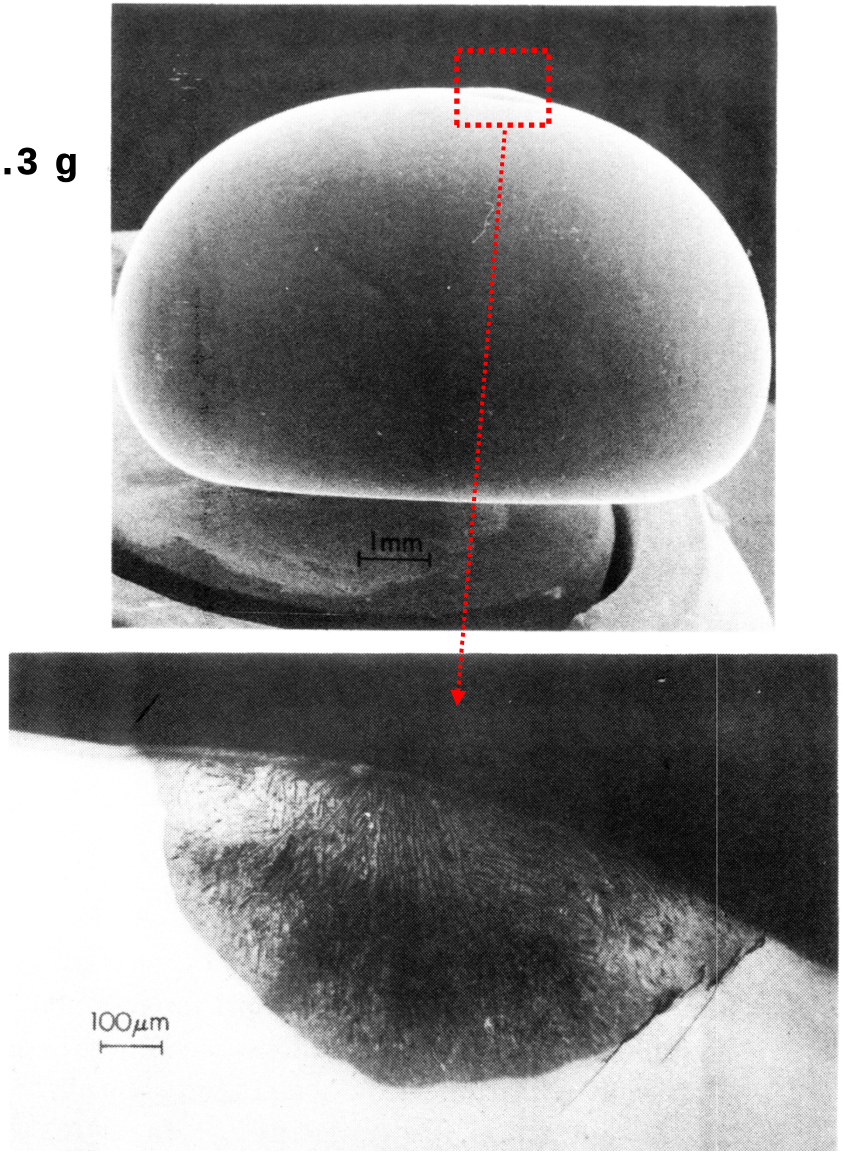

OM image of the cross section of a crystalline inclusion showing the eutectic structure

Formation of bulk metallic glass by fluxing

- **Heterogeneous nucleation**

1. **Surface oxide layer**
2. **Container walls**
3. **Motes in the liquid**

→ **Suppression**

1. Ingot = Chemical etching
by dilute aqua regia (HNO_3 + HCl)

2. Interior of the vessel = Cleaning
by hydrofluoric acid

3. Impurities = Successive heating-cooling cycles in a molten oxide flux

B_2O_3 melting point 723 K, boiling point <40,000 K

After gravity segregation to the oxide-metal interface most heterophase impurities presumably are dissolved or deactivated (e.g., by being wet) by the molten oxide

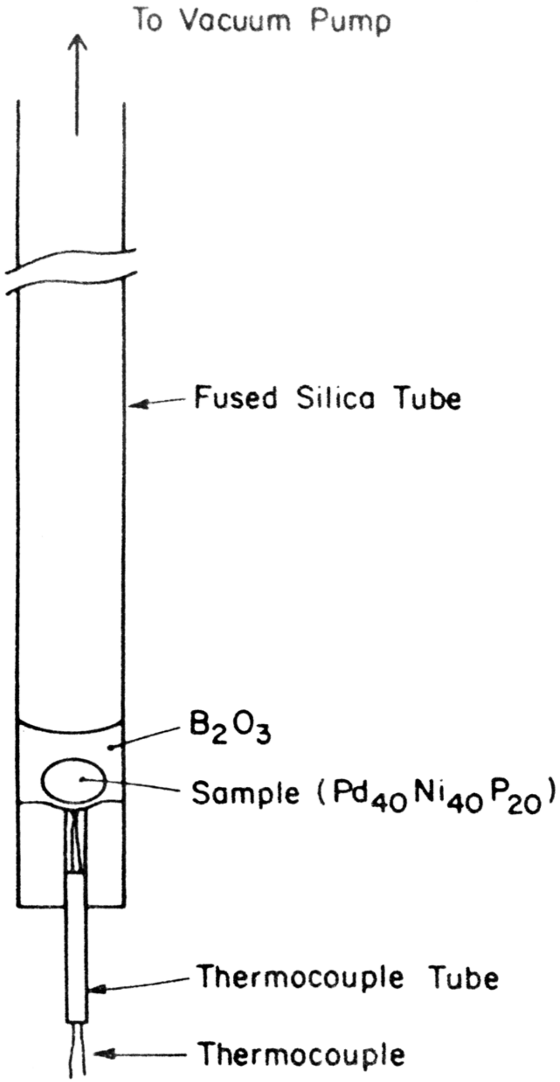

Schematic process of fluxing

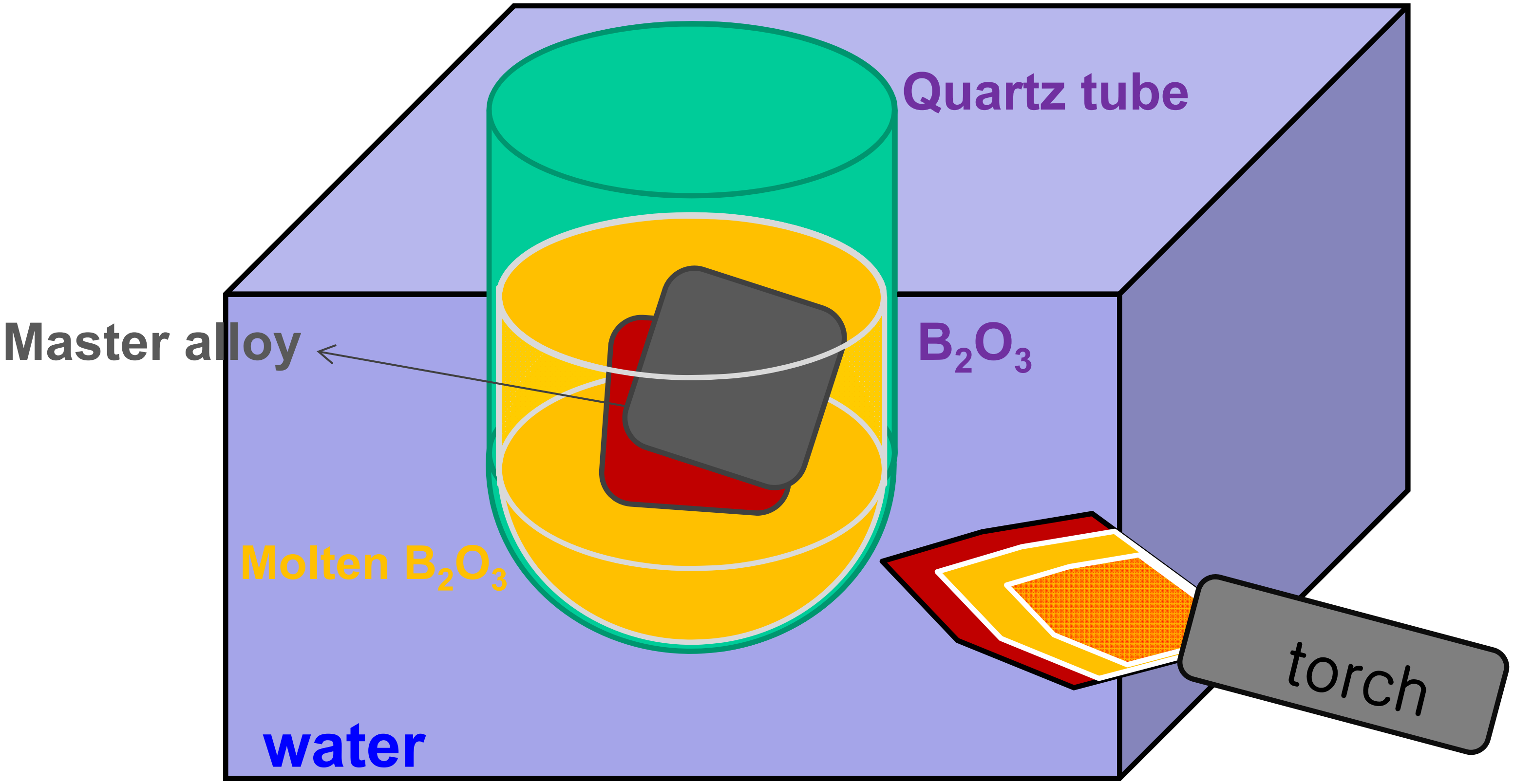

B_2O_3 melting point 723 K, boiling point <40,000 K

Formation of centimeter-sized BMG by fluxing

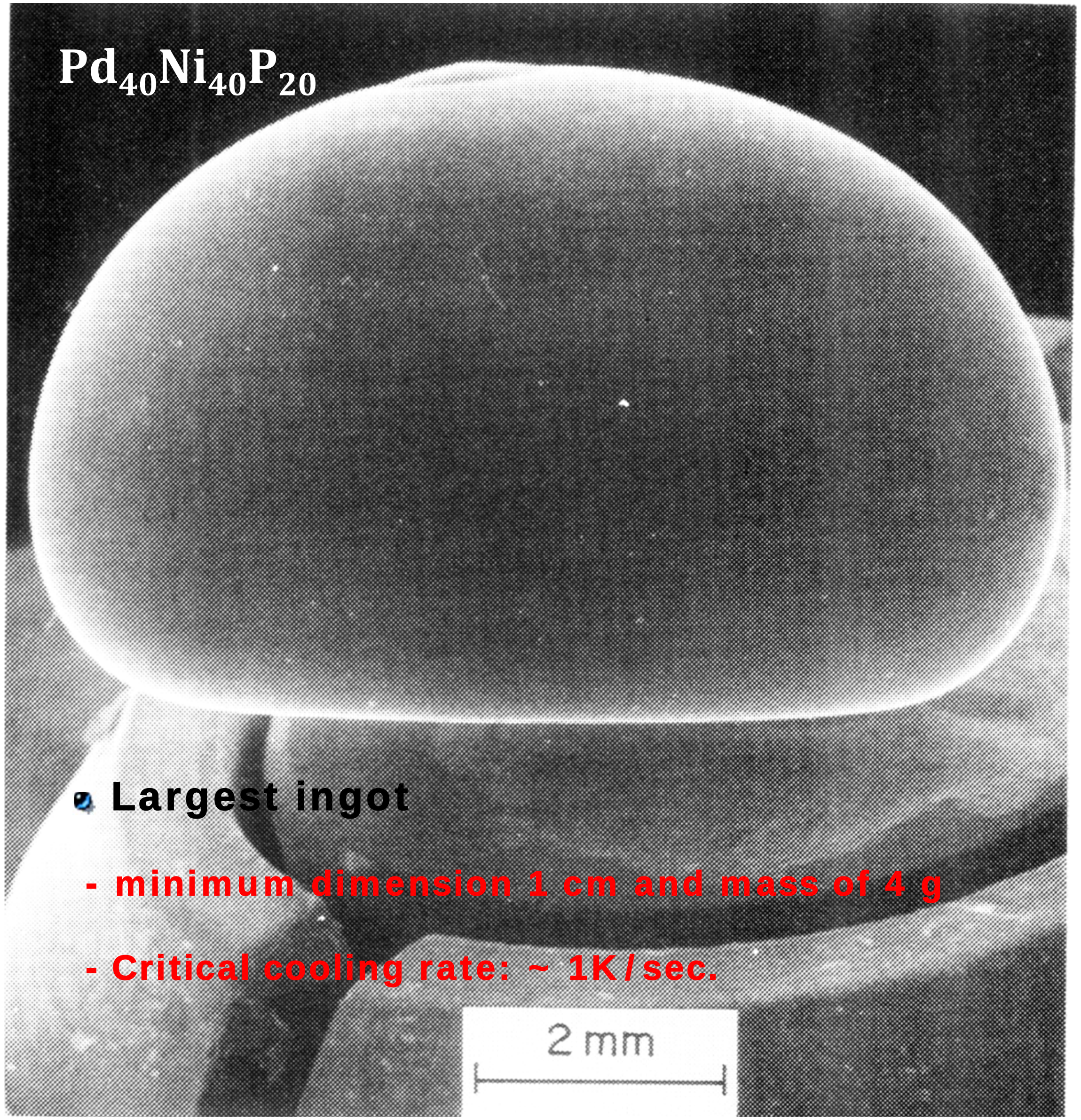

- **Largest ingot**
  - minimum dimension 1 cm and mass of 4 g
  - Critical cooling rate: ~ 1K/sec.

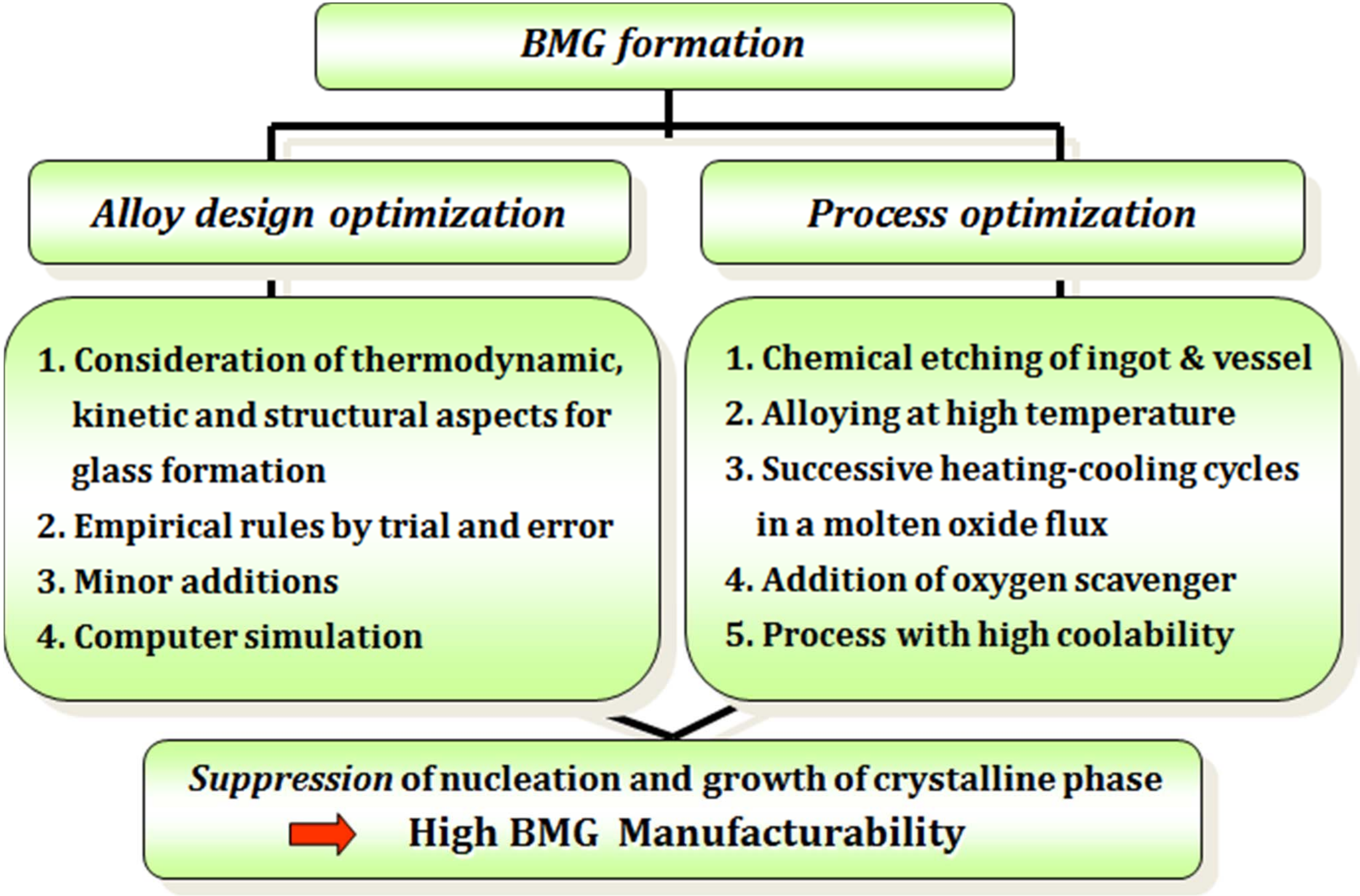

BMG formation

Alloy design optimization

1. **Consideration of thermodynamic, kinetic and structural aspects for glass formation**
2. **Empirical rules by trial and error**
3. **Minor additions**
4. **Computer simulation**

Process optimization

1. **Chemical etching of ingot & vessel**
2. **Alloying at high temperature**
3. **Successive heating-cooling cycles in a molten oxide flux**
4. **Addition of oxygen scavenger**
5. **Process with high coolability**

***Suppression* of nucleation and growth of crystalline phase**

➡ **High BMG Manufacturability**

Formation of centimeter-sized BMG by fluxing

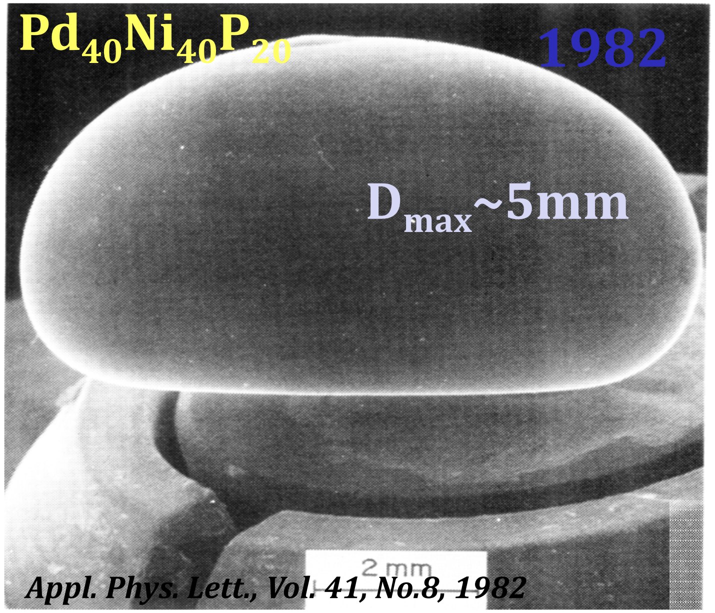

$Pd_{40}Ni_{40}P_{20}$

1982

D_{max}~5mm

Appl. Phys. Lett., Vol. 41, No.8, 1982

1984

→

D_{max}~10mm

After fluxing treatment

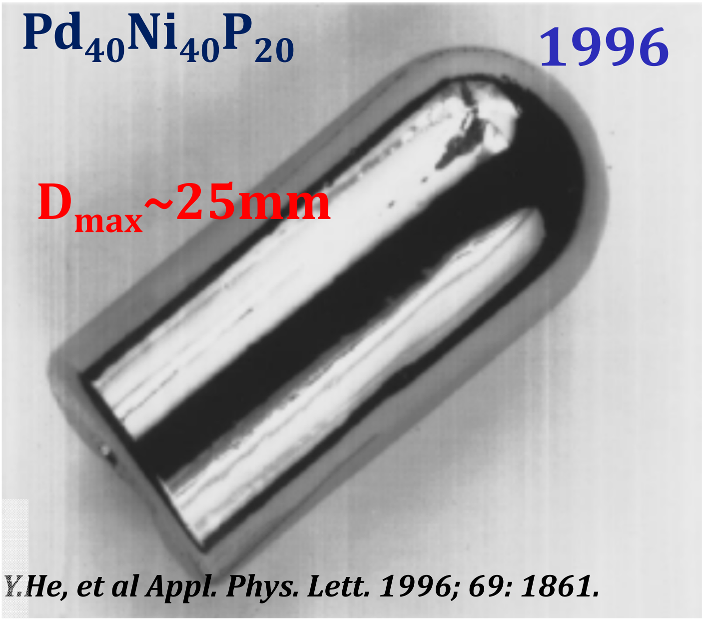

$Pd_{40}Ni_{40}P_{20}$

1996

D_{max}~25mm

Y.He, et al Appl. Phys. Lett. 1996; 69: 1861.

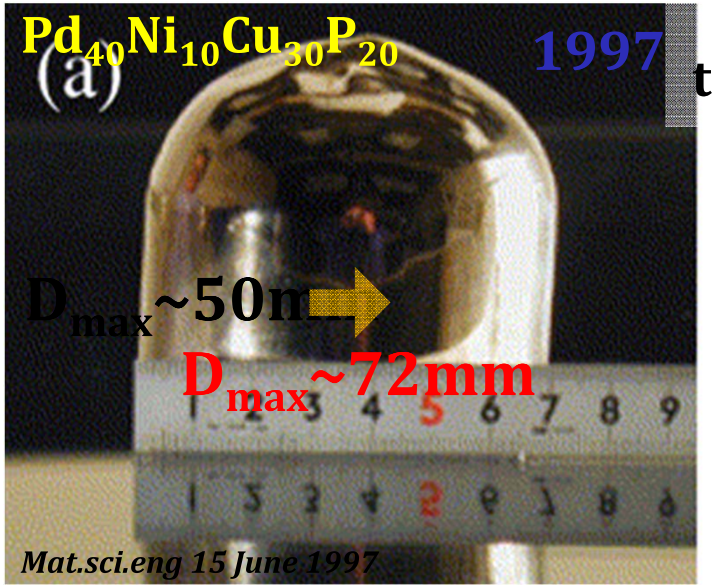

$Pd_{40}Ni_{10}Cu_{30}P_{20}$

1997

D_{max}~50m

→

D_{max}~72mm

Mat.sci.eng 15 June 1997

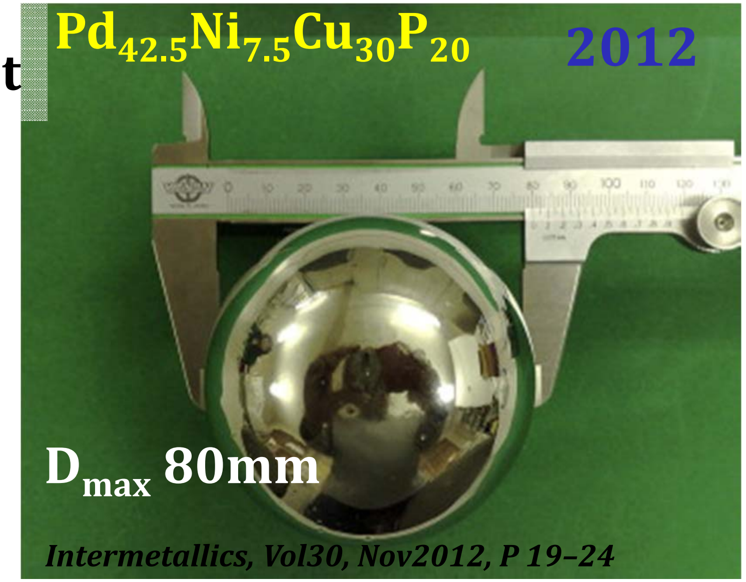

$Pd_{42.5}Ni_{7.5}Cu_{30}P_{20}$

2012

D_{max} 80mm

Intermetallics, Vol30, Nov2012, P 19–24

Starting in the late 1980s, the RSP group at Tohoku University in Sendai, Japan, has systematically investigated the glass-forming ability (GFA) of different alloy systems and was able to produce bulk glassy alloys in some of the systems at solidification rates of 10^3 K s^{-1} or lower. A brief account of the development of BMGs at Tohoku University is described below.

Al–La–Ni [67] and Mg–Ni–La [68] glassy alloys were produced in a wide composition range → The ΔT_x values reported were 69 K for the $La_{55}Al_{25}Ni_{20}$ glass and 58 K for the $Mg_{50}Ni_{30}La_{20}$ glass. These ΔT_x values are much larger than those reported for the noble-metal-based glasses, Pd–Ni–P and $Pt_{60}Ni_{15}P_{25}$ (35–40 K) reported earlier.

Figure 2.6

X-ray diffraction patterns of La55Al25Ni20 glassy samples in the water-quenched rod (0.8 mm dia. → D_{max} = 1.2 mm) and melt-spun ribbon (20µm) conditions. Note that in both the cases, the diffraction pattern shows only a broad peak and sharp peaks indicative of any crystalline phase are absent. Furthermore, the position of the broad peak is the same in both the samples, suggesting that the glassy phase produced in same in both the cases.

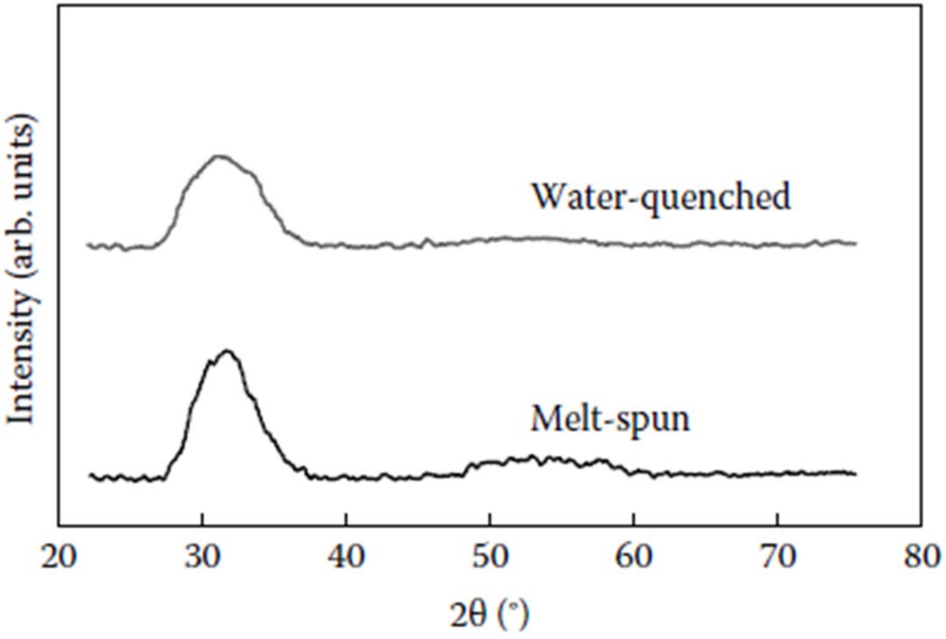

** Inoue A, et al., Mater. Trans. JIM, 30, 722, 1989.*

These observations have subsequently been confirmed in a number of other alloy systems and by several researchers. Subsequent to this initial discovery, Peker and Johnson [70] produced a 14 mm diameter fully glassy rod in the composition $Zr_{41.2}Ti_{13.8}Cu_{12.5}Ni_{10.0}Be_{22.5}$ (most commonly referred to as Vitreloy 1 or Vit 1, and now redesignated as liquid metal or LM-001), and since then there has been an explosion in the research activity in this area all over the world.

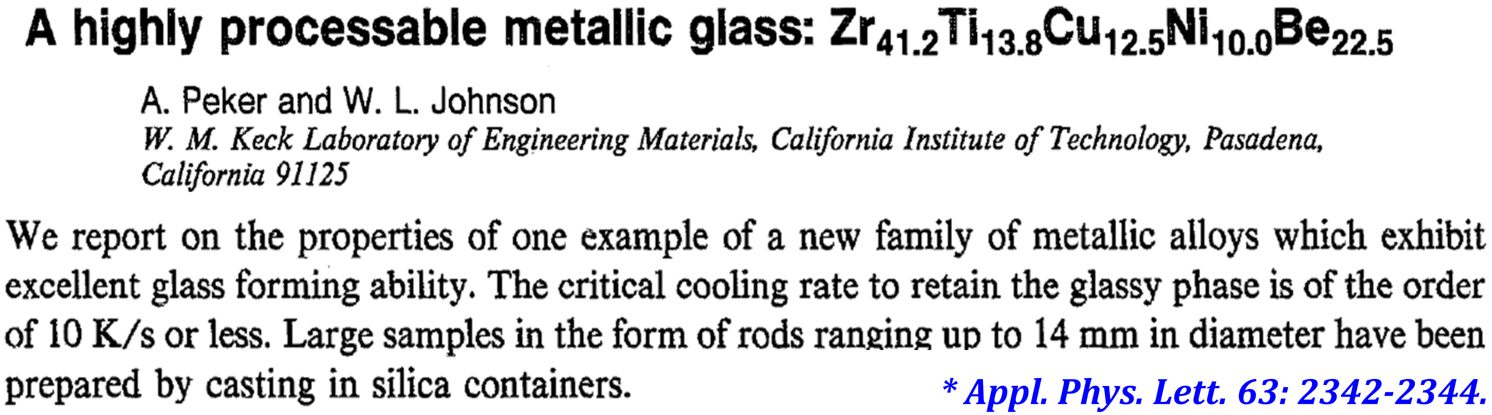

A highly processable metallic glass: $Zr_{41.2}Ti_{13.8}Cu_{12.5}Ni_{10.0}Be_{22.5}$

A. Peker and W. L. Johnson
W. M. Keck Laboratory of Engineering Materials, California Institute of Technology, Pasadena, California 91125

We report on the properties of one example of a new family of metallic alloys which exhibit excellent glass forming ability. The critical cooling rate to retain the glassy phase is of the order of 10 K/s or less. Large samples in the form of rods ranging up to 14 mm in diameter have been prepared by casting in silica containers.

**** Appl. Phys. Lett. 63: 2342-2344.***

Starting with the initial discovery of the formation of BMGs in the La–Al–Ni system, the Tohoku group has produced a very large number of BMGs in different alloy systems based on Mg, Zr, Ti, Pd, Fe, Co, Ni, and Cu. They have been able to produce several new alloys in the BMG state and also increase the critical (or maximum) diameter of the BMG alloy rods during the last nearly 20 years.

Recent BMGs with critical size ≥ 10 mm

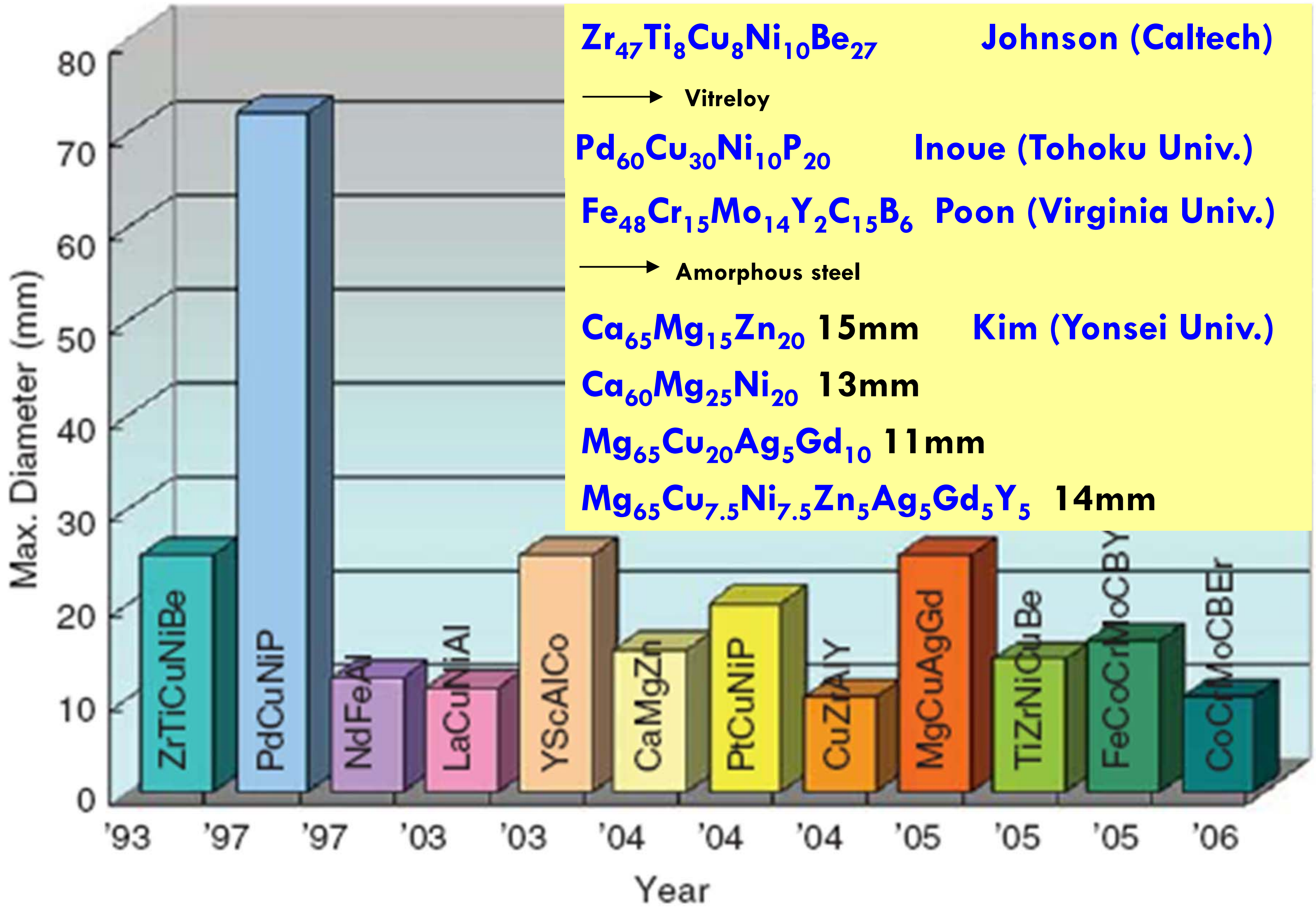

$Zr_{47}Ti_8Cu_8Ni_{10}Be_{27}$ Johnson (Caltech)

→ **Vitreloy**

$Pd_{60}Cu_{30}Ni_{10}P_{20}$ Inoue (Tohoku Univ.)

$Fe_{48}Cr_{15}Mo_{14}Y_2C_{15}B_6$ Poon (Virginia Univ.)

→ **Amorphous steel**

$Ca_{65}Mg_{15}Zn_{20}$ 15mm Kim (Yonsei Univ.)

$Ca_{60}Mg_{25}Ni_{20}$ 13mm

$Mg_{65}Cu_{20}Ag_5Gd_{10}$ 11mm

$Mg_{65}Cu_{7.5}Ni_{7.5}Zn_5Ag_5Gd_5Y_5$ 14mm

Bulk glass formation in the Pd-/Ni-/Cu-/Zr-element system

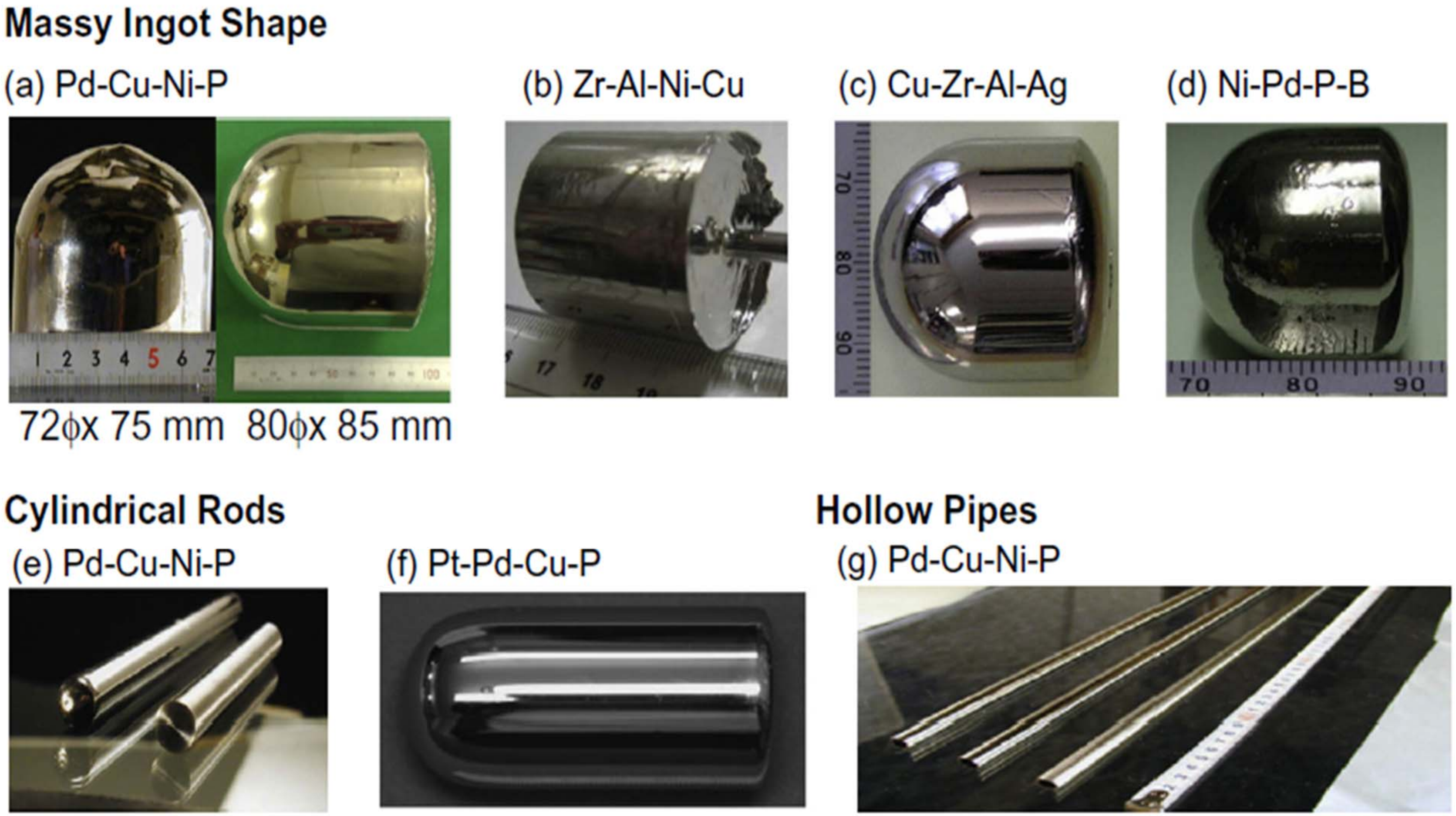

Recent BMGs with critical size ≥ 10 mm